Bullard

The American Mineralogist

Journal of the Mineralogical Society of America

Vol. 34 NOVEMBER-DECEMBER, 1949 Nos. 11 and 12

Contents

Fourier summations for symmetrical crystals . . . . M. J. Buerger 771
Dedolomitization, and its relation to a possible derivation of a magnesium-rich hydrothermal solution . . . . George T. Faust 789
On the symmetry and crystal structure of bornite . . G. Tunell and C. E. Adams 824
Petrographic distinction of xenotime and bastnäsite . . . . Wilfrid R. Foster 830
Geikielite, a new find from California . . . . . . Joseph Murdoch and J. J. Fahey 835
Improved differential thermal analysis apparatus . . . J. L. Kulp and P. F. Kerr 839
Linear thermal expansion of calcite, var. Iceland spar, and Yule marble . . . . Joseph L. Rosenholtz and Dudley T. Smith 846
Absorption of infrared radiation by powdered silica minerals . . . . W. D. Keller and E. E. Pickett 855
Suppression of thermal reactions in kaolinite . . . . R. M. Gruver, E. C. Henry and H. Heystek 869
Mineral isograds in southeastern Pennsylvania . . . . Hugh McKinstry 874
Notes and news: Refractive indices of high index liquids by the prism method on the two-circle goniometer . . . . C. W. Wolfe and Virginia Franklin 893
Note on the fluorescence test of bentonite . . . . Yi Hseung and C. C. Yeh 896
Index to volume 34; Title page; Table of contents 899

MCMXIX

EDITOR
WALTER F. HUNT

ASSOCIATE EDITORS
MICHAEL FLEISCHER, ESPER S. LARSEN,
AUSTIN F. ROGERS, M. N. SHORT AND GEORGE TUNELL

Published bi-monthly by the Society

Mineralogical Society of America

ASSOCIATED WITH THE GEOLOGICAL SOCIETY OF AMERICA

President: **John W. Gruner**, University of Minnesota, Minneapolis, Minnesota.

Vice President: **J. D. H. Donnay**, The Johns Hopkins University, Baltimore, Maryland.

Secretary: **C. S. Hurlbut, Jr.**, Harvard University, Cambridge, Massachusetts.

Treasurer: **Earl Ingerson**, U. S. Geological Survey, Washington 25, D.C.

Editor: **Walter F. Hunt**, University of Michigan, Ann Arbor, Michigan.

Councilors: **Joseph Murdoch**, University of California at Los Angeles, Los Angeles, California.
H. H. Hess, Princeton University, Princeton, New Jersey.
Clifford Frondel, Harvard University, Cambridge, Massachusetts.
Lewis S. Ramsdell, University of Michigan, Ann Arbor, Michigan.
M. A. Peacock, University of Toronto, Toronto, Canada.

The enlarged issues of this journal for 1949 are made possible by a grant from the Penrose Fund of the Geological Society of America.

The American Mineralogist—Journal of the Mineralogical Society of America

A journal containing articles on mineralogy, crystallography, petrography, and allied sciences, issued every two months. Contributions are invited from everyone.

Office of Publication, Mineralogical Laboratory, Ann Arbor, Mich.

The general conduct of the journal is in the hands of the Editor, **Walter F. Hunt**, Ann Arbor, Michigan. The council of the Mineralogical Society has appointed the following board of associate editors, to whom should be sent articles dealing with the special subjects indicated:

Michael Fleischer, U. S. Geological Survey, Washington, D.C., *New minerals.*
Esper S. Larsen, U.S. Geological Survey, Washington, D.C., *Optical crystallography.*
Austin F. Rogers, Stanford University, California, *Geometrical crystallography.*
M. N. Short, University of Arizona, Tucson, Arizona, *Mineralography.*
George Tunell, University of California at Los Angeles, *Structural crystallography.*

Contributors of leading articles are given without charge 100 reprints (without covers) of their article. If additional reprints are desired these can be purchased at the following rates:

Pages	*1–4*	*5–8*	*9–12*	*13–16*	*17–20*	*21–24*	*25–28*	*29–32*	*Covers*
Copies									
25	$3.50	$5.00	$ 8.00	$ 9.50	$11.00	$13.00	$15.00	$16.00	$4.90
50	3.80	5.55	8.80	10.40	12.10	14.20	16.40	17.50	5.50
75	4.10	6.10	9.60	11.30	13.20	15.40	17.80	19.00	6.10
100	4.40	6.65	10.40	12.20	14.30	16.60	19.20	20.50	6.70
Addl. C's	1.20	2.20	3.20	3.60	4.40	4.80	5.60	6.00	2.40

Cover Composition $1.55.

Sent to all members and fellows of the Mineralogical Society of America. Subscription price, $4.00 per year (single copies of normal issues, $1.00 plus postage).

Entered as second class matter at the post office at Menasha, Wis., under Act of March 3, 1879. Acceptance for mailing at the special rate of postage provided for in section 1103, Act of Oct. 3, 1917, paragraph 4 section 429 P. L. & R. authorized March 13, 1922.

Notices of change of address, orders, and remittances should be sent to Dr. Earl Ingerson, U.S. Geological Survey, Washington 25, D. C.

Printed by the George Banta Publishing Company, Menasha, Wisconsin

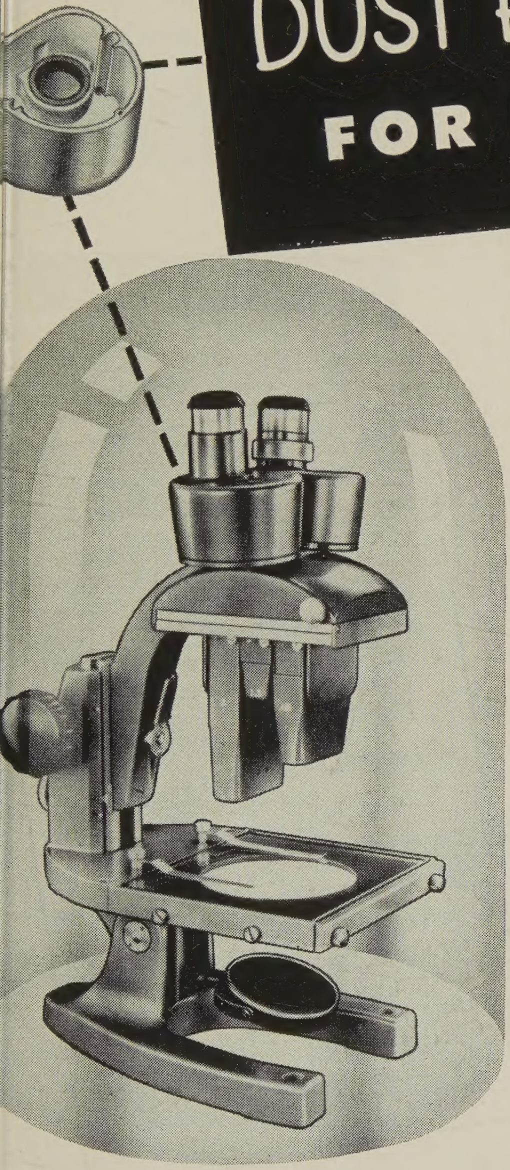

DUST PROOF

FOR LIFE!

Patented design *seals off* upper surface of each prism with Neoprene ring . . . Protects precision optics from dust and dirt . . . Assures maximum clarity and accuracy, *life-long* service.

WIDER FIELDS!

Critical focus on larger area than ever before . . . Advanced design optical system insures *true stereopsis* . . . Finest optics ever produced for wide field work.

Plus

Higher eyepoint • Dustproof nosepiece • Sturdier mechanical construction • and many other advantages you'll want.

Write today for complete information and demonstration. Bausch & Lomb Optical Co., 676-K St. Paul St., Rochester 2, N. Y.

ausch & Lomb *Stereoscopic* **Wide Field Microscopes**

A **NEW** SPENCER STEREOSCOPIC MICROSCOP

NEW Double Revolving Nosepiece

NEW Black Satin-Smooth Finish

NEW Platen Type Stage

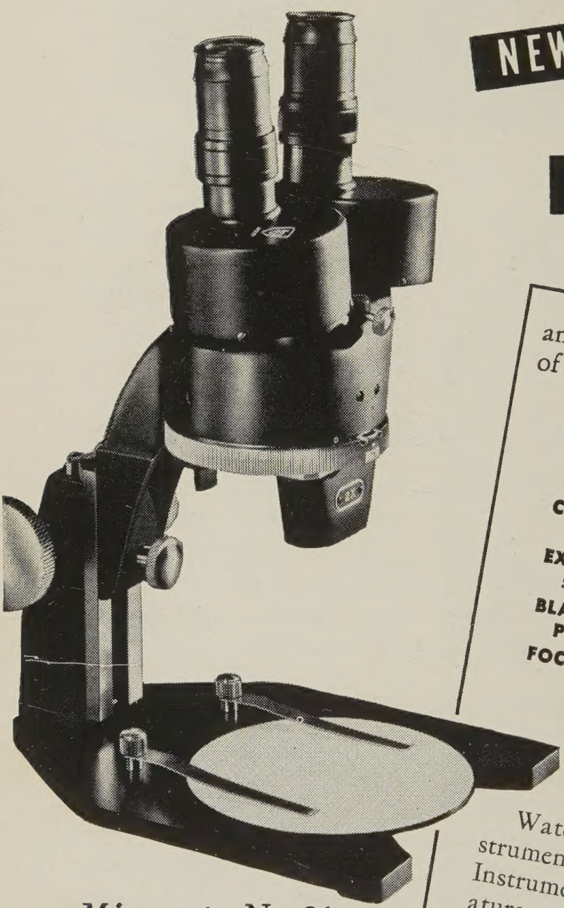

and all of these time-proven features of Spencer Stereoscopic Microscopes:

- **UNUSUALLY WIDE, FLAT FIELDS**
- **ENHANCED STEREOSCOPIC EFFECT** from paired objectives converging at 12°
- **COMFORTABLE VISION** through normal eyetube convergence of 8°
- **EXTENDABLE DOVETAIL BODY SLIDE** supplements focusing mechanism
- **BLACK AND WHITE REVERSIBLE STAGE PLATEN**
- **FOCUSING SLIDEWAYS GROOVED** to retain lubricant
- **DUSTPROOF NOSEPIECES** protect objectives
- **DUSTPROOF GEARING** for interpupillary distance control

Watch for this outstanding instrument. See your AO Scientific Instrument Distributor or for literature write Dept. Y7, American Optical Company, *Scientific Instrument Division*, Buffalo 15, N. Y.

Microscope No. 21

PRICES START AT $194.00

including optics

Model illustrated—No. 21X with 1.0X and 2.0X paired Objectives, 9X paired Wide Field Eyepieces and cabinet—is priced at $254.00.

Makers of Microscopes for over 100 Years

AO

SPENCER

TRANSPARENT SPECIMEN BOXES

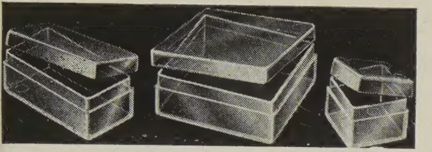

Five Sizes: (Outside Dimensions)

A: 15/16" x 15/16" x 3/4"
B: 1-7/8" x 15/16" x 3/4"
C: 1-7/8" x 1-7/8" x 3/4"
D: 3-1/4" x 2-3/4" x 1-1/4"
E: 6" x 7/8" x 3/4"

Prices:		
A:	**20** for $1;	**100** for $4.60
B:	**15** for $1;	**100** for $5.60
C:	**12** for $1;	**100** for $6.60
D:	**5** for $1;	**100** for $17.50
E:	**6** for $1;	**100** for $16.00

Assortments:

No. 1: 8 **A**, 4 **B**, 4 **C** $1.00
No. 2: 60 **A**, 20 **B**, 16 **C** $5.00
No. 3: 10 each **A**, **B**, **C**, **D**, **E**, $5.50
No. 3A: 20 each **A**, **B**, **C**, **D**, **E** $10.00

Specimen Boxes **A**, **B**, and **C** are furnished in flat, white cardboard trays that hold 100 A's or 50 B's or 25C's. Convenient for keeping the boxes in order.

FOR
STORING, HANDLING and
EXHIBITING SPECIMENS and
SMALL OBJECTS
In Convenient, Orderly
Arrangement

ADVANTAGES

- Keep specimens dust-free
- Contents are completely visible
- Protect fragile specimens from damage by rough handling

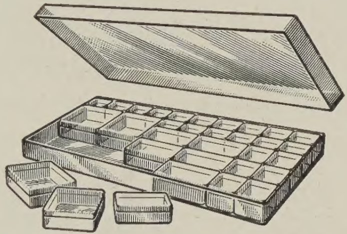

Transparent Boxes in Transparent Cases

For arranging specimens in sets, and for passing the sets around classes or other groups.

Full details on leaflet PB-AM
Write for it

SHILLABER'S

CERTIFIED INDEX OF REFRACTION LIQUIDS

Immersion media for use on the microscope that offer the following **outstanding advantages:**

Range: 1.400 to 1.700—**Intervals:** 0.002 index—**Adjustment:** 0.0002 index (D line, 25° C)
Very inert and non-volatile. Index remains unchanged.

Additional liquids now available in the range 1.71—1.83 Index; Intervals 0.01 Index.
Liquids of higher indices are in preparation.

Just write for latest "Index Data"

DENSITY LIQUIDS FOR THE SINK-AND-FLOAT TEST

For determining the specific gravity of minerals, gems and other substances

Range: 1.50-4.00 Density. **Intervals:** 0.10, or as selected.

Containers designed for convenience in making the tests;
Sets can be assembled in convenient wooden block with cover.

Write for Leaflet 50-D

R. P. CARGILLE

118 LIBERTY STREET, NEW YORK 6, N.Y.

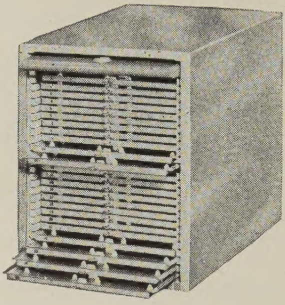

Eberbach

PETROGRAPHIC SLIDE FILING CABINETS

These cabinets provide an expandable filing system. They may be stacked beside or on top of each other as the collection increases. The cabinets hold 750 slides, each of the 25 aluminum trays holding thirty 2″ x 1″ slides. The door disappears, as shown, into the top of the cabinet which measures 10″ high, 8½″ wide by 12″ deep. The cabinets are sturdily constructed of seasoned hardwood which is carefully filled and lacquered to retain the attractive light oak hue. The cabinet carries catalog number 60-664 and sells for $42.50

Eberbach & Son Company
LABORATORY APPARATUS & SUPPLIES
ANN ARBOR, MICH.
ESTABLISHED 1843

Bravais Memoir Now Available In English

A. BRAVAIS, MEMOIR ON THE SYSTEMS FORMED BY POINTS REGULARLY DISTRIBUTED ON A PLANE OR IN SPACE; Journal de l'École, Polytechnique, Cahier 33, Tome XIX, pp. 1-128, 1850. Translated by AMOS J. SHALER, Massachusetts Institute of Technology, 1949. Memoir No. 1 of The Crystallographic Society of America, $3.90 per copy, postpaid.

It is a well known fact that there are fourteen space-lattice types, but very few people know just why there are fourteen. It is in this classical memoir that these results were first developed. Here also, the polar lattice (now known as the "reciprocal lattice") was first presented. In other words, this is *the* source work on lattices. The development of the subject is easy to understand and requires no knowledge of advanced mathematics.

The original is published in French in a journal which is available in only a few of the larger libraries. It has been considered of such importance that it has been translated into other languages. The present publication makes this classic work available, for the first time, to English-speaking crystallographers.

The low price of the book is made possible by the generous financial assistance of several anonymous friends. Remittance ($3.90) must accompany order which should be sent to

WILLIAM PARRISH
c/o Philips Laboratories, Inc.
Irvington-on-Hudson, N.Y., U.S.A.

INDEX MEDIA

LIQUID IMMERSION MEDIA—Original series, colorless, orderless, stable, exact specified indices, range Nd 1.41 to 1.65, steps of .01, in twenty-five 1-ounce applicator vials, with cabinet $27.50

Set of thirty-eight Immersion Media Nd 1.41 to 1.78 in steps of .01, in ⅛ fl. oz. each, applicator vials with cabinet $35.00

J. T. Rooney, Chemist, P.O. Box 358, Buffalo, N.Y.

W. HAROLD TOMLINSON

Petrographic Laboratory

260 N. ROLLING RD., SPRINGFIELD, PA.

ROCK SECTIONS **ORIENTATED MINERAL SECTIONS**

WANTED

The Mineralogical Society of America is in special need of certain issues of *The American Mineralogist* to complete full sets. The Society will pay $1.00 each for the following issues if returned to the Editor in such condition as to make resale possible.

Year 1942	*Year 1943*	*Year 1944*	*Year 1945*
January February	March	January-February	March-April

Also Vol. 1 is desired.

Address: W. F. Hunt, Editor: Mineralogical Laboratory, University of Michigan, Ann Arbor, Michigan.

CRYSTALLOGRAPHY

Specializing in choice crystals, singles, groups, from world wide sources. Catalog free.

V. D. HILL

Complete Gem & Mineral Establishment
Route 7-F, Box 188, Salem, Oregon

The Recently Prepared 200 page Author-Subject
INDEX TO VOLUMES 21-30, 1936-1945, of

THE AMERICAN MINERALOGIST

by
Earl Ingerson, Geophysical Laboratory
and
Michael Fleischer, U.S. Geological Survey

is now available

The price is $2.00 to members and subscribers and $3.00 to non-members. The Treasurer will be glad to receive your order now. Address, Dr. Earl Ingerson, U.S. Geological Survey, Washington 25, D.C.

Two-Circle Goniometer

$1000

(without head)

Developed by Prof. C. W. Wolfe, Boston University

Manufactured and Sold by

LABORATORY ASSOCIATES
60 White Street, Belmont, Mass.

For detailed information write to Laboratory Associates.

MINERAL SPECIMENS

SHORTITE CRYSTALS for crystallography classes. Well formed isolated simple crystals especially well adapted to illustrate orthorhombic pyramidal (hemimorphic) symmetry. The crystals are nearly perfect but not transparent, show the forms (100) (011) (00$\bar{1}$), and vary in size from ¼ to ⅜ inch. Price $3.00 per dozen crystals.

Perfect transparent shortite crystals are available in the ¼ inch size @ $1.00 each or $10.00 per dozen; ⅜ inch @ $1.50 each.

ANDALUSITE. Excellent examples of columnar andalusite from a pegmatite near Sweetwater, Nevada. 1 x 2, 25¢; 2 x 2, 50¢; 2 x 3, 75¢; 3 x 4, $1.50.

ANTLERITE. Northern Lights Mine, Wassuk Range, Nevada. A basic copper sulfate from one of the few established localities for this mineral. The antlerite occurs as friable green crusts on ore. 2 x 2, $1.00; 2 x 3, $1.50; 3 x 4, $3.50.

BINDHEIMITE. Mineral County, Nevada. A lead antimonate as nearly pure, yellow-brown masses. 1 x 1½, 25¢; 2 x 2, 75¢; 2 x 3, $1.00; 3 x 4, $2.50.

CELADONITE. Washoe County, Nevada. Hydrous silicate of iron, magnesium and potassium. Soft earthy masses in cavities of amygdaloid. 1 x 1½, 25¢; 2 x 2, 75¢; 2 x 3, $1.00; 3 x 4, $2.00.

CHALCOPHYLLITE. Majuba Hill, Nevada. An arsenate and sulfate of copper. Light blue hexagonal plates on matrix. 3 x 3½, $5.00; 2 x 3½, $3.00; 1½ x 2½, $2.00; 1 x 1½, $1.00.

CLINOCLASITE. Majuba Hill, Nevada. A hydrous copper arsenate occurring as small beautiful blue crystals. Two specimens showing clinoclasite crystals with zeunerite crystals on quartz porphyry whose phenocrysts are smoky quartz. 1½ x 4¼, $5.00; 1½ x 3, $2.50. One specimen of clinoclasite crystals with olivenite crystals on quartz porphyry, 2¼ x 3½, $2.50.

KALINITE. Esmeralda County, Nevada. An anisotropic potassium alum as columnar, vitreous, pure masses. 1 x 2, 35¢; 2 x 2, 75¢; 2 x 3, $1.00; 3 x 4, $2.50.

LEUCOCHALCITE. Majuba Hill, Nevada. A rare and *white* copper arsenate as fibrous crusts and delicate fibers on matrix. 3 x 3¼, $5.00; 2¼ x 3, $3.50; 1 x 2, $2.50, $2.00, $1.50; 1 x 1, $1.00.

MAGNESIOCHROMITE. Madison County, Montana. Pure black masses. 1 x 2, 20¢; 2 x 2, 35¢; 2 x 3, 50¢; 3 x 4, $1.25.

PALYGORSKITE. La Table, Savoy, France. An interesting hydrous silicate of aluminum and magnesium in sheets somewhat resembling mountain leather. 2 x 3, 75¢; 3 x 4, $1.50.

PICROLITE. Jamestown, California. Excellent, long fibrous examples of this serpentine variety: 1 x 2, 25¢; 1 x 4 and 2 x 2, 50¢; 2 x 3, 75¢; 3 x 5, $2.00.

SPANGOLITE. Majuba Hill, Nevada. A rare sulfate of aluminum and copper. Aggregates of greenish-blue crystals with chalcophyllite and tyrolite on matrix. Two specimens: 2½ x 3, $12.50; 2½ x 2½, $10.00.

THULITE. Yerington, Nevada. Good pink masses of the manganiferous clinoziosite. 1 x 1½, 25¢; 1½ x 2, 50¢; 2 x 3, $1.00; 3 x 4, $2.50.

TRONA. Green River, Wyoming. Very choice cleavages. 1 x 1½, 25¢; 2 x 2, 50¢; 2 x 3, 75¢; 3 x 4, $1.50.

WAPPLERITE. Manhattan, Nevada. A hydrous calcium arsenate as thin white coatings on realgar and orpiment. 1 x 1½, 50¢; 1½ x 2, $1.50; 2 x 3, $3.00; 3 x 4, $6.00.

Sizes approximate in inches. ***Prices F.O.B. Yerington, Nevada***

HATFIELD GOUDEY

Box 529 **Yerington, Nevada**

FINE MINERAL SPECIMENS

KEILHAUITE, Norway. A large, brown, *twin* crystal. Rare and unusual. 1¼ x 2, $7.50.

BARYSILITE, New Jersey. Fine, cream-colored, pearly, foliated on massive yellow axinite. 3 x 4½, $10.00.

INESITE, Sweden. Pink radiating in calcite. 1 x 3, $5.00.

WITHERITE, Illinois. Fine, pseudo-hexagonal twinned crystals, associated with fluorite, calcite and sphalerite. Brilliantly fluorescent. 1 x 1½, $2.00, $2.50 and $3.00; 1½ x 2 x 2, $5.00; 1¾ x 2, $4.00; 2 x 2½, $5.00; 3 x 3 x 2½, $10.00.

YTTERGARNET, Norway. Black modified dodecahedrons in syenite. Slightly radioactive. 2 x 2½ x 1½, $5.00.

SMOKY QUARTZ, Switzerland. Superb pale smoky *twisted* doubly terminated xls, delicately sprinkled with chlorite. An outstanding specimen. 2 x 3 x 4½, $12.50.

URANINITE, Norway. Variety Cleveite. Black massive in matrix with gummite. 1 x 1½, $5.00.

TENGERITE, Norway. Yellowish-white pseudomorphous after hellandite crystal. Rare. ¾ x 1½, $10.00.

All prices F.O.B. Berkeley, California. Approval orders invited.

The above specimens are from the MINERALS UNLIMITED Fine Mineral Lists. If you would like a free copy with many other rare, fine, and unusual specimens listed, *send* for it today.

Among our expected shipments are the following rare and fine minerals from Italy: Metavoltine, Avogadrite, Palmierite, Cossyrite, Rinneite, Zebedassite, Taramellite, Celestite, Melanite, Sulfur, Aragonite, Hessonite, Orthoclase (Baveno twins from the type locality), Hematite and many others.

MINERALS UNLIMITED

1724 University Avenue
Berkeley 3, California

Articles to appear in early issues of The American Mineralogist include the following:

●

The lazulite-scorzalite isomorphous series by W. T. Pecora and J. J. Fahey

Arrojadite, hühnerkobelite and graftonite by Marie Louise Lindberg

On the nature of the opal-like outer layer of coated diamonds by J. F. H. Custers

Three new polymorphs of zinc sulfide by Clifford Frondel and Charles Palache

Occurrence of polymorphous wurtzite in Western Pennsylvania and Eastern Ohio by David M. Seaman and Howard Hamilton

Wherryite, a new mineral from the Mammoth Mine, Arizona by Joseph J. Fahey, E. B. Daggett and Samuel G. Gordon

Age of uraninite from a pegmatite near Singar, Gaya District, India by Arthur Holmes

Composition of veatchite by George Switzer and W. W. Brannock

Thermal study of the potash-soda feldspars by Milton T. Heald

The differential thermal analysis of certain phosphates by Robert L. Manly, Jr.

Phosphate-Allophane in an epidosite from North Carolina by Howard W. Jaffe and Alexander M. Sherwood

The crystal structure of cryptomelane by A. McL. Mathieson and A. D. Wadsley

Cordierite in pegmatite near Micanite, Colorado by E. Wm. Heinrich

SARTORIUS
SPECIFIC GRAVITY BALANCE

NEW IMPROVED MODEL
LITERATURE NOW AVAILABLE

LEITZ

4-CIRCLE UNIVERSAL STAGE
BEREK COMPENSATORS
STEREOGRAPHIC NETS
UM-OBJECTIVES
QUARTZ WEDGES
CM — RESEARCH } Polarizing Microscopes
III M STUDENT }
NOW IN STOCK

STOE

GONIOMETERS
X-RAY GONIOMETER HEADS
PRICES CONSIDERABLY REDUCED

SPENCER

ABBE REFRACTOMETERS
PROMPT DELIVERY

GAMMA SCIENTIFIC COMPANY
261-263 GREAT NECK RD.
GREAT NECK, N. Y.

THE AMERICAN MINERALOGIST
JOURNAL OF THE MINERALOGICAL SOCIETY OF AMERICA

Vol. 34 NOVEMBER-DECEMBER, 1949 Nos. 11 and 12

FOURIER SUMMATIONS FOR SYMMETRICAL CRYSTALS

M. J. BUERGER,
Massachusetts Institute of Technology, Cambridge, Massachusetts.

ABSTRACT

This paper is concerned with the application of symmetry principles to the reduction of terms in Fourier synthesis. For this purpose two theorems are first given, the reciprocal symmetry theorem and the additivity theorem. To illustrate the use of these in performing summations for symmetrical crystals, the form of the electron density function is derived for Fourier syntheses of projections corresponding to the 17 plane groups. The extension of the method to three-dimensional syntheses is also discussed in sufficient detail so that it can be applied to any space group.

INTRODUCTION

In performing Fourier summations, it appears to be a common practice to disregard the symmetry of the crystal and fit the summation into the classical case of centrosymmetry [1] if possible, otherwise into the nonsymmetrical case. Failure to make use of the symmetry of the crystal requires the summation to be made for a great number of unnecessary terms, and thus increases the labor of performing the summation. It also produces a summation in which the errors accumulate in an unsymmetrical way. When symmetry-equivalent segments are selected from such a synthesis, their edges usually do not match, and in order to make the segments fit together, an adjustment of the values in the neighborhood of the edges is necessary.

In this paper, some general devices for utilizing symmetry in performing the summation for symmetrical crystals are discussed. Specific forms for the Fourier summations for the symmetries of the various projections are derived, and the extension of the methods to three-dimensional summations is outlined.

GENERAL FORM OF THE FOURIER SUMMATION

The Fourier summation for electron density has the following form:

$$\rho(xyz) = \frac{1}{V} \sum_{h} \sum_{k=-\infty}^{\infty} \sum_{l} F_{hkl} e^{-2\pi i(hx+ky+lz)}. \quad (1)$$

Since this form involves phases, it is convenient for computational purposes to recast it in such a way that the real and imaginary parts are separated. The decomposition of the complex terms into real and imaginary components is as follows:

$$F_{hkl} = A_{hkl} + iB_{hkl} \tag{2}$$

$$e^{-i\phi} = \cos\phi - i\sin\phi. \tag{3}$$

Making this substitution in (1), it becomes

$$\rho(xyz) = \frac{1}{V}\sum_h \sum_{k\atop -\infty}^{\infty} \sum_l \left\{A_{hkl} + iB_{hkl}\right\}\left\{\cos 2\pi(hx+ky+lz) - i\sin 2\pi(hx+ky+lz)\right\}. \tag{4}$$

$$\begin{aligned} &= \frac{1}{V}\sum_h \sum_{k\atop -\infty}^{\infty} \sum_l A_{hkl}\cos 2\pi(hx+ky+lz) \\ &\qquad - iA_{hkl}\sin 2\pi(hx+ky+lz) \\ &\qquad + iB_{hkl}\cos 2\pi(hx+ky+lz) \\ &\qquad - i^2B_{hkl}\sin 2\pi(hx+ky+lz). \end{aligned} \tag{5}$$

This summation is made over all indices from $-\infty$ to ∞. If reflections *hkl* and $\overline{hkl}$ are considered in pairs, then Friedel's law can be applied to the members of the pairs. Friedel's law can be stated in the following form:

$$\begin{aligned} F_{\overline{hkl}} &= A_{\overline{hkl}} + iB_{\overline{hkl}} \\ F_{\overline{hkl}} &= A_{hkl} - iB_{hkl}. \end{aligned} \tag{6}$$

From this statement of the law it is obvious that

$$\begin{aligned} A_{hkl} &= A_{\overline{hkl}} \\ B_{hkl} &= -B_{\overline{hkl}}. \end{aligned} \tag{7}$$

Furthermore, for pairs of reflections *hkl* and $\overline{hkl}$, the following relations hold in the trigonometric parts of (5):

$$\begin{aligned} \cos 2\pi(hx+ky+lz) &= \cos 2\pi(\bar{h}x+\bar{k}y+\bar{l}z) \\ \sin 2\pi(hx+ky+lz) &= -\sin 2\pi(\bar{h}x+\bar{k}y+\bar{l}z). \end{aligned} \tag{8}$$

In (5), the second line involves the sine, and according to (8) every term in the summation for a particular *hkl* is exactly cancelled by a similar term for the corresponding $\overline{hkl}$. Similarly, the third line involves a *B*, and according to (7) every term in the summation for a particular *hkl* is exactly cancelled by a similar term for the corresponding $\overline{hkl}$. The last line does not cancel for *hkl* and $\overline{hkl}$, because two sign changes are involved in the relation between *hkl* and $\overline{hkl}$.

These considerations leave a comparatively simple form for Fourier summation in terms of the real and imaginary components:

$$\rho(xyz) = \frac{1}{V}\sum_h \sum_{k\atop -\infty}^{\infty} \sum_l A_{hkl}\cos 2\pi(hx+ky+lz) + B_{hkl}\sin 2\pi(hx+ky+lz). \tag{9}$$

Basic Principles for Combination

Introduction. In performing a Fourier summation, it should be possible to limit the actual summation to a representative section of the data and then derive the rest of the summation by principles of symmetry. This derivation, or combination, can be carried on either in reciprocal space or in direct space. If it is carried out in reciprocal space, it is necessary to know the effect of crystal symmetry in reciprocal space. If it is carried out in direct space, it is necessary to know how to make the combination. For these two situations, the following two theorems, respectively, are very useful and are stated without proof [5].

Theorem of Reciprocal Symmetry. *The symmetry of reciprocal space is the same as the isomorphous point-group symmetry of direct space, except that every symmetry element containing the origin produces a phase change in its equivalent space fields of* $e^{2\pi ih/n}$. Here a/n is the translation component of the symmetry operation. Note that the phase shift becomes zero for $n=0$, i.e., for pure reflections and pure rotations.

This theorem makes it unnecessary to derive phase relations between F's by the tedious method of using structure factors [2]. All possible relations for any given space group can be written down by inspection with the aid of the theorem.

Theorem of Additivity. It is convenient to regard the process of Fourier synthesis as a transformation from a space to its reciprocal. For combinations occurring in the new space, the theorem of additivity can be employed. In the present application, the transformation is from reciprocal space to direct space. The following theorem, of course, is valid for either direction of transformation:

The transform of a sum is the sum of the transforms, i.e.,

$$T_{xyz}(M+N) = T_{xyz}(M) + T_{xyz}(N). \tag{10}$$

In the present problem, this can be applied in the following way: If reciprocal space is divided into blocks in any desired way, and if the synthesis is carried out for each block, the complete synthesis is equal to the sum of the separate syntheses of the blocks. In particular, each block of reciprocal space may be one of the unsymmetrical fields related by the several symmetry elements. Actually, since all fields are the same except for orientation, the synthesis need be carried on for only one field. If the resulting transform for this single field is then displaced in accordance with the requirements of the operations of crystal symmetry, and the several results at xyz added, the sum is the complete transform at xyz. An equivalent way of performing the final summation is to start with the transform of a single data field, then add together the value of the transform at xyz and all symmetry-equivalent points, recording the sum at xyz.

This scheme provides a perfectly general way of performing the Fourier synthesis for a symmetrical crystal. If it is pursued blindly, however, it sometimes involves unnecessary labor because in the process of combining, some of the components of symmetrically related fields cancel. For this reason, it is important to first study the consequences of the first theorem, which often reveals the manner in which certain components of the unsymmetrical fields cancel when combined in symmetrical manners.

Additional Aids to Synthesis. By the aid of the two theorems just mentioned, the appropriate form of the synthesis for any plane group or space group can be written down by inspection. If this is to be done in a systematic way for a large number of groups, extensive use may be made of generating operations. Thus, in deriving space groups, a group may be derived from any of its subgroups by adding a generating operation to the subgroup. Similarly, in reciprocal space, a symmetry combination can be derived from a subgroup symmetry by adding a generating operation. This involves an additional phase relation. Therefore, the form for symmetrical Fourier synthesis may be derived from the form appropriate to a subgroup by imposing upon it the appropriate additional phase relationship of the added generating operation.

When the symmetry operations of the crystal transform each axis into itself, then it is also possible to make the form of the synthesis more compact by making use of the symmetrical properties of the trigonometric functions for positive and negative indices with respect to the same axes. For brevity this property is called "interchange symmetry." This kind of compaction is not possible when the symmetry operation does not cause this particular type of transformation. It does not occur, therefore, for trigonal or hexagonal crystals, nor for diagonal reflections.

SYMMETRICAL SYNTHESES FOR THE PLANE PROJECTIONS

Introduction. Since the most common Fourier synthesis is probably the plane projection, the derivation of symmetrical syntheses will be illustrated by deriving the appropriate forms of the summations for plane projections of the several possible plane symmetries. The form of the summation corresponding to the electron density projected on a plane normal to some rational axis is the two-dimensional equivalent of (9). For clearness, suppose specifically that the electron density is desired as projected on a plane normal to the c axis. The form of the summation is then

$$\rho(xy) = \frac{1}{S} \sum_{h}\sum_{k}{}_{-\infty}^{\infty} A_{hk0} \cos 2\pi(hx + ky) + B_{hk0} \sin 2\pi(hx + ky). \qquad (11)$$

Here S is the area of the section of the cell perpendicular to the direction of the projection, in this case normal to the c axis.

To recast this in a form more convenient for computational procedures, the trigonometric functions of sums of angles are expressed as products, as first suggested by Beevers and Lipson [3] by the use of the identities

$$\begin{aligned}\cos(\alpha+\beta) &= \cos\alpha\cos\beta - \sin\alpha\sin\beta\\ \sin(\alpha+\beta) &= \sin\alpha\cos\beta + \cos\alpha\sin\beta.\end{aligned}\qquad(12)$$

Making these substitutions in (11) it takes the form

$$\begin{aligned}\rho(xy) = \frac{1}{S}\sum_h\sum_k{}_{-\infty}^{\infty}\, & A_{hk0}\cos 2\pi hx\cos 2\pi ky\\ & - A_{hk0}\sin 2\pi hx\sin 2\pi ky\\ & + B_{hk0}\sin 2\pi hx\cos 2\pi ky\\ & + B_{hk0}\cos 2\pi hx\sin 2\pi ky.\end{aligned}\qquad(13)$$

Symmetry $p1$. Friedel's law provides the relation between the phases of any two halves of reciprocal space. For symmetry $p1$, therefore, reciprocal space may be divided into any two halves and the Fourier summation may be expressed in terms of either one. Furthermore, since the symmetry operation 1 transforms each axis into itself, there is a second relation between the indices with respect to positive and negative ends of the same axis which arises due to the symmetrical properties of the trigonometric functions. To take advantage of these two symmetries, divide reciprocal space into four segments along the reciprocal axes. The four segments now contain F's having indices $hk0$, $\bar{h}k0$, $\overline{hk}0$, and $h\bar{k}0$, respectively. Now, the summation (13) extends over all reciprocal space. It can be rewritten in terms of the summations over these four segments of reciprocal space. In doing this a precaution should be observed: the division lines of the reciprocal space into four segments occur through the lines $h00$, $0k0$, $\bar{h}00$, and $0\bar{k}0$. Each of these lines, therefore, belong to its two adjoining sectors equally, while the origin point belongs to all four segments. The lines $h00$, $0k0$, $\bar{h}00$, and $0\bar{k}0$ should be counted only at half value for each segment, and the origin point only at quarter value. The special nature of the multiplicity of the edges and point of each segment is indicated by adding a prime to the summation, thus: $\sum'$. With this convention, the expansion of (12) into separate summations for each of the four sectors is

$$) = \frac{1}{S}\sum_h{}'\sum_k{}'_{0}^{\infty}$$

$$\begin{aligned}&{}_{hk0}\cos 2\pi hx\cos 2\pi ky + A_{hk0}\cos 2\pi\bar{h}x\cos 2\pi ky + A_{h\bar{k}0}\cos 2\pi\bar{h}x\cos 2\pi\bar{k}y + A_{h\bar{k}0}\cos 2\pi hx\cos 2\pi\bar{k}y\\ &{}_{hk0}\sin 2\pi hx\sin 2\pi ky - A_{hk0}\sin 2\pi\bar{h}x\sin 2\pi ky - A_{h\bar{k}0}\sin 2\pi\bar{h}x\sin 2\pi\bar{k}y - A_{hk0}\sin 2\pi hx\sin 2\pi\bar{k}y\\ &{}_{hk0}\sin 2\pi hx\cos 2\pi ky + B_{\bar{h}k0}\sin 2\pi\bar{h}x\cos 2\pi ky + B_{hk0}\sin 2\pi\bar{h}x\cos 2\pi\bar{k}y + B_{h\bar{k}0}\sin 2\pi hx\cos 2\pi\bar{k}y\\ &{}_{hk0}\cos 2\pi hx\sin 2\pi ky + B_{\bar{h}k0}\cos 2\pi\bar{h}x\sin 2\pi ky + B_{\bar{h}\bar{k}0}\cos 2\pi\bar{h}x\sin 2\pi\bar{k}y + B_{hk0}\cos 2\pi hx\sin 2\pi\bar{k}y.\end{aligned}\qquad(14)$$

Friedel's law provides symmetry relations between alternate columns. According to (7) the A's of alternate columns have the same sign, but the B's have opposite signs. Furthermore, the cosines in alternate columns are equal and have the same signs, while the sines are equal but with opposite signs. Note, now, that alternate columns are related by zero or two sign changes in the trigonometric functions if the coefficient is an A, whereas if the coefficient is a B, they are related by one sign change in the trigonometric part. Since B also contributes a sign change according to (7), alternate columns are related by an even number of sign changes, and are, therefore, identical. As a consequence, (14) can be more compactly expressed as twice the sum of the first two columns, namely

$$\begin{aligned}\rho(xy) = \frac{2}{S}\sum_{h}{}'^{\infty}_{-\infty}\sum_{k}{}' A_{hk0}\cos 2\pi hx\cos 2\pi ky &+ A_{\bar{h}k0}\cos 2\pi\bar{h}x\cos 2\pi ky\\ - A_{hk0}\sin 2\pi hx\sin 2\pi ky &- A_{\bar{h}k0}\sin 2\pi\bar{h}x\sin 2\pi ky\\ + B_{hk0}\sin 2\pi hx\cos 2\pi ky &+ B_{\bar{h}k0}\sin 2\pi\bar{h}x\cos 2\pi ky\\ + B_{hk0}\cos 2\pi hx\sin 2\pi ky &+ B_{\bar{h}k0}\cos 2\pi\bar{h}x\sin 2\pi ky.\end{aligned} \tag{15}$$

The reduction of terms just discussed makes use of Friedel symmetry only. Interchange symmetry is also present in $p1$. To take advantage of this, express $\cos 2\pi\bar{h}x$ as $\cos 2\pi hx$ and express $\sin 2\pi\bar{h}x$ as $-\sin 2\pi hx$. This expresses (15) in terms of functions of positive angles only:

$$\begin{aligned}\rho(xy) = \frac{2}{S}\sum_{h}{}'^{\infty}_{0}\sum_{k}{}' A_{hk0}\cos 2\pi hx\cos 2\pi ky &+ A_{\bar{h}k0}\cos 2\pi hx\cos 2\pi ky\\ - A_{hk0}\sin 2\pi hx\sin 2\pi ky &- A_{\bar{h}k0}(-\sin 2\pi hx)\sin 2\pi ky\\ + B_{hk0}\sin 2\pi hx\cos 2\pi ky &+ B_{hk0}(-\sin 2\pi hx)\cos 2\pi ky\\ + B_{hk0}\cos 2\pi hx\sin 2\pi ky &+ B_{\bar{h}k0}\cos 2\pi hx\sin 2\pi ky.\end{aligned} \tag{16}$$

Interchange symmetry provides no relations among A's or among B's. Therefore, although the first and second columns have similar trigonometric forms, they have different coefficients. Nevertheless, a more compact expression, which represents a great reduction in the labor of the synthesis, can be had by combining the trigonometric parts as follows:

$$\begin{aligned}\rho(xy) = \frac{2}{S}\sum_{h}{}'^{\infty}\sum_{k}{}' (A_{hk0} + A_{\bar{h}k0})&\cos 2\pi hx\cos 2\pi ky\\ - (A_{hk0} - A_{\bar{h}k0})&\sin 2\pi hx\sin 2\pi ky\\ + (B_{hk0} - B_{\bar{h}k0})&\sin 2\pi hx\cos 2\pi ky\\ + (B_{hk0} + B_{\bar{h}k0})&\cos 2\pi hx\sin 2\pi ky.\end{aligned} \tag{17}$$

Symmetry $p2$. Symmetry* $p2$ may be derived from symmetry $p1$ by adding to it the generating operation 2. According to the reciprocal symmetry theorem, this operation causes the symmetry

$$\begin{aligned} F_{hk0} &= F_{\bar{h}\bar{k}0} \\ \therefore \quad A_{hk0} + iB_{hk0} &= A_{hk0} - iB_{hk0}, \\ \therefore \quad B_{hk0} &= B_{\bar{h}\bar{k}0} = 0, \\ \text{and} \quad A_{hk0} &= F_{hk0}. \end{aligned} \tag{18}$$

Evidently the appropriate form of the symmetrical summation for symmetry $p2$ can be derived from that of symmetry $p1$ by applying the last two conditions of (18) to (17). This provides the following form for $p2$:

$$\begin{aligned} \rho(xy) = \frac{2}{S} \sum_{h}{}'^{\,\infty}_{\,0} \sum_{k}{}' (F_{hk0} + F_{\bar{h}k0}) \cos 2\pi hx \cos 2\pi ky \\ - (F_{hk0} - F_{\bar{h}k0}) \sin 2\pi hx \sin 2\pi ky. \end{aligned} \tag{19}$$

This is equivalent to the classical form of Beevers and Lipson [1] for projections with centro-symmetry.

Symmetries $pm1$ and $cm1$. Both of the symmetries $pm1$ and $cm1$ have identical symmetries in reciprocal space; these plane groups differ only in the locations of points where the value of the transform does not vanish. These symmetries can be derived from symmetries $p1$ and $c1$, respectively, by the addition of the generating operation m parallel to b. According to the reciprocal symmetry theorem, this imposes the additional relation

$$\begin{aligned} F_{hk0} &= F_{\bar{h}k0}, \\ \therefore \quad A_{hk0} &= A_{\bar{h}k0}, \\ \text{and} \quad B_{hk0} &= B_{\bar{h}k0}. \end{aligned} \tag{20}$$

Under these conditions, the second and third rows of (17) vanish, leaving the simpler form

---

* The nomenclature of the plane groups used here differs somewhat from that given inside the covers of the writer's book *X-Ray Crystallography*. The correspondence table is as follows:

This paper	X. R. C.	This paper	X. R. C.
$p1$	$P1$	$p3$	$C3$
$pm1$	Pl	$p3m1$	$C3l1$
$pg1$	Pb	$p31m$	$C31l$
$cm1$	Cl	$p4$	$P4$
$p2$	$P2$	$p4mm$	$P4ll$
$p2mm$	Pll	$p4gg$ (origin on 4)	$P4bl$
$p2gg$	Pba	$p6$	$P6$
$p2gm$	Pbl	$p6mm$	$C6ll$
$c2mm$	Cll		

$$\rho(xy) = \frac{4}{S} \sum_{h}{}' \overset{\infty}{\underset{0}{}} \sum_{k}{}' \quad A_{hk0} \cos 2\pi hx \cos 2\pi ky$$

$$+ \quad B_{hk0} \cos 2\pi hx \sin 2\pi ky \tag{21}$$

$$= \frac{4}{S} \sum_{h}{}' \left[\sum_{k}{}'^{\infty}_{0} A_{hk0} \cos 2\pi kx + B_{hk0} \sin 2\pi ky \right] \cos 2\pi hx. \tag{22}$$

The latter form implies a considerable saving in labor. It indicates that for each available value of h, a summation over k can be made for h constant. This first summation requires both a cosine and a sine summation. But once this preliminary summation is complete, the resulting coefficient requires only a cosine summation over the available values of h.

Symmetry $pg1$. Symmetry $pg1$ can be derived from $p1$ by the addition of a generating operation g parallel to b. According to the reciprocal symmetry theorem, this symmetry element gives rise to the additional relation

$$F_{hk0} = e^{2\pi ik/2} F_{\bar{h}k0}. \tag{23}$$

Therefore, the reflections can be grouped into two classes:

$$\begin{aligned} &\text{for } k \text{ even:} \quad F_{hk0} = F_{\bar{h}k0} \\ &\text{for } k \text{ odd:} \quad F_{hk0} = -F_{\bar{h}k0}. \end{aligned} \tag{24}$$

This circumstance requires the summation to be split into two summations, one with k even and the other with k odd. For k even, the conditions are exactly the same as in the last section, and consequently (22) holds for this half of the summation. For k odd, substitution of the real and imaginary parts of the second half of (24) into (17) causes the first and last rows to vanish, leaving

$$\underset{k \text{ odd}}{\rho(xy)} = \frac{4}{S} \sum_{h}{}' \overset{\infty}{\underset{0}{}} \sum_{k}{}' - A_{hk0} \sin 2\pi hx \sin 2\pi ky$$

$$+ B_{hk0} \sin 2\pi hx \cos 2\pi ky$$

$$= \frac{4}{S} \sum_{\substack{h \\ 0}}{}' \left[\sum_{\substack{k \\ 0}}{}'^{\infty} - A_{hk0} \sin 2\pi ky + B_{hk0} \cos 2\pi ky \right] \sin 2\pi hx. \tag{25}$$

The entire summation includes summation over both k even and k odd, namely an expression like (22) for k even, plus (25) for k odd. The complete form is

$$\rho(xy) = \frac{4}{S} \sum_{\substack{0 \\ h}}^{\infty}{}' \left[\sum_{\substack{0 \\ k \text{ even}}}^{\infty}{}' A_{hk0} \cos 2\pi ky + B_{hk0} \sin 2\pi ky \right] \cos 2\pi hx$$

$$- \left[\sum_{\substack{0 \\ k \text{ odd}}}^{\infty}{}' A_{hk0} \sin 2\pi ky - B_{hk0} \cos 2\pi ky \right] \sin 2\pi hx. \tag{26}$$

This form looks somewhat formidable, but by appropriate selection of masks for the Patterson-Tunell method [4], or Beevers-Lipson method [1], it is no more difficult than (22). It merely requires different treatment of even and odd terms.

For computations of projections having this symmetry, the preferred form of the summation is (26). For the subsequent derivation of $p2gg$, however, it is desirable to have the origin of the plane group chosen halfway between neighboring glide-lines, the glides remaining parallel to b. It can be easily shown [5] that a change of origin of a reflection parallel to b by amount a/m produces a phase change of $e^{2\pi i 2h/m}$. For the new origin shifted $a/4$ from the first origin, (23) is, therefore, replaced by

$$\begin{aligned} F_{hk0} &= e^{2\pi ih/2}\, e^{2\pi ik/2}\, F_{\bar{h}k0} \\ &= e^{2\pi i(h+k)/2}\, F_{hk0}. \end{aligned} \tag{27}$$

By imposing this condition on (17) in exactly the same way it was done for the first origin, the following form of the synthesis results:

$$\begin{aligned} \rho(xy) = \frac{4}{S}\Bigg\{ & \underset{\substack{h \\ h+k \text{ even}}}{\sum_{0}^{\infty}}{}' \left[\underset{k}{\sum_{0}^{\infty}}{}' A_{hk0}\cos 2\pi ky + B_{hk0}\sin 2\pi ky \right] \cos 2\pi hx \\ & - \underset{\substack{h \\ h+k \text{ odd}}}{\sum_{0}^{\infty}}{}' \left[\underset{k}{\sum_{0}^{\infty}}{}' A_{hk0}\sin 2\pi ky - B_{hk0}\cos 2\pi ky \right] \sin 2\pi hx. \Bigg\} \end{aligned} \tag{28}$$

Symmetries $p2mm$ and $c2mm$. These symmetries have subgroups $p2$ and $pm1$, or $c2$ and $cm1$, respectively. They can, therefore, be derived from the first subgroup by adding m parallel to b, or from the second by adding the operation 2. Either derivation may be used to find the appropriate form of the Fourier summation. In the first derivation, conditions (20) are imposed on (19), which causes the vanishing of the second line; in the second derivation, conditions (18) are imposed on (22), which causes the B parts to vanish. By either route, the Fourier summation reduces to the very simple form

$$\rho(xy) = \frac{4}{S} \underset{0}{\overset{\infty}{\sum_{h}{}' \sum_{k}{}'}} F_{hk0}\cos 2\pi hx \cos 2\pi ky. \tag{29}$$

Symmetry $p2gm$. This symmetry can be derived from its subgroup $pg1$ by adding the generating operation 2. This imposes conditions (18) on (26), causing the B terms to vanish. The summation then assumes the simpler form

$$\begin{aligned} \rho(xy) = \frac{4}{S}\Bigg\{ & \underset{0}{\overset{\infty}{\sum_{h}{}' \sum_{k \text{ even}}{}'}} F_{hk0}\cos 2\pi hx \cos 2\pi ky \\ & - \underset{0}{\overset{\infty}{\sum_{h}{}' \sum_{k \text{ odd}}{}'}} F_{hk0}\sin 2\pi hx \sin 2\pi ky \Bigg\}. \end{aligned} \tag{30}$$

Symmetry *p2gg*. If the origin of this group is placed at a 2-fold rotor, with glide lines parallel to a and b, the glides are located at $a/4$ and $b/4$. A subgroup of this is $pg1$. The form of the Fourier summation for this subgroup with the glide line removed from the origin by an amount $a/4$ was given in (28). The appropriate form for $p2gg$ can be derived from (28) by imposing the conditions of the generating operation 2 on (28). These conditions are given in (18). They cause the B terms in (28) to vanish, leaving the simpler form

$$\rho(xy) = \frac{4}{S}\left\{ \underset{h+k \text{ even}}{\sum_{h}{}'\,{}^{\infty}_{0}\sum_{k}{}'} F_{hk0} \cos 2\pi hx \cos 2\pi ky \right.$$

$$\left. - \underset{h+k \text{ odd}}{\sum_{h}{}'\,{}^{\infty}_{0}\sum_{k}{}'} F_{hk0} \sin 2\pi hx \sin 2\pi ky \right\}. \tag{31}$$

Symmetry *p4*. According to the reciprocal symmetry theorem, the reciprocal to a crystal of symmetry $p4$ also has 4-fold symmetry. Therefore, the following relations hold

$$F_{hk0} = F_{\bar{k}h0} = F_{\bar{h}\bar{k}0} = F_{k\bar{h}0}. \tag{32}$$

Since alternate terms of (32) correspond to symmetry 2, conditions (18) can be imposed at once on the general form of the Fourier summation (13) causing the last two lines involving B components to vanish. The summation then involves only A components, but the summation limits extend over all reciprocal space. To take advantage of the 4-fold symmetry, reciprocal space is divided along the h and k axes into four equivalent parts and the entire summation split into four summations, one for each of these quadrants. The summation then has a somewhat similar form to (14), but with the B terms eliminated and A's replaced by the first two coefficients of (32). Using the arguments outlined following equation (14), the summations of opposite quadrants can be added, giving a form somewhat similar to (15), specifically

$$\rho(xy) = \frac{2}{S} \sum_{h}{}'\,{}^{\infty}\sum_{k}{}' F_{hk0} \cos 2\pi hx \cos 2\pi ky + F_{\bar{k}h0} \cos 2\pi \bar{k}x \cos 2\pi hy$$

$$- F_{hk0} \sin 2\pi hx \sin 2\pi ky - F_{\bar{k}h0} \sin 2\pi \bar{k}x \sin 2\pi hy. \tag{33}$$

All the F's in this summation are equal, according to (32). The trigonometric functions can also be changed into functions of positive angles, as follows:

$$\rho(xy) = \frac{2}{S} \sum_{h}{}'\,{}^{\infty}_{0}\sum_{k}{}' F_{hk0} \cos 2\pi hx \cos 2\pi ky + F_{hk0} \cos 2\pi kx \cos 2\pi hy$$

$$- F_{hk0} \sin 2\pi hx \sin 2\pi ky + F_{hk0} \sin 2\pi kx \sin 2\pi ky. \tag{34}$$

The summation is now expressed in terms of the positive quadrant of reciprocal space. Because of the equivalence of the a_1 and a_2 axes, it is possible to reduce the number of terms in this summation still further. To accomplish this, each column of (34) is split into two columns, one for each half-quadrant. The two halves of the quadrant are related by interchange of h and k indices. The limits of the original summation were from 0 to ∞, but with the split summation, the lower limit becomes the diagonal (labelled D) of the positive quadrant. This effectively reduces the number of terms in the summation by half. Let this summation be represented by $\sum_{D}^{\infty}{}'$. Then the Fourier expression is

$$) = \frac{2}{S} \sum_{h}{}' \sum_{D}^{\infty} \sum_{k}{}'$$

$$_{hk0} \cos 2\pi hx \cos 2\pi ky + F_{kh0} \cos 2\pi kx \cos 2\pi hy + F_{hk0} \cos 2\pi kx \cos 2\pi hy + F_{kh0} \cos 2\pi hx \cos 2\pi ky$$
$$_{hk0} \sin 2\pi hx \sin 2\pi ky - F_{kh0} \sin 2\pi kx \sin 2\pi hy + F_{hk0} \sin 2\pi kx \sin 2\pi hy + F_{kh0} \sin 2\pi hx \sin 2\pi ky. \quad (35)$$

It will be observed that, although the F's are of two kinds, the trigonometric parts of columns 1 and 4 are the same, and that the trigonometric parts of columns 2 and 3 are the same. The summation can, therefore, be more compactly expressed as

$$\rho(xy) = \frac{2}{S} \sum_{h}{}' \sum_{D}^{\infty} \sum_{k}{}' (F_{hk0} + F_{kh0}) \cos 2\pi hx \cos 2\pi ky + (F_{hk0} + F_{kh0}) \cos 2\pi hy \cos 2\pi kx$$
$$- (F_{hk0} - F_{kh0}) \sin 2\pi hx \sin 2\pi ky + (F_{hk0} - F_{kh0}) \sin 2\pi hy \sin 2\pi kx. \quad (36)$$

The form of (36) looks rather formidable. Actually the summation is easy to perform. Since the parts of first and second columns are identical except for interchange of x and y, (and the sign of the second row) only the summations of the first column need be performed. The summations of the second column can then be derived from them by interchanging the axes of x and y. The entire summation consists of adding the results of the two summations and recording them at coordinates xy.

Symmetry $p4mm$. Plane group $p4mm$ can be derived from $p4$ by the addition of the generating operation m parallel to a diagonal and through the origin. According to the reciprocal symmetry theorem, this entails the condition

$$F_{hk0} = F_{kh0}. \quad (37)$$

If this is applied to (36), it causes the sine terms to vanish, leaving only

$$\rho(xy) = \frac{4}{S} \sum_{h}{}' \sum_{D}^{\infty} \sum_{k}{}' F_{hk0} \cos 2\pi hx \cos 2\pi ky + F_{hk0} \cos 2\pi hy \cos 2\pi kx. \quad (38)$$

To perform the summation, only the first term need be summed. The second term is derived from it by interchange of x and y. The entire summation is the sum of these two summations.

Symmetry $p4gg$. Plane group $p4gg$ can be derived from $p4$ by the addition of glide through the origin and diagonal to the axes. The glide component is $a/2+b/2$. According to the reciprocal symmetry theorem, this gives rise to the reciprocal symmetry

$$F_{hk0} = e^{2\pi i(h+k)/2}F_{kh0}. \tag{39}$$

There are, therefore, two classes of reflections:

$$\begin{aligned} &\text{for } h+k \text{ even:} \quad F_{hk0} = F_{kh0} \\ &\text{for } h+k \text{ odd:} \quad F_{hk0} = -F_{kh0}. \end{aligned} \tag{40}$$

For the first class of reflections, the second line of (36) vanishes, and for the second class of reflections, the first line vanishes. Therefore, the entire summation for $p4gg$ is

$$\begin{aligned} \rho(xy) = \frac{4}{S}\Bigg\{ &\underset{\substack{D\\ h+k \text{ even}}}{\sum_{h}{}'\overset{\infty}{\,}\sum_{k}{}'} F_{hk0}\cos 2\pi hx \cos 2\pi ky + F_{hk0}\cos 2\pi hy \cos 2\pi kx \\ &+ \underset{\substack{D\\ h+k \text{ odd}}}{\sum_{h}{}'\overset{\infty}{\,}\sum_{k}{}'} - F_{hk0}\sin 2\pi hx \sin 2\pi ky + F_{hk0}\sin 2\pi hy \sin 2\pi kx \Bigg\}. \end{aligned} \tag{41}$$

As before, Fourier summations need be made only for the parts of the first column of (41). The summations of the second column are derived from the first by interchanging the axes of x and y. The summation is completed by adding together the separate summations.

Symmetry $p3$. The symmetry of trigonal crystals is best displayed by choosing axes a_1, a_2, and a_3 at 120° intervals. With respect to these axes the indices are h, k, and i, such that $h+k+i=0$. According to the reciprocal symmetry theorem, the relations between F's is

$$F_{hk0} = F_{ki0} = F_{ih0}. \tag{42}$$

According to the additivity theorem, the Fourier synthesis can be written as the sum of three syntheses, one for each of the symmetrically equivalent sectors of the trigonally symmetrical reciprocal structure. Since each sector is nonsymmetrical, the summation for a sector has the form of (13) but with summation limits 0 to ∞. The entire summation is

$$\begin{aligned} \rho(xy) = \frac{1}{S}\underset{0}{\sum_{h}{}'\overset{\infty}{\,}\sum_{k}{}'} \\ &A_{hk0}\cos 2\pi hx \cos 2\pi ky + A_{ki0}\cos 2\pi kx \cos 2\pi iy + A_{ih0}\cos 2\pi ix \cos 2\pi hy \\ &- A_{hk0}\sin 2\pi hx \sin 2\pi ky - A_{ki0}\sin 2\pi kx \sin 2\pi iy - A_{ih0}\sin 2\pi ix \sin 2\pi hy \\ &+ B_{hk0}\sin 2\pi hx \cos 2\pi ky + B_{ki0}\sin 2\pi kx \cos 2\pi iy + B_{ih0}\sin 2\pi ix \cos 2\pi hy \\ &+ B_{hk0}\cos 2\pi hx \sin 2\pi ky + B_{ki0}\cos 2\pi kx \sin 2\pi iy + B_{ih0}\cos 2\pi ix \sin 2\pi hy. \end{aligned} \tag{43}$$

The symmetry of this summation is not appropriate for utilizing interchange symmetry of the trigonometric parts, so (43) is the final form of the summation for trigonal crystals. It has a formidable appearance. Actually, however, only the summation represented by the first column need be carried out. The summations represented by the other two columns are identical with that of the first column except for rotation of axes by 120° and 240° respectively. To perform the summation represented by (43), therefore, it is only necessary to make a Fourier summation of the first column, then add values for symmetrically equivalent points, recording the sum of the values at xy.

Symmetry $p31m$. Plane group $p31m$ can be derived from $p3$ by the addition of a symmetry line diagonally between the axes. According to the reciprocal symmetry theorem, this causes the additional relation

$$F_{hk0} = F_{kh0}. \tag{44}$$

To take advantage of this in reducing the number of terms involved in the summation, reciprocal space is divided into the three sectors of the summation (43), then each sector is divided into two segments along the diagonal. The appearance of the summation is twice as large as (43), since each column has a corresponding column with interchanged indices. The summation has a formidable appearance. Actually, the Fourier part of the summation need be performed on only one of these six columns. The final part of the summation consists of recording at coordinate xy, the sum of the results for this one summation which appear at the six sets of coordinates related to xy by the symmetry of the projection, namely $31m$.

A convenient way of performing the summation is to choose new axes for the purposes of the summation. Instead of using a_1 and a_2 as axes for the synthesis, the axes a_1 and D (the diagonal) are used. The work of the Fourier summation then consists of summing over indices h and k', where k' is the index on D, namely,

$$\begin{aligned}\sum_{h}{}'\sum_{k'}{}'_{0}^{\infty} A_{hk'0} &\cos 2\pi hx \cos 2\pi k'y \\ - A_{hk'0} &\sin 2\pi hx \sin 2\pi k'y \\ + B_{hk'0} &\sin 2\pi hx \cos 2\pi k'y \\ + B_{hk'0} &\cos 2\pi hx \sin 2\pi k'y.\end{aligned} \tag{45}$$

Symmetry $p3m1$. Plane group $p3m1$ can be derived from $p3$ by the addition of a reflection parallel to the long diagonal of the cell. This causes a_1 and $-a_2$ to become equivalent. According to the reciprocal symmetry theorem, the following symmetry arises in reciprocal space:

$$F_{hk0} = F_{\bar{k}\bar{h}0}. \tag{46}$$

To reduce the number of terms of the summation, reciprocal space is divided into the three sectors of (43), then each sector subdivided into segments along the two long diagonals extending from the origin. A convenient way to perform the actual summation is to choose these two diagonals in reciprocal space as new axes, h' and k'. The actual Fourier part of the summation then consists of the single summation

$$\sum_{h'}{}' \overset{\infty}{\underset{0}{}} \sum_{k'}{}' A_{h'k'0} \cos 2\pi h'x \cos 2\pi k'y$$
$$- A_{h'k'0} \sin 2\pi h'x \sin 2\pi k'y$$
$$+ B_{h'k'0} \sin 2\pi h'x \cos 2\pi k'y$$
$$+ B_{h'k'0} \cos 2\pi h'x \sin 2\pi k'y. \tag{47}$$

The summation is completed by adding the values of this summation at the six points related by the symmetry $3m1$ and recording the sum at xy.

Symmetry $p6$. Plane group $p6$ can be derived from $p3$ by the addition of the operation 2. Therefore, the appropriate form of the symmetrical Fourier summation can be found by imposing conditions (18) on the form of (43). To take full advantage of the hexagonal symmetry, however, it is more convenient to rewrite (43) in six parts, which is equivalent to dividing reciprocal space into six sectors which are equivalent by hexagonal symmetry. The edges of each sector are an a axis and a diagonal, D. These edges may be chosen as axes on which the indices are h and k'. If the sectors are considered in centrosymmetrical pairs, one member of the pair has indices like $hk0$, while the other has the corresponding negative indices, $\overline{hk}0$. Thus the summation consists of three columns, each column including opposite sectors, with summation limits from $-\infty$ to ∞, namely

$$\rho(xy) = \frac{1}{S} \sum_{h}{}' \overset{\infty}{\underset{-\infty}{}} \sum_{k'}{}'$$
$$A_{h\bar{i}0} \cos 2\pi hx \cos 2\pi \bar{i}y + A_{k\bar{h}0} \cos 2\pi kx \cos 2\pi \bar{k}y + A_{i\bar{k}0} \cos 2\pi ix \cos 2\pi \bar{k}y$$
$$- A_{h\bar{i}0} \sin 2\pi hx \sin 2\pi \bar{i}y - A_{k\bar{h}0} \sin 2\pi kx \sin 2\pi \bar{k}y - A_{i\bar{k}0} \sin 2\pi ix \sin 2\pi \bar{k}y$$
$$+ B_{h\bar{i}0} \sin 2\pi hx \cos 2\pi \bar{i}y + B_{k\bar{h}0} \sin 2\pi kx \cos 2\pi \bar{k}y + B_{i\bar{k}0} \sin 2\pi ix \cos 2\pi \bar{k}y$$
$$+ B_{h\bar{i}0} \cos 2\pi hx \sin 2\pi \bar{i}y + B_{k\bar{h}0} \cos 2\pi kx \sin 2\pi \bar{k}y + B_{i\bar{k}0} \cos 2\pi ix \sin 2\pi \bar{k}y. \tag{48}$$

The number of terms in this summation may be reduced by a factor of 4 by applying conditions (18) for the two-fold operation. This eliminates the B terms and doubles up the A terms, changing the summation limits from $-\infty$ to ∞, to 0 to ∞. The simplified summation appropriate to $p6$ is therefore

$$\rho(xy) = \frac{2}{S} \sum_{h}{}' \overset{\infty}{\underset{0}{}} \sum_{k'}{}'$$
$$A_{h\bar{i}0} \cos 2\pi hx \cos 2\pi \bar{i}y + A_{k\bar{h}0} \cos 2\pi kx \cos 2\pi \bar{h}y + A_{i\bar{k}0} \cos 2\pi ix \cos 2\pi \bar{k}y$$
$$- A_{h\bar{i}0} \sin 2\pi hx \sin 2\pi \bar{i}y - A_{k\bar{h}0} \sin 2\pi kx \sin 2\pi \bar{h}y - A_{i\bar{k}0} \sin 2\pi ix \sin 2\pi \bar{k}y. \tag{49}$$

As in the case of the trigonal summations, only the Fourier summation for the first column of (49) need be performed. The summation is completed by adding together the results found for three coordinate positions separated by 120° and recording the sum at the first of the three points.

Symmetry *p6mm*. Plane group *p6mm* can be derived from its subgroup *p6* by the addition of a reflection parallel to an axis. This provides the additional relation

$$F_{hk0} = F_{kh0}. \tag{50}$$

This permits changing the summation limits of (49) from 0 to ∞, to D to ∞. Otherwise the form of the summation is the same. To perform the summation, the Fourier part consists of summing for the first column only. The summation is completed by adding together at coordinates xy the six results found at points related to xy by symmetry $3mm$.

THREE DIMENSIONAL SUMMATIONS

Introduction. The computation of three-dimensional summations, one level at a time, can be referred to the pattern established for two-dimensional summations. In the following discussion, it is assumed, for sake of clearness, that it is desired to compute the electron density at level z_1. The value of z is, therefore, constant for the level.

The form of the Fourier summation for the general, non-symmetrical case was given in (9). Since z_1 is constant for the level, it is convenient to separate the trigonometric parts of (9) into constant and variable portions. This can be done by utilizing relations (12). Making these substitutions, (9) becomes

$$\rho(xyz_1) = \frac{1}{V}\sum_h \sum_{k=-\infty}^{\infty} \sum_l A_{hkl}\cos 2\pi(hx+ky)\cos 2\pi lz_1 - A_{hkl}\sin 2\pi(hx+ky)\sin 2\pi lz_1$$
$$+ B_{hkl}\sin 2\pi(hx+ky)\cos 2\pi lz_1 + B_{hkl}\cos 2\pi(hx+ky)\sin 2\pi lz_1. \tag{51}$$

Now, for any selected level, z_1, the values of

$$\begin{aligned} C_{A,hkl} &= \sum_l A_{hkl}\cos 2\pi lz_1 \\ S_{A,hkl} &= \sum_l A_{hkl}\sin 2\pi lz_1 \\ C_{B,hkl} &= \sum_l B_{hkl}\cos 2\pi lz_1 \\ S_{B,hkl} &= \sum B_{hkl}\sin 2\pi lz \end{aligned} \tag{52}$$

are fixed, and can be computed in advance of making the Fourier summation proper. Therefore, the summations over l can be eliminated in (51) and it assumes the simpler form

$$\rho(xyz_1) = \frac{1}{V}\sum_h \sum_{k=-\infty}^{\infty} C_{A,hkl}\cos 2\pi(hx+ky) - S_{A,hkl}\sin 2\pi(hx+ky)$$
$$+ S_{B,hkl}\cos 2\pi(hx+ky) + C_{B,hkl}\sin 2\pi(hx+ky) \tag{53}$$

$$= \frac{1}{V}\mathop{\sum_h\sum_k}_{-\infty}^{\infty} (C_A + S_B)_{hkl} \cos 2\pi(hx + ky) + (C_B - S_A) \sin 2\pi(hx + ky). \quad (54)$$

For compactness, if one takes

$$(C_A + S_B)_{hkl} = A'_{hkl}$$

and

$$(C_B - S_A)_{hkl} = B'_{hkl} \quad (55)$$

then (54) has the form

$$\rho(xyz_1) = \frac{1}{V}\mathop{\sum_h\sum_k}_{-\infty}^{\infty} A'_{hkl} \cos 2\pi(hx + ky) + B'_{hkl} \sin 2\pi(hx + ky). \quad (56)$$

This is exactly the same form as (11) for the non-symmetrical two-dimensional summation. Obviously, therefore, the three-dimensional summation can be handled exactly like the two-dimensional one after the coefficients (55) have been computed from (52). In practical summation, (56) should be recast into product form exactly the same as (13) except for primes indicating the composite nature of the coefficients in (55).

SYMMETRY BETWEEN UPPER AND LOWER RECIPROCAL SPACE

If the upper and lower halves of the crystal are related by any symmetry, the upper and lower halves of reciprocal space have a corresponding symmetry according to the reciprocal symmetry theorem. This specializes the forms of the coefficients in (55). To see how this affects (54), split each coefficient into a part pertaining to the upper half of reciprocal space and another pertaining to the lower half. Then (54) becomes

$$\rho(xyz_1) = \frac{1}{V}\mathop{\sum_h\sum_k}_{-\infty}^{\infty} (C_{A+} + C_{A-} + S_{B+} + S_{B-})_{hkl} \cos 2\pi(hx + ky)$$
$$+ (C_{B+} + C_{B-} - S_{A+} - S_{A-})_{hkl} \sin 2\pi(hx + ky). \quad (57)$$

Under the following headings, the way in which these coefficients are related in important cases, according to the reciprocal symmetry theorem, are tabulated. The simplified form of (57) is also listed:

Inversion center:

$$F_{h\overline{kl}} = F^*_{h\overline{kl}},$$

$$\therefore \quad A_+ = A_- \qquad C_+ = C_-$$

and

$$B_+ = -B_- \qquad S_+ = -S_-$$

$$\therefore \quad C_{A+} = C_{A-},$$
$$C_{B+} = -C_{B-},$$
$$S_{B+} = S_{B-},$$
$$S_{A+} = -S_{A-}.$$

$$\rho(xyz_1) = \frac{2}{V}\sum_h\sum_k (C_{A+} + S_{B-}) \cos 2\pi(hx + ky). \quad (58)$$

Reflection:

$$\begin{aligned} & F_{hkl} = F_{hk\bar{l}}, \\ \therefore\quad & A_+ = A_- \\ \text{and}\quad & B_+ = B_-. \end{aligned}$$

$$\rho(xyz_1) = \frac{2}{V}\sum_h \sum_k C_{A+}\cos 2\pi(hx+ky) + C_{B+}\sin 2\pi(hx+ky). \tag{59}$$

Glide, translation-component a/2:

$$\begin{array}{lll} & h \text{ even} & h \text{ odd} \\ & F_{hkl} = F_{\overline{hkl}}, & F_{hkl} = -F_{hkl} \\ \therefore & A_{hkl} = A_{hk\bar{l}}, & A_{hkl} = -A_{hk\bar{l}} \\ \text{and} & B_{hkl} = B_{hk\bar{l}}, & B_{hkl} = -B_{hk\bar{l}}. \end{array}$$

$$\rho(xyz_1) = \frac{2}{V}\left\{\sum_{\substack{h\\ \text{even}}} \sum_k C_{A+}\cos 2\pi(hx+ky) + C_{B+}\sin 2\pi(hx+ky) + \sum_{\substack{h\\ \text{odd}}} \sum_k S_{B+}\cos 2\pi(hx+ky) - S_{A+}\sin 2\pi(hx+ky)\right\}. \tag{60}$$

2-fold rotation $\|a$*:*

$$\begin{aligned} & F_{hkl} = F_{h\overline{kl}}, \\ \therefore\quad & A_{hkl} = A_{hkl}, \\ \text{and}\quad & B_{hkl} = B_{h\overline{kl}}. \end{aligned}$$

$$\rho(xyz_1) = \frac{2}{V}\sum_h \sum_k C_{A+}\cos 2\pi(hx+ky) + C_{B+}\sin 2\pi(hx+ky). \tag{61}$$

2-fold screw $\|a$*, translation-component a/2:*

$$\begin{array}{lll} & h \text{ even} & h \text{ odd} \\ & F_{hkl} = F_{h\overline{kl}}, & F_{hkl} = -F_{hk\bar{l}} \\ \therefore & A_{hkl} = A_{h\overline{kl}}, & A_{hkl} = -A_{h\overline{kl}} \\ \text{and} & B_{hkl} = B_{hkl}, & B_{hkl} = -B_{h\overline{kl}}. \end{array}$$

$$\rho(xyz_1) = \frac{2}{V}\left\{\sum_{\substack{h\\ \text{even}}} \sum_k C_{A+}\cos 2\pi(hx+ky) + C_{B+}\sin 2\pi(hx+ky) + \sum_{\substack{h\\ \text{odd}}} \sum_k S_{B+}\cos 2\pi(hx+ky) - S_{A+}\sin 2\pi(hx+ky)\right\}. \tag{62}$$

Computation. The computation of a three-dimensional summation has the symmetry of the section at which the summation is made. This is usually lower than the symmetry of the projection on a plane parallel to the section. On the other hand, the trigonometric part of the summation may have the same symmetry as that of the projection. In any case, when it is necessary to utilize the symmetry of the section, the same system can be followed which was discussed in detail for the projections, except that the coefficients involved are those shown in detail in (57) instead of A_{hkl} and B_{hkl}.

The additivity theorem suggests a general method of computing which can be used for three dimensional summations; the Fourier synthesis is performed at z_1 and $-z_1$ for data contained in a representative unsymmetrical block of the reciprocal structure. (In this synthesis, terms which the previous section indicates will cancel on combination may be omitted.) This gives the Fourier transform at xyz_1 and $xy\bar{z}_1$ for one block of the reciprocal structure. The summation is completed by adding together at xyz_1 the results obtained for the several points equivalent by symmetry to xyz_1.

REFERENCES

1. LIPSON H. AND BEEVERS, C. A., An improved numerical method of two-dimensional Fourier synthesis for crystals: *Proc. Phys. Soc.*, **48,** 772–780 (1936).
2. LONSDALE, KATHLEEN, Simplified structure factor and electron density formulae for the 230 space groups of mathematical crystallography. (G. Bell & Sons Ltd , London) 1936, esp. pp. 7–8.
3. BEEVERS, C. A., AND LIPSON, L., A rapid method for the summation of two-dimensional Fourier series: *Phil. Mag.*, (7) **17,** 855–859 (1934).
4. PATTERSON. A. L., AND TUNELL, GEORGE, A method for the summation of the Fourier series used in x-ray analysis of crystal structures: *Am. Mineral.*, **27,** 655–679 (1942).
5. BUERGER, M. J., Crystallographic symmetry in reciprocal space: *Proc. Nat. Acad. Sci.*, **35,** 198–201 (1949).

DEDOLOMITIZATION, AND ITS RELATION TO A POSSIBLE DERIVATION OF A MAGNESIUM-RICH HYDROTHERMAL SOLUTION*

GEORGE T. FAUST, *U. S. Geological Survey, Washington, D. C.*

CONTENTS

	Page
ABSTRACT	789
INTRODUCTION	789
THERMAL DISSOCIATION OF DOLOMITE	791
OCCURRENCE OF THERMALLY METAMORPHOSED DOLOMITES	795
SOURCE OF HEAT FOR METAMORPHISM	797
PHYSICAL CHEMICAL DATA ON THE SYSTEM MgO-CaO-CO_2-H_2O AND RELATED SYSTEMS	803
The system: MgO-H_2O	804
The system: H_2O-CO_2; The solubility of carbon dioxide in water	804
The system: MgO-CO_2-H_2O	805
The system: CaO-CO_2-H_2O	809
The system: MgO-CaO-CO_2-H_2O	811
THE PROCESS OF DEDOLOMITIZATION	814
LATER STAGES OF HYDROTHERMAL ACTIVITY AND THE DEVELOPMENT OF MAGNESIUM-RICH SOLUTIONS	815
(a) Leaching of dedolomitized rocks by hydrothermal solutions poor in carbon dioxide	815
(b) Reaction of dedolomitized rocks with hydrothermal solutions rich in carbon dioxide	816
(c) Subsequent reactions of hydrothermal solutions rich in magnesium and carbon dioxide with the country rock	817
SUMMARY OF THE DOLOMITE RELATIONSHIPS	819
SUMMARY AND CONCLUSIONS	820
ACKNOWLEDGMENTS	821
BIBLIOGRAPHY	822

ABSTRACT

This paper presents an interpretation, based on physical-chemical principles and data, of the phenomena arising in the aureole of metamorphism, resulting from the intrusion of a magma into dolomitic rocks. It is assumed that dedolomitization takes place in those beds closest to the magma. It also suggests a mechanism by which hydrothermal solutions passing through the zone of dedolomitized rocks may become rich in magnesium. A summary is given of the available data on the system MgO-CaO-CO_2-H_2O and its subsidiary systems. Probable phase equilibrium diagrams have been drawn for the systems MgO-CO_2-H_2O and CaO-CO_2-H_2O. The course of the reactions, involved in hydrothermal dolomitization of limestones, and the special conditions necessary for the formation of magnesite, are discussed.

INTRODUCTION

A fundamental object in geochemistry is the development of theories to explain the origin of rocks formed or altered by hydrothermal solu-

---

* Published by permission of the Director of the U. S. Geological Survey.

tions. Such theories should minimize the use of unusual constituents whose former presence cannot be established by a study of the rocks and minerals of the deposit and the associated rocks. The hydrothermally formed brucite, dolomite, and magnesite deposits constitute a typical group of such rocks and have been under study by the writer for the past six years. The hydrothermal solutions which formed the carbonate deposits were rich in magnesium and carbon dioxide.

Hydrothermal dolomitization of limestones in the aureole of mineralization in ore deposits has been recognized for many years. An especially fine contribution by Hewett (1928) has refocussed attention upon this phenomenon. Hewett made a field study of the association of dolomitized limestones and ore deposits of zinc and lead both in this country and in Europe, and he emphasizes the frequency of this relationship. He also points out that in some deposits there is zoning among the carbonates and in others, particularly at Iglesias in Sardinia, islands of unreacted limestone are contained within the dolomite. Concerning magnesite he writes (page 856):

> Magnesite is uncommon, if not very rare, near zinc and lead deposits, and similarly zinc and lead minerals are rare or unknown near the larger replacement magnesite deposits. Viewed broadly, such magnesite deposits are very uncommon, whereas dolomitized limestone near the zinc and lead deposits is rather common.

Hewett concludes his paper with a discussion of the possible sources of the magnesium.

A great many interesting geochemical problems are posed by these phenomena. In this study we are particularly concerned with (*a*) a mechanism or mechanisms by which hydrothermal solutions rich in magnesium and carbon dioxide may be derived, and (*b*) the manner in which these solutions will react with the preexisting limestones which they traverse.

In a study of the magnesite deposits of Currant Creek, Nev., Faust and Callaghan (1948) proposed a mechanism for the derivation of solutions, rich in magnesium and carbon dioxide, namely through the attack of hydrothermal solutions charged with carbon dioxide upon dolomitic rocks. The derivation proposed in that paper was one that seemed to fit best the geological relationships of the area. In addition, through a correlation of the physical chemistry, the observed mineralogical character and the texture and structure of the deposits, an explanation was offered for the formation of the dolomite, zoning, the presence of relicts of calcite (limestone), and the formation of magnesite. The comparative rarity of magnesite with respect to dolomitized limestone was also explained.

The present paper goes beyond the limitations imposed by the geology at Currant Creek, Nev., and proposes another mechanism for the derivation of solutions rich in magnesium and carbon dioxide.

The hydrothermal solutions which accomplished these reactions must have contained significant quantities of magnesium and carbon dioxide because, first, these substances are essential constituents of dolomite and magnesite and were introduced into the system; and second, from considerations of the phase rule, carbon dioxide is present both in the liquid and vapor phases whenever carbonates are precipitated from solutions.

The term carbon dioxide is used in this discussion for the sake of simplicity. In a solution of carbon dioxide in water, the following equilibria exist (1)

$$[H_2O + CO_2 \rightleftarrows H_2CO_3 \rightleftarrows H^+ + HCO_3^- \rightleftarrows 2H^+ + CO_3^{--}]. \tag{1}$$

In addition carbon dioxide is present as a gas dissolved in the solution.

The purpose of this paper is to show how magnesium-rich solutions may also be derived from the attack of hydrothermal solutions upon dolomites thermally metamorphosed by intrusives. Such dedolomitized rocks have been called predazzite, pencatite, and brucite marble. Harker (1904) has defined these rocks as follows:

> It is most in accordance with the original usage to employ the name pencatite for an aggregate of calcite and brucite in equal molecular proportions, i.e. with the percentage composition of 63.3 calcite to 36.7 brucite, reserving the predazzite for varieties richer in calcite.

Periclase, MgO, was the magnesium mineral present in these rocks after thermal metamorphism. Brucite, $Mg(OH)_2$, belongs to a later period in the genesis of the rock.

The structure, texture, and mineralogy of these metamorphic rocks will influence the character and rate of the reactions with the later hydrothermal solutions which traverse them.

Thermal Dissociation of Dolomite

In order to gain an understanding of the origin of these dedolomitized rocks, the physical chemistry of the dissociation of dolomite is considered here.

The dissociation of dolomite may take place in two stages as is shown in the following equations:

At temperatures sufficient to cause the complete decarbonatization of the dolomite the over-all reaction will give the products outlined in boxes:

(2)

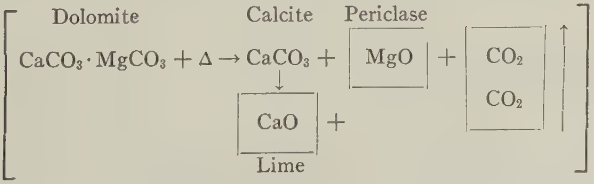

$$\left[\begin{array}{l} \overset{\text{Dolomite}}{CaCO_3\cdot MgCO_3} + \Delta \rightarrow \overset{\text{Calcite}}{CaCO_3} + \overset{\text{Periclase}}{\boxed{MgO}} + \boxed{\begin{matrix}CO_2\\ CO_2\end{matrix}}\uparrow \\ \qquad\qquad\qquad\qquad\qquad\quad \downarrow \\ \qquad\qquad\qquad\qquad\quad \underset{\text{Lime}}{\boxed{CaO}} + \end{array}\right].$$

At somewhat lower temperatures, incomplete dissociation occurs:

$$\left[\overset{\text{Dolomite}}{CaCO_3\cdot MgCO_3} + \Delta \rightarrow \overset{\text{Calcite}}{\boxed{CaCO_3}} + \overset{\text{Periclase}}{\boxed{MgO}} + \boxed{CO_2} \uparrow\right] \tag{3}$$

The dissociation of dolomite may be therefore either partial or complete and the heat necessary to bring about the reactions is quite different.

The course of these two reactions may be followed by means of the method of thermal analysis. A study of many thermal curves prepared in the petrology laboratory of the U. S. Geological Survey [Faust (1944–48)] demonstrates that the temperatures at which dolomite dissociates into calcite and periclase and at which calcite subsequently decomposes to form CaO are somewhat variable, and depend chiefly upon the grain size and the rate of heating.

Typical thermal analysis curves for calcite, magnesite, and dolomite obtained in this laboratory are given in Fig. 1. Reactions (2) and (3), as given above are irreversible in an open system because the system loses CO_2. Some studies have been made under conditions which are essentially reversible. Thus Smyth and Adams (1923) present equilibrium data for the reversible dissociation of calcite, as expressed in equation (4) (double arrow).

$$\lfloor CaCO_3 + \Delta \rightleftarrows CaO + CO_2 \rfloor . \tag{4}$$

In the natural process of thermal metamorphism of dolomite (or a magnesian limestone), the following factors will affect the process: grain size, rate of heating, pressure, closure of system, and associated minerals.

Laboratory studies indicate that the finer the grain size of dolomite, the lower will be the temperature of dissociation. The data suggest that a similar condition may hold under natural conditions of metamorphism and that this may explain the failure of some dolomites to undergo dissociation while other beds nearby are changed into new rock types.

The rate of heating of the carbonate rocks is difficult to evaluate. Aside from the heat transmitted by conduction through the solid rock, it is necessary to consider the thermal energy transported by the emanations, chiefly water vapor, from the cooling magma, and also that contributed to the advancing heat front by the CO_2 arising from the dissociation of the dolomite. This subject is discussed more fully below.

Hydrostatic pressure alone may influence the dissociation of dolomite so much as to prevent its decomposition. Halla (1936) has calculated the effect of pressure on the stability of dolomite. A translation of his views follows:

> From the values of $\Delta F°$ and the "means" of the known molecular volumes of dolomite, magnesite, and calcite, the conclusion is allowed that increased pressure (Gebirgsdrucke an der Erdoberfläche) has the effect of stabilizing dolomite.

The difference between the reaction studied by Halla, equation (5)

$$(5)\quad \left[\begin{array}{c}\text{Dolomite}\\ CaCO_3\cdot MgCO_3\end{array} \rightarrow \begin{array}{c}\text{Calcite}\\ CaCO_3\end{array} + \begin{array}{c}\text{Magnesite}\\ MgCO_3\end{array}\right] \text{system closed, } P=\text{very high}$$

and equations (2) and (3) should be noted. Bowen (1940) has treated the more complicated effect of pressure on the thermal metamorphism of siliceous limestone and dolomite, and has given the phase assemblages stable at various temperatures and pressures.

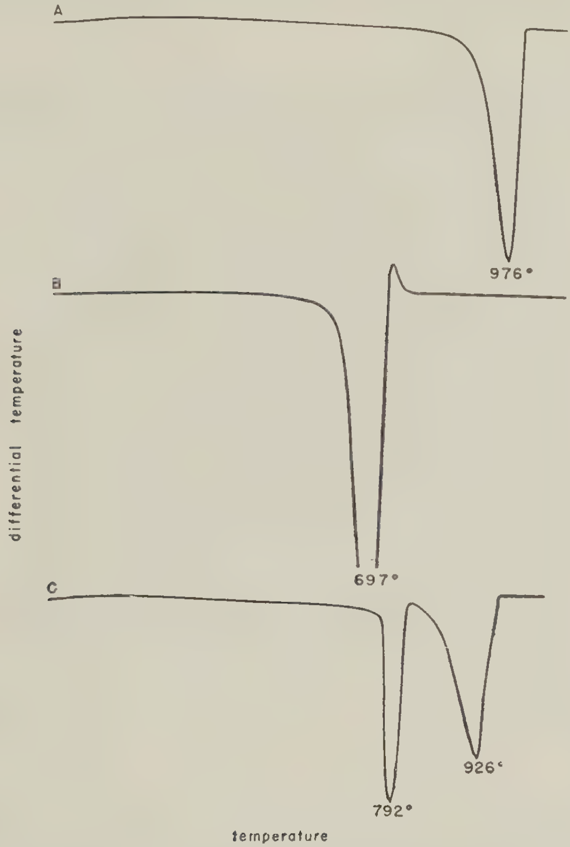

Fig. 1. Thermal analysis curves of calcite, magnesite, and dolomite. (A, calcite, Joplin, Missouri, analyzed sample—pure, resistance in series with galvanometer 999.9 ohms. Record C-89. (B, magnesite, Currant Creek, Nevada, analyzed sample—pure, resistance in series with galvanometer 999.9 ohms. Record C-79. (C, dolomite, Millville, West Virginia, analyzed sample, resistance in series with galvanometer 900 ohms. Record F-3.

From these observations and equations (2 and 3) it is evident that thermal dissociation of dolomite is also dependent on the state of closure of the system. If the system is closed so that CO_2 cannot escape, then the effects of thermal metamorphism will consist largely of recrystallization of the dolomite to a dolomite marble, marmorization. Griggs (1946) recrystallized the Yule marble to a new texture in the presence of H_2O and CO_2 at a high confining pressure and at a temperature of only 150° C. If the system is open and CO_2 can escape, then periclase can form and the dolomite will be dedolomitized.

This reaction of dissociation is also dependent upon the kind and amount of the associated minerals in the original dolomite. Bowen (1940) has treated these relations for siliceous dolomites and has shown the effect in producing new phase assemblages at given temperatures and pressures.

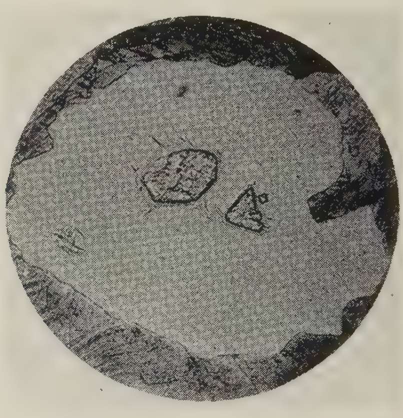

FIG. 2. Unaltered cores of periclase enclosed within brucite Pencatite from the Organ Mountains, New Mexico. Plane-polarized light. Mag. 70×.

In summary of the data of thermal dissociation studies and their application to thermal metamorphism, it is evident that natural metamorphic processes introduce factors difficult to assess and do not permit the direct use of such data as fixed points in geological thermometry. Thermal analysis data do show, however, how minerals break down at higher temperatures. They indicate an upper limit to the temperature of dissociation and they furnish in a general way the range of temperatures at which the process may occur.

The thermal dissociation of dolomite is accompanied by a change in volume. If reaction (3) goes to completion, the volume change is a decrease of 22 per cent. The change in volume accompanying reaction (2) is 38 per cent. As both of these reactions result in a diminution in volume, hydrostatic pressure will favor the thermal dissociation of dolomite *if*

CO_2 can escape, according to the principle of LeChatelier and Braun [see Rivett (1923)]. An examination of thin sections of predazzite and pencatite, which contain unaltered cores of periclase (see Fig. 2), shows this mineral to be present in dense form. Periclase, formed by the thermal dissociation of magnesite in the laboratory, is a pseudomorph after magnesite (see Fig. 3). Faust (1944) has studied these pseudomorphs and found that, following thermal dissociation, the resulting periclase consists of a skeletal boxwork inheriting the rhombohedral form of magnesite. This aggregate is composed of crystallites of periclase and air-filled spaces. Upon longer heating, this unstable structure collapses.

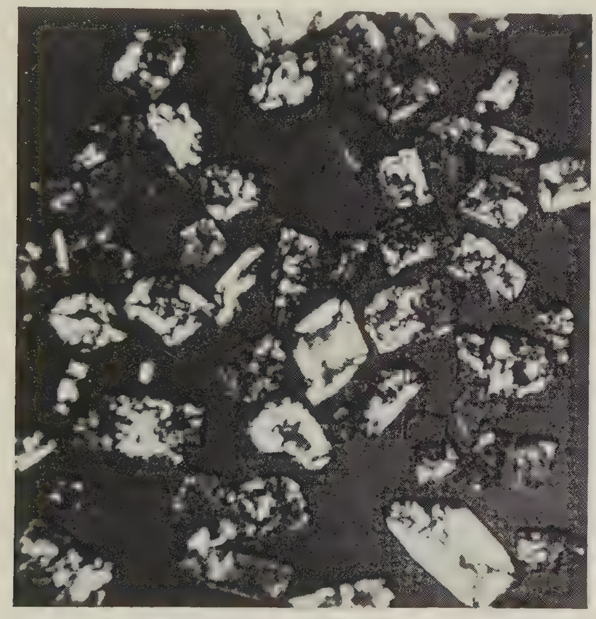

FIG. 3. Optically anomalous periclase resulting from the conversion of magnesite grains (−150+200 mesh) to the oxide by heating. Crossed nicols. Mag. about 75×.

Thermal metamorphism under geologic conditions would not permit an unstable structure, such as described above, to exist; for the hydrostatic pressure and the continuous passage of heat would jointly serve to produce a dense form of periclase.

OCCURRENCE OF THERMALLY METAMORPHOSED DOLOMITES

Thermal analysis data show that contact metamorphism of dolomites can produce two types of rocks. If the temperature and the thermal

TABLE 1. FIELD RELATIONSHIPS OF THE OCCURRENCES OF PREDAZZITE AND PENCATITE

Locality	Intrusive rock responsible for thermal metamorphism	Name given to metamorphosed dolomites	Characteristics of the original carbonate rock	Reference
Near heads of Big Cottonwood and Little Cottonwood Creeks, S.E. of Salt Lake City, Utah.	Granodiorite and quartz diorite.	Metamorphosed dolomite.	Dolomitic beds in the Maxfield (Cambrian) Jefferson (?) (Devonian) and Deseret (Mississippian) limestones.	Calkins, F. C., and Butler, B. S., Geology and ore deposits of the Cottonwood-American Fork Area, Utah: *U.S. Geol. Survey, Prof. Paper* **201** (1943). Also Calkins, F. C., Oral Communication, Dec. 1946.
Philipsburg Quadrangle, Montana.	Granodiorite (?)	Metamorphosed dolomite.	Dolomite of the Hasmark formation (Cambrian)	Emmons, W. H., and Calkins, F. C., Geology and ore deposits of the Philipsburg Quadrangle, Montana: *U.S. Geol. Survey, Prob. paper* **78** (1913). Also Calkins, F. C., Oral Communication, Dec. 1946.
Organ Mountains, New Mexico.	Quartz monzonite.	Pencatite, predazzite.	Dolomites of lower Paleozoic age.	Dunham, C. K., The Geology of the Organ Mts.: *New Mexico School of Mines, Bull.* **11** (1935). Hunt, W. F. and Faust, G. T., Pencatite from the Organ Mts., New Mexico: *Am. Mineral.*, **22,** 1151–1160 (1937).
Crestmore, near Riverside, California.	Porphyritic quartz monzonite. The predazzite occurs as a roof pendant.	Predazzite.	Magnesian limestone of upper Paleozoic age.	Rogers, A. F., Periclase from Crestmore near Riverside, California, with a list of minerals from this locality: *Am. Mineral.*, **14,** 462–469 (1929). Woodford, A. O., Crestmore minerals: *California Jour. Mines and Geology*, 333–365 (1943).
Near Wakefield, Quebec, Canada.	Hastingsite syenite. The brucitic limestone occurs as roof pendants in a batholith.	Brucitic limestone.	Dolomites of pre-Cambrian age (Grenville).	Ambrose, J. W., Brucitic limestones and hastingsite syenite near Wakefield, Quebec: *Royal Soc. Canada, Proc. and Trans.*, 3rd Ser., **37,** 9–22 (1943).
Near Wilkinson, Ontario, Canada.	Granites or syenites. The brucite limestone occurs as roof pendants in a batholith.	Brucite limestone.	Magnesian limestones.	Brown, I. C., Brucite in limestone near Wilkinson, Ontario; *Econ. Geology*, **38,** 408–419 (1943).
Assynt district, Sutherland, Scotland.	Loch Borolan granite, syenites.	Marbles.	Cambrian dolomites and limestones.	Teall, J. J. H., *Mem. Geol. Survey, United Kingdom,* 453–462 (1907).
Island of Skye, Scotland.	"In the area of extreme metamorphism next the granite."	Predazzite. Pencatite.	Dolomitic limestones of Cambrian age.	Harker, A., The tertiary igneous rocks of Skye: *Mem. Geol. Survey, United Kingdom,* 144–151, especially p. 150 (1904).
Predazzo, Tyrol, Province of Veneto, Italy.	Monzonite.	Predazzite. Pencatite.	Triassic Kalken Mendelund-Latemar-Kalk. Unteren Muschelkalks.	Klebelsberg, R. von., Geologie von Tirol: Gebrüder Borntraeger, Berlin, p. 354 (1935).
Nantei mine, Suian, Tyôsen (Korea).	Granodiorite. A small batholith.	Brucite marble (predazzite).	Pre-Cambrian dolomites and slates	Watanabe, Takeo, On the brucite-marble (Predazzite) from the Nantei Mine, Suian, Tyôsen, (Korea): *Jour. Fac. Sci. Hokkaidô Imp. Univ.*, 4th Ser., **3,** No. 1, 49–59 (1935).

energy are sufficient to dissociate dolomite completely, the resulting minerals would be lime (CaO) and periclase (MgO). No geologic occurrence of a completely dissociated dolomite which contains lime is known. Only one occurrence of lime as a mineral has so far been reported. Zambonini (1935) has listed lime as a mineral occurring in the blocks of calcareous rock enclosed within lava at Vesuvius. Such highly dissociated rocks, if they exist, are stable only when protected from solutions and water vapor and presumably at some depth within the earth's crust.

The partly calcined dolomites called predazzite and pencatite, on the other hand, have been observed in many places. Rogers (1918, 1929) has summarized their distribution in California, Utah, and Montana. Hunt and Faust (1937) and Dunham (1935) have described them from New Mexico.

Recently, Goudge (1939), Ambrose (1943), and Brown (1943) have described brucitic limestones from Canada.

An interesting relationship exists between the metamorphic rocks, predazzite and pencatite, and the type of intrusive rocks which are responsible for their metamorphism. Table 1 shows this relationship. The intrusive rocks are chiefly granites, granodiorites, and less commonly, quartz diorites. These rocks are predominantly the siliceous types and their close association with the dedolomitized rocks suggests that the composition of the intrusive rock is a factor in determining the degree of metamorphism of the dolomite. The reasons for this interrelation are developed in the following section on the source of heat for metamorphism.

The association of certain types of mineralization with certain types of rocks has long been observed by geologists. A comprehensive review of this association has been given by Buddington (1933) and the reader is referred to his paper.

SOURCE OF HEAT FOR METAMORPHISM

It is assumed in this paper that a magma supplied the heat necessary for metamorphism.

A study of the conduction of heat through rocks by Birch and Clark (1940) shows that the chemical composition of the magma is a relatively unimportant factor, for at depths of about 10 to 20 km., and at elevated temperatures, the differences in the constants of thermal conductivity are very small. The thermal characteristics of the magma type are thus not important factors in determining the degree of thermal metamorphism of the intruded rocks.

The conductivity of rocks is so low and the resultant rate of conduction of heat is so low that additional sources of heat are required for the thermal energy necessary to bring about the remarkable changes produced in the process of dedolomitization.

Intensive studies of contact-metamorphic ore deposits and of the aureole of metamorphism associated with igneous intrusion have been made during the last three decades. These studies have shown that the contact zones are not all alike in character nor are the resultant effects indicative of an equality in intensity. The effects produced depend upon many factors of which the following are very important: size of the intrusive; structural relation of the complex assemblage; amount of cover and the closure of the system; composition and texture of the country rock; and the abundance of gaseous and hydrothermal emanations. The importance of emanations from a magma to the process of contact metamorphism is now gaining wide acceptance. Ross (1928) has commented on the importance of emanations as follows (p. 873):

> The almost complete absence of recognizable contact-metamorphic effects in the wall rock of even the relatively hot magmas that have formed basalt dikes or diabase sills is noteworthy. Hypabyssal intrusive magmas, even those that are known to have had high temperatures, were in general able to exert little effect on most enclosing rocks by means of their heat energy unassisted by hydrothermal or gaseous emanations, and without doubt vein-forming materials are cooler than basalt magma.

The relative quantity of gaseous and hydrothermal emanations associated with "basic" and "acid" magmas has been discussed by many geologists and petrologists, and Bowen (1933) in particular has considered this relationship with respect to the differentiation of magma:

> Page 113, In a full differentiation sequence from basic types to acid types, there will be a natural tendency to this greater concentration of hyperfusibles in the acid types.

and again,

> Page 115, Generally speaking it is in the granitic and related magmas that the greater concentration of the hyperfusibles come into being.

Buddington (1933) likewise writes:

> Page 354, The percentage and the kinds of volatiles may vary widely with different kinds of magma, and this must affect the resultant mineralization. It is generally accepted that the percentage of H_2O and other volatiles is usually considerably greater in siliceous magmas than in basic varieties.

Gaseous and hydrothermal emanations are responsible for the transportation of and transfer of heat into the country rock. It is generally conceded that the principal constituents of emanations are chiefly H_2O and CO_2, with the former more abundant. The emanations from a magma have a very low viscosity and hence are very mobile. This mobility permits the gases and solutions to move out into the country rock, and accordingly is an important factor in the transfer of heat from the magma to the country rock by the emanations. In addition, the heat capacities of the gaseous and hydrothermal emanations are significantly larger than that of a molten magma itself. The heat capacities of (H_2O) vapor, (H_2O) liquid, (CO_2) vapor, together with those of molten magma, and of several types of granitic rocks are given in Table 2, and in Fig. 4.

TABLE 2. HEAT CAPACITY OF GASES, WATER (LIQUID), AND ROCKS AT HIGH TEMPERATURES. HEAT CAPACITY, CP IN JOULES PER GRAM[1]

Substance	Temperature in degrees centigrade						
	0°	200°	220°	400°	600°	800°	1200°
CO_2 (gas)[2]	0.82			1.12			1.32
H_2O (gas)[2]	1.847			2.052			2.478
H_2O (liquid)[3]	4.219	4.341	4.376				
Granite[2]	0.65	0.95		1.07		1.13	
Granodiorite[2]	0.70	0.97		1.08_5		1.17_5	
Diorite[2]	0.71	0.99		1.09		1.18	
Molten magma[4]				0.8			1.2

[1] One joule is equivalent to 0.23895 gram calorie at 15°C.

[2] Data from: Birch, F., Schairer, J. F., and Spicer, H. C., Handbook of Physical Constants: *Geol. Soc. Am., Special Paper* no. **36** (1942).

[3] Data from: Kaye, G. W. C., and Laby, T. H., Tables of Physical and Chemical Constants and Some Mathematical Functions. London, Longmans, Green and Co., 8th ed., p. 59. 1935.

[4] Data from: Barus, Carl, High Temperature Work in Igneous Fusion and Ebullition Chiefly in Relation to Pressure: *U. S. Geol. Survey, Bull.* **103,** 53–54 (1893). An estimated curve is sketched in figure 4 based on Barus' data.

The contribution of heat transferred by the gases CO_2 and, to a very minor extent H_2O, released by the heating and thermal dissociation of dolomite rock, is also significant. These gases may be released: (*a*) by the ingestion of masses of dolomite or limestone entrapped within the magma as it stopes its way upward. Evidence for such relations is found at some of the localities in the form of xenoliths of predazzite, Dunham (1936); (*b*) by the transmission of heat to the dolomite directly in contact with the magma. The gases when released are at a high temperature and have a relatively high specific heat. They can escape into the country rock or move along the contact and mingle with the gaseous emanations of the magma and then escape into the country rock. As more and more dolomite is dissociated, they continue to be released and are available for transmitting heat. As long as dolomite is being dissociated, there will be CO_2 gas available for thermal metamorphic processes.

The available thermal energy for metamorphism is the sum of the heat

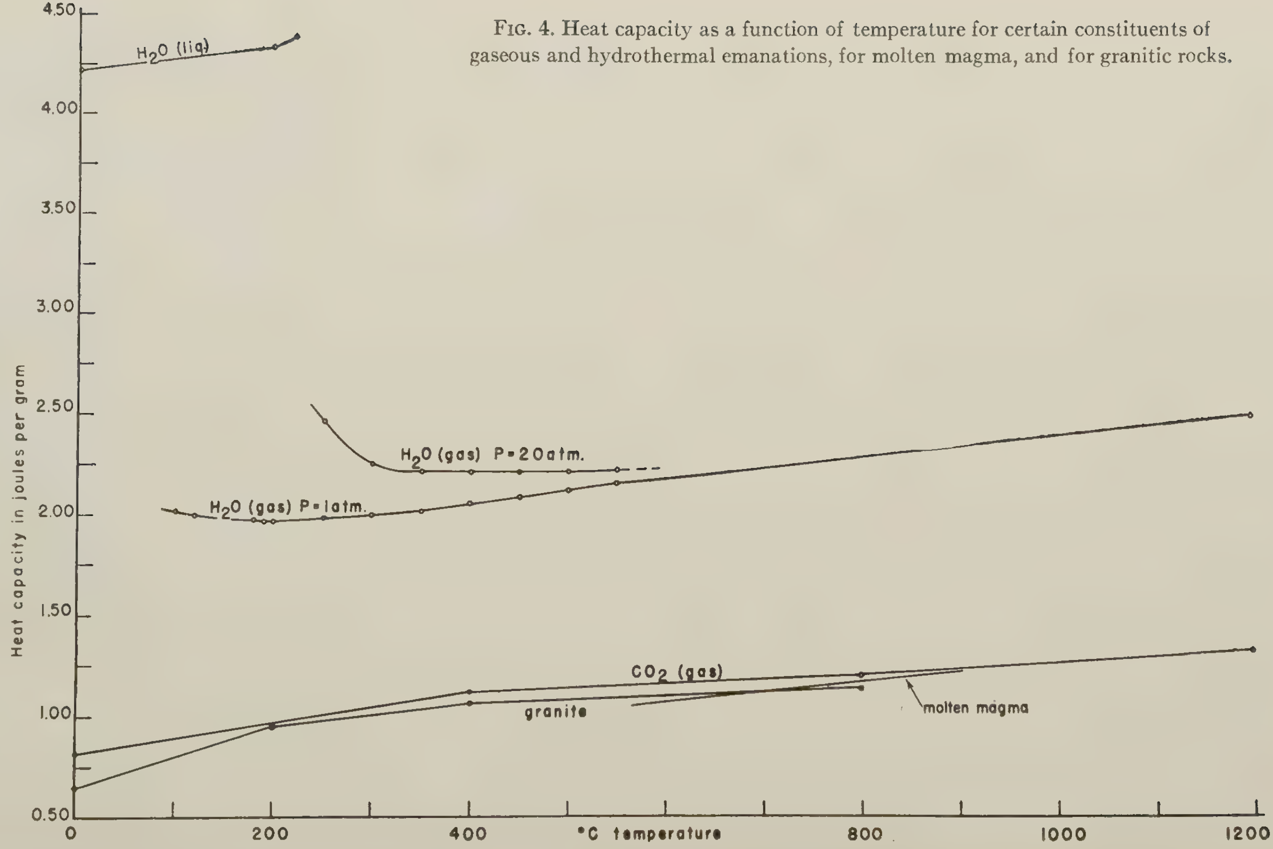

FIG. 4. Heat capacity as a function of temperature for certain constituents of gaseous and hydrothermal emanations, for molten magma, and for granitic rocks.

transmitted by conduction through the magma, the heat contributed by the emanations from the magma, the heat carried by the CO_2 gas resulting from the dissociation of dolomite; and the heat contributed by miscellaneous processes such as radiation, radioactivity, etc. For present purposes, the miscellaneous contributions may be neglected because of their small effect. The quantity of heat transmitted by conduction through the country rock is generally expressed as follows:

$$\left[Q = k\frac{(\theta_1 - \theta_2)At}{X}\right] \tag{6}$$

in which k is the thermal conductivity; θ_1 is the temperature of the magma and θ_2 that of the country rock; X the distance; A the area; and t the time. This equation implies a continuous function, as the time t is included. In other words, heat flow is a continuous process. A more complete statement of the problem requires the use of the diffusivity h, defined as, $h^2 = k/c\rho$, in connection with equation (6). In the definition of the diffusivity h, c, and ρ represent the specific heat and density respectively.

In order to simplify the presentation, we will treat the relations as an instantaneous matter and express Q_i as the maximum heat available, assuming that all the heat is given up to the pencatite or predazzite. The quantity of heat, Q_i, available at the earliest stage of metamorphism when the gaseous constituents are the dominant part of the emanations, is:

$$\left[Q_i = \underbrace{C_p(T_m - T_{cr})M_m}_{\text{Heat available for transmission by conduction.}} + \underbrace{C_p{}^1(T_m - T_{cr})M_e}_{\text{Heat available for transportation by the gaseous emanations.}}\right] \tag{7}$$

where C_p, C_p' are the specific heats of the magma and the gaseous emanations, and T_m, T_{cr} are the temperatures of the magma and country rock and M_m and M_e the masses of the magma and emanations, respectively.

The heat contributed by the gaseous phase for the same weight in grams, is two to three times as large as that available from the magma. The relative masses of magma and emanations are, however, greatly different. At the earliest stage of intrusion of magma, the emanations are at a minimum; as time passes and the magma crystallizes and cools, the amount of emanations increases. At a still later stage in the history of the magma when the magmatic solution contains a preponderance of H_2O, the amount of emanation reaches its maximum. An exception to these relations occurs when a magma that has intruded or entrapped xenoliths of a carbonate-rich rock, such as dolomite or limestone, is hot enough and has sufficient heat content to dissociate these carbonate rocks, liberating hot gaseous carbon dioxide and thus bringing about a local enrichment of the emanations.

The available heat conducted into the dolomite, if the temperature is sufficient to dissociate dolomite, will be consumed in raising the temperature of the dolomite to the dissociation temperature, dissociating the dolomite, and then finally spent in raising the temperature of the periclase, calcite, and the gaseous carbon dioxide.

The heat content of the first-formed pencatite or predazzite is as follows:

$$Q_D = \left[C_p^{\mathrm{II}}\left(\frac{T_m - T_{cr}}{2}\right)\mathrm{M}_{\mathrm{MgO}}\right] + \left[C_p^{\mathrm{III}}\left(\frac{T_m - T_{cr}}{2}\right)\mathrm{M}_{\mathrm{CO_2}}\right] + \left[C_p^{\mathrm{IV}}\left(\frac{T_m - T_{cr}}{2}\right)\mathrm{M}_{\mathrm{Calcite}}\right] \tag{8}$$

in which C_p^{II}, C_p^{III}, C_p^{IV}, are the specific heats respectively of periclase, carbon dioxide (gas), and calcite; and $\mathrm{M}_{\mathrm{MgO}}$, $\mathrm{M}_{\mathrm{CO_2}}$, $\mathrm{M}_{\mathrm{Calcite}}$) are the respective masses of periclase, carbon dioxide (gas), and calcite. An examination of the physical meaning of the mathematical statements in the three members of this equation shows that the heat content of the solid phases expressed in the first and third terms of equation (8) may be dissipated by conduction; whereas the heat content of the gaseous phase, CO_2, given in the second term, is available for thermal processes because the gaseous phase is mobile and can transfer its heat content elsewhere. When mixed with the emanations from the magma its temperature may be raised. It is this phenomenon of the release of CO_2 gas by carbonate rocks that undergo dissociation that modifies a straightforward mathematical treatment of heat conduction such as can be used for most country rock that is essentially thermally inert.

At a later stage in the cooling of the intrusive, when the temperatures are lower and the emanations from the magma are chiefly hydrothermal solutions, the last term in equation (7) must be modified to take into account the very much greater value of the specific heat of water (liquid), which is about four times larger than that of a crystallizing intrusive. The volume of hydrothermal solution may be very large, and these solutions are very important agents in the process of contact metamorphism.

Adams (1924) has pointed out another type of thermal effect which for liquids is always a heating effect and for gases is either a heating or cooling effect. This effect, termed the "porous-plug expansion," applies to the escape of gases and solutions through capillary and subcapillary openings, and along intergrain boundaries. As it is difficult to evaluate, it is only mentioned here, but it is recognized that because such escape of gases will take place in metamorphic processes, this effect may affect the heat content of the system.

There are thus three factors which make magmatic emanations important in contact metamorphism: their greater specific heat; their mobility, which transports the heat quickly to the country rock; their ability to enter into reaction with the country rock while at elevated temperatures. These characteristics contrast markedly with the slow, short-distance effects of heat conduction.

A unique reaction, involving one of the major components of the rock which undergoes decomposition to yield a gaseous phase, differentiates dedolomitization from simpler thermal metamorphism. The complete miscibility relations existing among gases permits the hot, released CO_2 to mix with gaseous emanations of the magma and to undergo an increase in temperature. Such a mixture of gases is a powerful agent in metamorphism.

From the foregoing discussion of the field relations of the aureoles of metamorphism associated with granitic rocks, it is here believed that the association of granitic or related types of rocks with the dedolomitized rocks, predazzite and pencatite, is not a fortuitous one. It is further held that most of the heat necessary for dedolomitization is transported by emanations from the magma.

PHYSICAL CHEMICAL DATA ON THE SYSTEM MgO-CaO-CO_2-H_2O AND RELATED SYSTEMS

As described above, the complete or selective dissociation of dolomite gives rise to definite assemblages of the following solid phases: lime, periclase, and calcite. These substances can react with carbonate-rich, hot solutions in various ways depending upon the variables: temperature, pressure of carbon dioxide in the system, total pressure on the system, and the presence of other ions in the solutions. A discussion of the pertinent physico-chemical relations applying to the above-mentioned system is given herewith.

Data are available on the systems MgO-H_2O; H_2O-CO_2; CaO-CO_2-H_2O; and MgO-CO_2-H_2O, which are parts of the quaternary system. However, to define completely the relationships in the complex natural system, we would require the data for the water-rich portions of the multicomponent system MgO-CaO-CO_2-H_2O-Cl-SO_4-Na_2O-K_2O. In the absence of such complete information, it is necessary to consider the available data on the subsystems mentioned above and to evaluate the effects of the Cl, SO_4, Na, and K content from existing studies on the solubilities of carbonates in salt solutions.

The system MgO-H_2O

One of the sides of the tetrahedron of the quaternary system MgO-CaO-CO_2-H_2O is the subsystem MgO-H_2O. Complete equilibrium relations in the system MgO-H_2O are not available at present. Considerable data are, however, to be found in the literature for the phases in this system, periclase, brucite, and water in its various forms. Complete data on the equilibrium thermal relations have been determined for periclase and the various phases of H_2O. The equilibrium-dissociation relations for brucite have just been published by Bowen and Tuttle (1949), who found that brucite is remarkably stable thermally, dissociating into periclase at a temperature of approximately 880° C. at a pressure of about 1,000 pounds per square inch (68 atmospheres) and at about 910° at a pressure of 32,000 pounds per square inch (2,176 atmospheres). The latter pressure corresponds to a depth of 5 miles in the earth (density of the rock assumed to be 2.7).

The statement of the equilibrium dissociation of brucite is given in equation (9)

$$[Mg(OH)_2 \rightleftarrows MgO + H_2O]. \tag{9}$$

This reaction is driven to the right by temperature and to the left by the pressure of H_2O.

These data suggest the view that dedolomitization of dolomite, in nature, at high temperatures (above the dissociation temperature of brucite) with the formation of periclase (MgO) may take place in the presence of vapors composed largely of H_2O.

As the temperature of the natural system consisting of the magma, the dedolomitized zone, and the emanations drop and the proportion of liquid phase increases, the stability of periclase (MgO) decreases rapidly, and it is converted into brucite ($Mg(OH)_2$).

The system: H_2O-CO_2; the solubility of carbon dioxide in water

When carbon dioxide gas is introduced into water the following equilibrium relations exist:

$$[CO_2 + H_2O \rightleftarrows H_2CO_3 \rightleftarrows H^+ + HCO_3^- \rightleftarrows 2H^+ + CO_3^{--}]. \tag{11}$$

In addition (CO_2) gas is dissolved as such in the solution. The solubility of carbon dioxide in pure water at high pressures and various temperatures has been measured by Wiebe and Gaddy (1939, 1940). These studies were made at pressures as high as 700 atmospheres and at temperatures of 12° to 100° C. More recently these data have been extended to 120° C. with pressures to 700 atmospheres by Prutton and Savage (1945). The solubility relations of carbon dioxide in water are shown graphically in Fig. 7. The unit of concentration should be carefully noted;

it is expressed as the number of cubic centimeters of carbon dioxide, at standard temperature (273° K = 0° C.) and pressure (1 atmosphere), contained in *one gram* of water. One cubic centimeter of carbon dioxide at (S.T.P.) weighs 0.00198 gram. Thus at 100° C. and at a *total pressure* of 25 atmospheres (pressure of CO_2 in the vapor phase plus the pressure of H_2O in the vapor phase), 5.365 cc. of carbon dioxide (S.T.P.) are dissolved in *one gram* of water. This is equivalent to 0.0106 gram of carbon dioxide per gram of water or approximately 10.62 grams of carbon dioxide per liter.

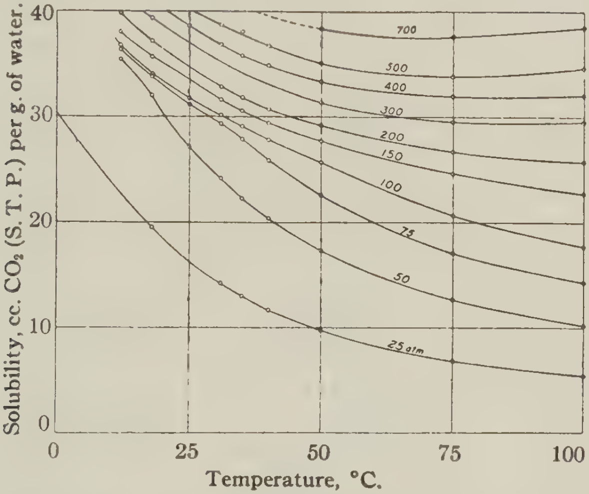

FIG. 5. The solubility of carbon dioxide, in cubic centimeters, (S.T.P.) per gram of water as a function of temperature and pressure. Wiebe and Gaddy (1939, 1940).

The solubility data for CO_2 in water as shown in Fig. 5 apply to pure water as the solvent. Prutton and Savage (1945) have studied the solubility of CO_2 in calcium chloride solutions and find that the solubility of the gas decreases as the concentration of the calcium chloride increases.

The system: MgO-CO_2-H_2O

The information available for this system consists of (*a*) the solubility data of magnesium carbonate trihydrate in water at various pressures of carbon dioxide, (*b*) the solubility data of magnesium carbonate (magnesite) in water at various pressures of carbon dioxide, and (*c*) some observations on the reaction relations betweeen magnesium oxide and solutions of carbon dioxide in water.

Engel and Ville (1881) measured the solubility of magnesium carbonate in water charged with carbon dioxide at temperatures from 13.4°

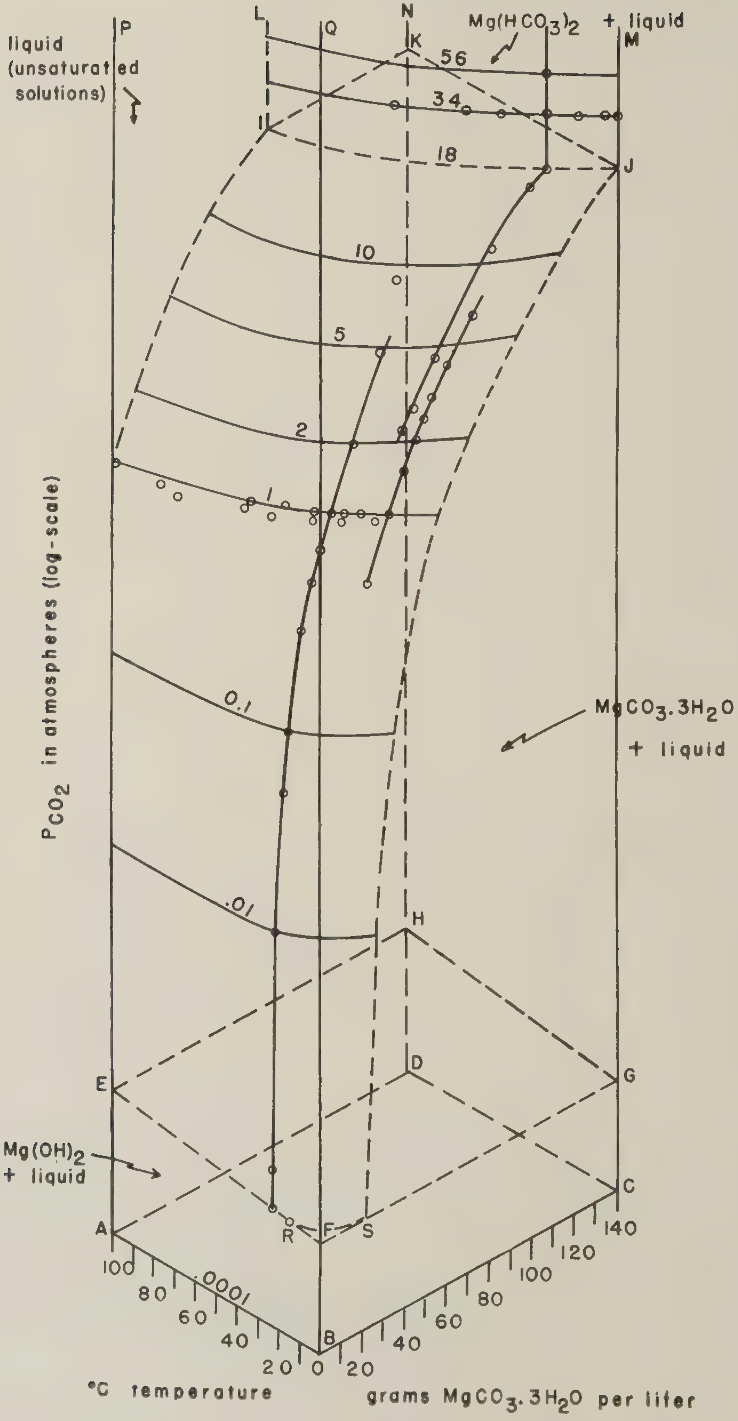
liquid
(unsaturated solutions)
P
L
Q
N
K
Mg(HCO$_3$)$_2$ + liquid
M
56
34
18
I
J
10
5
2
1
0.1
.01
H
D
E
G
C
A
R
F
S
B
Mg(OH)$_2$ + liquid
MgCO$_3$.3H$_2$O + liquid
P$_{CO_2}$ in atmospheres (log-scale)
.0001
100
80
60
40
20
0
20
40
60
80
100
120
140
°C temperature
grams MgCO$_3$.3H$_2$O per liter

to 100° C. and pressures from 1 to 9 atmospheres. Mitchell (1923) measured the solubility at 20° C. and at pressures of 6 to 21 atmospheres. Haehnel (1924) made measurements in the range to 0 to 60° C. and at pressures up to 56 atmospheres. Kline (1929) gives solubility data at 25° C. for pressures from 0.001 atmosphere to 15 atmospheres pressure of carbon dioxide. Bär (1932) has added to these data and summarized the results. Doerner, Holbrook, and Fortner (1946) have determined the solubility relations over the temperature range of 10° to 100° C. at a pressure of carbon dioxide of 700 millimeters (0.92 atmosphere). These data are given in Fig. 6, and the graphs show that the solubility of magnesium carbonate in a solution containing carbon dioxide increases rapidly with increasing CO_2 pressure for a given temperature. For a given pressure the solubility decreases with an increase in temperature.

The data of Haehnel show that the solubility becomes constant at 18 atmospheres and for a temperature of 18° C. and remains so, as far as he studied the relations, up to 56 atmospheres pressure of CO_2. This constancy in solubility means that a new solid phase has formed and Haehnel concludes this phase is magnesium bicarbonate, $Mg(HCO_3)_2$.

The probable phase relationships existing in the system $MgO\text{-}CO_2\text{-}H_2O$ from 0° C. to 100° C., and at pressures of CO_2 ranging from 1×10^{-4} atmospheres to 56 atmospheres have been sketched in Fig. 6. These phase boundaries have been drawn based on (*a*) the solubility data of magnesium carbonate trihydrate (nesquehonite), (*b*) the data on the transition of nesquehonite to brucite as related to the pressure of CO_2, (*c*) the stability relationships for magnesium bicarbonate. The field of magnesite lies at higher temperatures than those given here. The relationships at very low temperatures between nesquehonite ($MgCO_3 \cdot 3H_2O$) and lansfordite ($MgCO_3 \cdot 5H_2O$) have been ignored.

The presence of other ions in the solution also affects the solubility relations of magnesium carbonates in water that contains carbon dioxide. Cameron and his associates (1903, pp. 578–590; 1907, pp. 577–580) have studied qualitatively the solubility of magnesium carbonate and calcium carbonates in various aqueous solutions containing ions commonly present in natural waters. In general, the solubilities of these

---

FIG. 6. The solubility of magnesium carbonate in water as a function of temperature and pressure based on the data of Otto Haehnel, Kline, Engel and Ville, and Doerner, Holbrook and Fortner. The figure also portrays the probable phase relationships existing in the system $MgO\text{-}CO_2\text{-}H_2O$, within the temperature range of 0° C. and 100° C., and pressures of CO_2 ranging from 1×10^{-4} atmospheres to 56 atmospheres. The stability field of magnesite is situated at higher temperatures than those shown here. The stability relations of lansfordite $MgCO_3 \cdot 5H_2O$, at very low temperatures, have been ignored.

carbonates increase, with increasing quantities of the salts in the aqueous solutions, to a maximum, beyond which the solubility of the carbonates decreases. For solutions containing 100 grams of the salt per liter, sodium sulfate at 23° C. caused a four-fold increase in the solubility of magnesium carbonate while sodium chloride approximately doubled the solubility over that in pure water. These experiments were conducted in an atmosphere free of carbon dioxide. A notable exception is the solubility of magnesium carbonate in the presence of sodium carbonate which—for the same range of concentration as the other salts—shows a continuously rising curve of solubility.

The solubilities referred to above concern the relations for magnesium carbonate trihydrate (nesquehonite), and magnesium bicarbonate in equilibrium with solutions having definite carbon dioxide pressures above them. Haehnel (1924) found no difference in his solubility experiments whether he used artificial nesquehonite, magnesite from Snarum, Norway, or magnesium oxide as starting materials.

In the reaction between the dedolomitized rock and hydrothermal solutions charged with carbon dioxide, we are interested in the reaction between MgO (periclase) and a solution of water containing carbon dioxide. Doerner, Holbrook, and Fortner (1946) give the following two equations (12) and (13) to represent the conditions:

$$[MgO + 2CO_2 + H_2O \rightleftarrows Mg(HCO_3)_2] \tag{12}$$

or in two steps:

$$\left[\begin{array}{l} MgO + CO_2 + H_2O \rightleftarrows Mg(CO_3)(H_2O)_x \\ Mg(CO_3)(H_2O)_x + CO_2 \rightleftarrows Mg(HCO_3)_2 + (x-1)H_2O \end{array}\right] \tag{13}$$

they state further:

> Reaction (12) can be carried out in two steps (13) and no conclusive evidence that it occurs in a single step has been found.

According to these investigators, the result of the solution of MgO (periclase) in water charged with CO_2 is the production of a solution of magnesium bicarbonate. The proportion of MgO (periclase) converted to bicarbonate depends on the volume of the solution, amount of periclase, temperature, and the pressure of CO_2 in the system.

Terada (1928) made a study of the reaction of MgO and $Mg(OH)_2$ with waters saturated with CO_2, and on page 41 of the English abstract he writes:

> When MgO or $Mg(OH)_2$ is used as the sample, the water is charged with CO_2 gas so that it remains always at saturation, they dissolve very quickly, and soon attain a state of supersaturation, forming a meta-stable solution of $Mg(HCO_3)_2$.
>
> $MgCO_3 \cdot 3H_2O$, in the same condition as above stated, dissolves slowly; and only the stable saturated solution is obtained, forming no meta-stable solution.

He further found that the metastable solution decomposes just on standing and that the addition of a small quantity of magnesium carbonate crystals will destroy the metastability, causing CO_2 gas to escape and precipitating an undetermined solid phase.

It appears from the comprehensive studies of Terada that irrespective of the original starting materials, the resulting solution will stabilize itself and end as a solution of magnesium carbonate. Haehnel (1924) also found his solubility studies for $MgCO_3 \cdot 3H_2O$ to be independent of the starting materials.

The system: CaO-CO_2-H_2O

This system has been studied in considerable detail at relatively low temperatures by Johnston and his coworkers. Frear and Johnston (1929) have given a list of the reliable solubility determinations for calcite and have prepared a table of solubilities for 25° C. and for CO_2 pressures ranging from 3.2×10^{-4} to 10 atmospheres, based on the data of all workers (Fig. 7). Haehnel (1924) has measured the solubility of calcium carbonate between 10 and 56 atmospheres pressure of CO_2 at 18° C. and at temperatures from 18° to 55° C. at a constant pressure of CO_2 of 56 atmospheres.

The great difference in the solubility of calcium carbonate (calcite) and magnesium carbonate trihydrate (nesquehonite) is easily seen on comparing Figs. 6 and 7. In comparing these two diagrams, it should be observed that the scales along the axis representing the pressure of carbon dioxide are identical in both figures but that the scales along the other two axes are not the same. In Fig. 6, the temperature axis covers the range of 0° C. to 100° C. while the corresponding axis in Fig. 7 covers the range of 0° C. to 60° C. The scale representing composition in Fig. 6 covers the range of 0 to 140 grams per liter of $MgCO_3 \cdot 3H_2O$ while the same distance in Fig. 7 covers the range in composition of 0 to 5 grams per liter of $CaCO_3$. In other words the diagram for the solubility relations of calcite is greatly magnified in comparison with that of magnesium carbonate. This disproportionate solubility of the carbonates in water charged with carbon dioxide will permit the separation of one carbonate from the other. Thus at a pressure of carbon dioxide of 1 atmosphere and at a temperature of 19.5° C., magnesium carbonate trihydrate is soluble to the extent of 42.3 grams per liter of water, whereas calcium carbonate will only dissolve to the extent of 1.08 grams per liter at 18° C. At 10 atmospheres pressure of CO_2 and 18° C., calcium carbonate is soluble to the extent of 2.56 grams per liter, whereas magnesium carbonate trihydrate at 10 atmospheres pressure of carbon dioxide and at a temperature of 18° C. dissolves to the extent of 96.8 grams per liter.

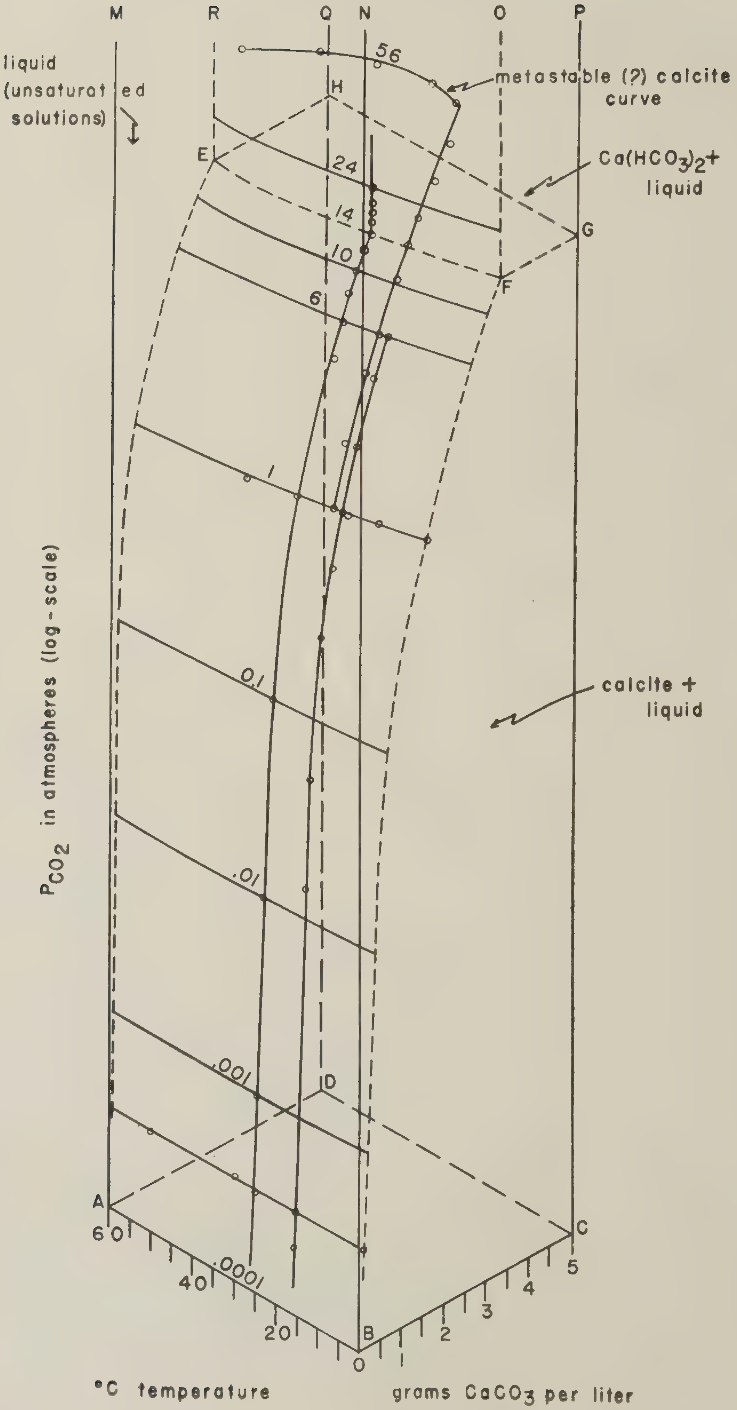
M
R
Q
N
O
P
56
liquid (unsaturated solutions)
H
metastable (?) calcite curve
E
24
$Ca(HCO_3)_2$ + liquid
14
G
10
F
6
1
P_{CO_2} in atmospheres (log-scale)
calcite + liquid
0.1
.01
.001
D
A
C
60
40
.0001
20
B
0
1
2
3
4
5
°C temperature
grams $CaCO_3$ per liter

According to Mitchell (1923) and others, at carbon dioxide pressures of 15 atmospheres and greater, the solid phase in equilibrium with the solution is calcium bicarbonate. Haehnel (1924), working at high pressures and temperatures, did not, according to his interpretation, find the solid phase calcium bicarbonate, but actually observed a decrease in the solubility of calcite. If this is the correct interpretation, it may be that Haehnel actually followed the metastable solubility curve of calcite in this region.

The phase relationships existing in the system CaO-CO_2-H_2O, from 0° C. to 100° C. and at pressures of CO_2 ranging from 1×10^{-4} atmospheres to 56 atmospheres, have been sketched in Fig. 7. These boundaries have been drawn based on (*a*) the solubility data of calcite, and (*b*) on the stability relations of calcium bicarbonate. The stability relationships of $CaCO_3 \cdot 6H_2O$ are not too well known and so have been ignored. They would not affect the thesis of this paper.

In the reaction between dedolomitized rock and hydrothermal solutions charged with carbon dioxide, we are concerned with the solubility of calcite in such solutions. According to Tillmans and Heublein (1912) this proceeds as follows:

$$[CaCO_3 + H_2O + nCO_2 \rightleftarrows Ca(HCO_3)_2 + (n-1)CO_2] \tag{14}$$

the reaction taking place in aqueous solution and at a definite pressure of carbon dioxide in equilibrium with the solution. The aforementioned data on the solubility of calcite show that although the solubility of calcite is low at low pressures of carbon dioxide it does increase somewhat with an increase in pressure of CO_2 and such an increase would drive the reaction, expressed in equation 14, to the right. The increase in solubility of calcite, however, does not compare with that of magnesium carbonate trihydrate.

The solubility of calcite generally increases in the presence of other ions and this has been studied by Frear and Johnston (1929), who give data for the solubility of calcite in solutions of NaCl and $CaSO_4 \cdot 2H_2O$. They found the solubility of calcite in one molal sodium chloride to be practically double that in the absence of the salt. Calcium sulfate slightly decreases the solubility of calcite.

The system: MgO-CaO-CO_2-H_2O

The data previously given are for the two ternary and two binary systems that belong to the quarternary system. Very little systematic data are available for the quarternary system and these data concern

---

FIG. 7. The solubility of calcium carbonate in water and in equilibrium with various carbon dioxide pressures. Based on data summarized by Frear and Johnston and the determinations of Haehnel. The field of stability of $CaCO_3 \cdot 6H_2O$ has been ignored.

the solubility of dolomite, a relationship not pertinent to this discussion.

A considerable amount of information on this system has been determined in connection with the recovery of magnesium compounds from calcined dolomite. The assemblage of phases in such calcined dolomites, particularly the partially calcined dolomite, corresponds closely to those present in the naturally occurring dedolomitized rocks. From the previous discussion we note (1) that calcite is much less soluble than magnesium carbonate in water containing carbon dioxide; (2) that MgO forms a highly soluble carbonate when it reacts with a solution rich in carbon dioxide. As a result of these relationships, a mixture of MgO and $CaCO_3$ will react with a solution of water rich in carbon dioxide, with the transference of most of the magnesium but with only a minor amount of the calcium into the liquid phase.

Experimental evidence supporting these conclusions is furnished by the work of Doerner, Holbrook, and Fortner (1946). These workers studied means of removing the magnesium from dolomite. They calcined dolomite selectively so that only the magnesium carbonate was dissociated and the resulting product consisted of MgO (periclase) and $CaCO_3$ (calcite). Their calcination studies were carried out under various conditions: (*a*) in the presence of CO_2; (*b*) in vacuo; (*c*) in air. Their experiments on the calcination of dolomite in the presence of CO_2 suggest parallelism with the conditions prevailing in the natural process of dedolomitization and so only these results are considered here.

Their procedure was as follows: dolomite was calcined selectively in a CO_2 atmosphere to give a mixture of MgO (periclase) and $CaCO_3$ (calcite), and this calcine was leached in a solution of water saturated with carbon dioxide at 20° C. The resulting solution was analyzed. They found that a dolomite calcined so that 47.8 per cent of it was dissociated gave up 90.8 per cent of its MgO in 40 minutes when leached by a solution of carbon dioxide in water at 20° C. The resulting solution contained *only 0.0008 gram of calcium oxide per liter.* The leaching reaction evolves heat. These authors also measured the pH of saturated solutions of the various components and these are given in Table 3.

TABLE 3. pH OF SATURATED SOLUTIONS OF THE VARIOUS COMPONENTS AT 20° C. DATA OF DOERNER, HOLBROOK, AND FORTNER (1946)

Saturated solution	pH
Carbon dioxide in water	5.0
MgO in water	10.6
$Mg(HCO_3)_2$ in water	7.5
CaO in water	13.0
$Ca(HCO_3)_2$ in water	6.35

They state further:

> A batch of calcine in water has a pH between 10.6 and 13.0. When it is charged with CO_2, the pH gradually drops to 7.5 as the concentration of MgO in the solution approaches the "saturation value" (10.0 grams per liter at 20° C.) and remains constant at 7.5 when supersaturation is attained. Since the pH of $Ca(HCO_3)_2$ is less than 7.5, the solubility of the lime is low in a saturated $Mg(HCO_3)_2$ solution.

Evidence that some of the reactions outlined above take place on a large scale is afforded in a brief description of a commercial chemical plant operation. The physical chemical relationships in the preparation of magnesium from dolomite at the Austin plant of the International Minerals and Chemical Corporation have been described by Manning and Kirkpatrick (1944). In this process dolomite is completely calcined to a mixture of CaO (lime) and MgO (periclase), and its mixture of oxides is slaked in water resulting in the formation of hydroxides and some unreacted oxides. The slurry so prepared is carbonated by the introduction of carbon dioxide gas under pressure. Calcium carbonate is precipitated as a finely divided solid and the magnesium is retained in the solution.

In summary of the foregoing chemical data on the system MgO-CaO-CO_2-H_2O, we find that dolomite which has been dissociated to a mixture of lime (CaO) and periclase (MgO) will react with a solution of water charged with carbon dioxide to yield a precipitate (or reaction product) of calcite and a solution containing magnesium carbonate and a disproportionately smaller amount of calcium bicarbonate. If such a solution is aerated or some of the carbon dioxide can escape in another way, much of the remaining calcium bicarbonate will be precipitated as calcite, and a still purer magnesium-rich carbonated solution will be formed. If, on the other hand, dolomite is partially dissociated to a mixture of calcite ($CaCO_3$) and periclase (MgO) and this is reacted with a solution of water charged with carbon dioxide, the periclase will be converted to magnesium carbonate and remain in the solution, whereas the calcite is only slightly dissolved and a relatively small amount enters into the solution. The relationships observed for the partially dissociated dolomite are of considerable interest in this discussion for they provide a mechanism for the derivation of magnesium-rich solutions from the brucite marbles (predazzite and pencatite).

The solubility data for magnesium carbonate trihydrate show that as the temperature is raised, the solubility is decreased and that an increase in the pressure of carbon dioxide offsets this decrease. A decrease in the solubility at higher temperatures changes the quantitative relations in that larger volumes of water charged with carbon dioxide will be needed to leach an equivalent amount of periclase in comparison with that reacted at lower temperatures.

It must be emphasized here that the reactions between a partially dissociated dolomite, consisting of periclase and calcite, and a hydrothermal solution charged with carbon dioxide and considered in this discussion, are entirely different from the relationships involved in the attack of the same solutions on the rock dolomite. Dolomite is another phase in the quaternary system $MgO\text{-}CaO\text{-}CO_2\text{-}H_2O$ and its solubility relationships have been discussed elsewhere by Faust and Callaghan (1948).

The Process of Dedolomitization

The process of dedolomitization may be considered to take place in the following manner. After the magma has been emplaced and has started to cool, heat will be conducted from it to the country rock and some of the vapor phase associated with the magma will try to escape at the periphery of the intrusive mass. This vapor phase will escape into the fracture system of the country rock, along intergrain boundaries, and through capillary and subcapillary openings in the rocks. At the contact with the dolomite, it will be joined by CO_2 liberated from xenoliths and CO_2 liberated by reaction with the wall rock. The resulting mixed-gas phase is no longer in equilibrium with the magma and is most certainly not in equilibrium with the country rock. The chemical species which make up the gaseous phase are dominantly H_2O and CO_2. In addition, minor amounts of B, Cl, S, etc., are present. In such an environment as this, the stability of the various phases will depend on temperature and pressure conditions. It is possible for anhydrous phases to exist in equilibrium with H_2O, most of which is in the gaseous phase. In this stage, periclase may form as a stable mineral. It is noteworthy also that the zone containing periclase is, as Harker (1904) remarks, closest to the intrusive mass. As the magma crystallizes, the proportion of emanations derived from the magma will increase in amount and at some later stage, the magmatic solution will be composed largely of water together with the residual constituents, "the hyperfusibles of Bowen." This fluid phase will migrate from the cooling rock and become the hydrothermal solution. As this solution and its accompanying vapor phase move into the country rock, they will react with the earlier formed periclase to produce brucite. This reaction, as judged from the texture of the brucite whorls, does not take place over a whole crystal of periclase at once, but rather is the result of successive stages of hydration (see Fig. 8). The periclase now present in these rocks was protected by an armor of brucite. As these hydrothermal solutions move through the country rock, they will dissolve some of the brucite.

The hydrothermal solutions which formed the brucite did not contain much CO_2, for brucite is unstable in contact with CO_2-bearing solutions except for very low concentrations. Kline (1929) states:

> For with decreasing partial pressure of carbon dioxide there corresponds an increase in the ratio $[(OH^-)/(CO_3^=)]$ and, owing to the fact that magnesium hydroxide is much less soluble than the carbonate there is a pressure below which the hydroxide becomes the stable solid phase. . . .

Many of those who have studied brucite marble, predazzite, and pencatite, both in the field and the laboratory, agree that the first stage in dedolomitization is the dissociation of dolomite to periclase and calcite. Keith (1946) believes that for the deposits studied by him, the brucite was formed by the action of superheated steam on dolomite. The absence of periclase in his rocks leads him to believe that it may never have been present.

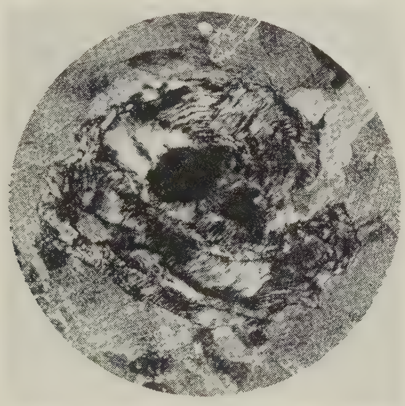

FIG. 8. Whorls of brucite surrounding periclase. Note that the oriented foliae in each whorl are not related to those in the adjacent whorls. This is a photograph of the same area recorded in Fig. 2, made with crossed nicols. Mag. 75×. Brucite and periclase in pencatite from the Organ Mountains, New Mexico.

LATER STAGES OF HYDROTHERMAL ACTIVITY AND THE DEVELOPMENT OF MAGNESIUM-RICH SOLUTIONS

(*a*) *Leaching of dedolomitized rocks by hydrothermal solutions poor in carbon dioxide.*

The more or less continuous migration of successive surges of hydrothermal solutions through the aureole of metamorphism in the carbonate rocks may dissolve some of the brucite. The amount dissolved will depend on the temperature, the ions present, and the volume of the hydrothermal solutions which traverse the rocks. Long-continued leaching by dilute solutions poor in carbon dioxide can remove appreciable quantities of brucite. Keith (1946) has observed a cellular limestone in the Rutherglen District, Ontario, which he attributes to the leaching of the brucite by dilute magmatic solutions. In some deposits the amount of leaching has been small, for in pencatite the ratio of magnesium to calcium is that required by the composition of dolomite. Analyses of several brucite marbles, the predazzites, show, on the other hand, less magnesium than the theoretical ratio. Some of these rocks may be metamorphosed magnesian limestones, whereas others may represent brucite marbles leached of part of their brucite. Evidence for the movement of brucite is given by Keith (1946), who noted that the ratio of magnesium to calcium in some rocks studied by him exceeded the theoretical values for dolomite. This certainly indicates that successive waves of hydrothermal solutions reworked the brucite. Some calcite may also have been reworked by these later solutions.

It is possible thus by reworking brucite and periclase, formed at an earlier stage, to derive a hydrothermal solution which will be able to deposit brucite. These relations probably account for the formation of brucite in and near some magnesite deposits and they also offer a mechanism for the migration of brucite in magnesite deposits.

(*b*) *Reaction of dedolomitized rocks with hydrothermal solutions rich in carbon dioxide.*

The passage of a hydrothermal solution rich in carbon dioxide over a completely dissociated dolomite will convert the lime to calcite and dissolve the periclase and yield a solution which will be rich in magnesium and poor in calcium. Calcium bicarbonate is much less stable than magnesium carbonate in such a solution and it tends to precipitate out as calcite. This process is similar to the industrial process at Austin, Texas, mentioned previously.

Where the hydrothermal solutions rich in carbon dioxide seek egress through partially dissociated dolomite, the reaction is still simpler. Calcite will be only slightly soluble while the periclase will be dissolved. The resulting hydrothermal solution will be rich in magnesium and carbon dioxide and relatively poor in calcium. The analogous chemical process has been studied at lower temperatures than those of hydrothermal solutions by Doerner, Holbrook, and Fortner (1946). Hydrothermal solutions rich in carbon dioxide which traverse predazzite and pencatite may react with the brucite and residual periclase to form a solution of magnesium carbonate. Some calcite may also dissolve but, as mentioned before, the concentration of calcium bicarbonate is not likely to be significant.

The mechanisms here proposed for deriving hydrothermal solutions, rich in magnesium and carbon dioxide and relatively poor in calcium, through the selective reaction of a hydrothermal solution rich in carbon dioxide upon dedolomitized rocks are simple, straightforward chemical processes which require no unusual chemical constituents.

(*c*) *Subsequent reactions of hydrothermal solutions rich in magnesium and carbon dioxide with the country rock.*

If the proposed mechanism produces, in nature, hydrothermal solutions rich in magnesium and carbon dioxide, the question arises as to the probable ways by which these hydrothermal solutions will give up their mineralizing constituents. If we assume that the solutions continue to migrate away from the zone of higher temperatures into the cooler country rock, these hydrothermal solutions will become cooler. If they enter zones of greater porosity, they may lose some of their carbon dioxide to the country rocks. Either, or both, of these changes may bring about the approach to saturation conditions for magnesium carbonate, (magnesite). The structural relationships of the country rock, its texture, and chemical and mineralogical character will determine the manner in which the magnesium and carbon dioxide will be removed from the solutions.

If the country rock is chemically inert with respect to the solutions, they will pass through the fracture systems, deposit magnesite in veins or fillings. However, they may continue and possibly move into the upper levels of the crust, mingle with cooler meteoric waters, and eventually emerge as springs at the earth's surface, where they may deposit hydromagnesite, $3MgCO_3 \cdot Mg(OH)_2 \cdot 3H_2O$, in "sinter" form.

In areas where hydrothermal solutions rich in magnesium and carbon dioxide enter limestone, dolomitization takes place. Armoring of the calcite by dolomite will protect larger masses of limestone from reaction. This phenomenon is well illustrated by the description and figures in Hewett (1928) concerning the islands of limestone in dolomite at Iglesias in Sardinia. Zoning, by dolomitization, about the fracture system, or between limestone and an inert rock may yield channelways along which the hydrothermal solutions can migrate without further reaction with the limestone. These magnesium-rich solutions, because of their failure to react with limestone protected by armoring or zoning, may deposit magnesite in the fracture system. Magnesite may form in direct contact with dolomite with which it is in equilibrium. Bain (1924) and Hewett (1928) have both pointed out examples of zoning. Hewett (1928) writes:

> Where magnesite appears to replace limestone near its contact with intrusive igneous rocks, especially in Styria, Austria; Stevens County, Washington; and Argenteuil County,

Quebec, there is a zone of dolomite between the limestone and the magnesite which lies next to the intrusive rock.

An examination of the literature on dedolomitized dolomites shows that in the vicinity of some of these rocks magnesite has been found, whereas in others it is lacking.

In the Organ Mountains in New Mexico, Dunham (1935) describes the presence of lenticular masses of magnesite as much as 5 feet in thickness. Concerning their origin he writes (p. 36):

> Metamorphism of the dolomite xenoliths by the quartz-monzonite converted them into periclase marbles, consisting essentially of periclase and calcite . . . at a later stage periclase and forsterite were in part converted into brucite and serpentine. Later still, the xenoliths were invaded by solutions, probably rich in carbon dioxide which were able to convert the marble into magnesite.

And again on page 104, Dunham writes:

> The further change of brucite marble into magnesite probably belongs to a much later stage in the history of the rock, but, as it is difficult to decide definitely the time of this change it will be considered here. The nature of the change is shown by the analyses. . . . There is a decrease in lime and an increase in magnesia and carbon dioxide; the reaction also involves the removal of water:
>
> $$[Mg(OH)_2 + CO_2 = MgCO_3 + H_2O].$$
>
> It is suggested that waters charged with carbon dioxide would be capable of effecting this reaction. The lime would be removed as calcium bicarbonate and the magnesia precipitated as the carbonate magnesite, which if the process is to work, must be supposed to be less soluble in carbonated water than calcium carbonate. Temperature may have been a controlling factor. A very porous rock was produced.

Magnesite has been reported from the 910-foot level of the Commercial quarry at Crestmore, Calif., by Woodford, Crippen, and Garner (1941).

Magnesite has not been found at Wakefield, Wilkinson, or Rutherglen in Ontario; in the Cottonwood-American Fork area, Utah; Philipsburg, Mont.; nor at the deposits of Korea. The chemical analyses of some of the specimens from the localities in Ontario suggest that magnesite may be present, Keith (1946). The author believes that the absence of magnesite at these localities arises from the reaction relationship pointed out previously. That is, any hydrothermal solution rich in magnesium and carbon dioxide was consumed in the process of dolomitizing the neighboring limestone rocks. Dolomitization of the limestones is recognized at the Cottonwood-American Forks area, Utah, and at Philipsburg, Mont.

Brown (1943) has noted that the chief constituents of the brucite-bearing lenses at Wilkinson, Ontario, are calcite, dolomite, and brucite; and that the proportions of these minerals vary from place to place. He states also that (page 410).

Calcite and dolomite (in the brucitic limestone) form a mosaic of closely interlocking grains traversed by tiny stringers of dolomite, which also cuts through the spherules of brucite. In places this later carbonate forms areas with micrographic texture, which are probably due to replacement of the older carbonate by later ones.

Dolomite is also present in the brucitic limestones at Rutherglen (Keith).

SUMMARY OF THE DOLOMITE RELATIONSHIPS

A summary of the dolomite relationships as given in the paper by Faust and Callaghan (1948) is presented here for purposes of comparison of the two proposed mechanisms.

The solubility of dolomite in solutions rich in carbon dioxide has been studied by several investigators and at present the following views are held:

(*a*) Dolomite is congruently soluble in carbon dioxide rich waters—that is, dolomite dissolves completely without the separation of a solid phase. Faust and Callaghan (1948) reasoned that the congruent solubility of dolomite might be the normal relationship and, by the use of the existing experimental data on the attempts at synthesis of dolomite, proposed a mechanism for deriving a magnesium- and carbon dioxide-rich solution. A solution of magnesium and calcium in the proportions necessary to form dolomite, and containing carbon dioxide may, under conditions of metastability, precipitate calcite, and leave a solution rich in magnesium and carbon dioxide. If these constituents are left together they will react to form dolomite, but if they can be separated, a magnesium-rich solution will result. It is necessary that there be sufficient CO_2 in the system to keep the magnesium in solution. Thus a hydrothermal solution rich in carbon dioxide may attack dolomite and dissolve it congruently. As the solutions move on, they may later precipitate their calcium content as calcite; the remaining solution will then be rich in magnesium and carbon dioxide. These solutions will dolomitize the calcite if left in contact with it, but if they move on, they can dolomitize other calcareous rocks.

(*b*) Dolomite is incongruently soluble in carbon dioxide-rich waters, that is, it dissolves to yield a solution and a solid phase other than dolomite. Two possibilities must be considered in this relationship. Incongruent solubility of dolomite may give rise, either (1) to a solution rich in magnesium with the separation of the solid-phase calcite, or, (2) to a solution rich in calcium with the separation of the solid-phase magnesite. If the solubility of dolomite takes place according to (1), the solution will be magnesium rich. After migration away from its source to areas of different porosity and temperature, the solution may deposit magnesite or react with limestones to form dolomite. If solubility of dolomite takes place according to (2), an insoluble residue of magnesite will result. A later surge of hydrothermal solutions may dissolve this residue, which thus will produce magnesium-rich solutions.

(*c*) Dolomite exhibits both congruent and incongruent solubility depending on the variables --temperature, pressure of carbon dioxide, or the concentration of other ions in solution. All these possibilities can be used to derive magnesium-rich solutions either by the selective leaching of magnesium or by the removal first of the calcium by leaching followed by the subsequent attack on a magnesium carbonate residue.

It should be re-emphasized that the two proposed mechanisms are not identical. The earlier mechanism proposed by Faust and Callaghan (1948) involves the attack of hydrothermal solutions rich in carbon dioxide upon dolomite. The phase relationships concerning this mechanism are referred to the quaternary system $MgCO_3$-$CaCO_3$-H_2O-CO_2. The second mechanism proposed by Faust, in this paper, involves the attack of hydrothermal solutions rich in carbon dioxide upon previously dedolomitized dolomites. They consist of periclase (MgO) and/or brucite ($Mg(OH)_2$) with calcite; and the phase relationships are referred to the quaternary system CaO-MgO-CO_2-H_2O.

Both mechanisms, however, do yield solutions rich in magnesium and carbon dioxide. It must not be concluded that the author believes that these are the only methods by which solutions may become enriched in magnesium and carbon dioxide. It is his belief that these two mechanisms offer a satisfactory explanation for the widespread dolomitization associated with ore deposition. The common association of magnesite and serpentinized peridotites and dunites requires another mechanism, and Bowen and Tuttle (1949) have proposed one. If the hydrothermal solutions rich in magnesium and carbon dioxide and derived from such intrusives migrate into the country rock and encounter limestone, the ensuing reactions between the hydrothermal solutions and the limestone will be governed by the same principles given in this paper and the paper by Faust and Callaghan (1948).

Summary and Conclusions

This paper describes a mechanism for the derivation of a magnesium-rich solution through the attack of hydrothermal solutions, rich in carbon dioxide, upon metamorphosed dolomites such as predazzite, pencatite, and brucite marble.

In order to gain an understanding of the origin of these dedolomitized rocks, the physical chemistry of the dissociation of dolomite is examined. Thermal analysis data show that contact metamorphism of dolomites can produce two types of rocks. The complete dissociation of dolomite results in the formation of lime and periclase. No geologic occurrence of a completely dissociated dolomite which contains lime is known. The partial dissociation of dolomite results in the formation of periclase and calcite, and rocks containing these minerals are well known. Periclase is quite unstable and alters to brucite.

From a study of the heat exchange relations between the hot magma, which supplied the heat necessary for metamorphism, and the country rock, it is concluded that heat conduction from solid to solid will not alone suffice to explain the relations in the process of dedolomitization. It is proposed, here, that the magmatic emanations and the carbon dioxide liberated in the process of dedolomitization served as important agents in the transfer of heat. Three factors which make the magmatic emanations important in contact metamorphism are (1) their greater specific heat (heat capacity); (2) their mobility, which serves to transport the heat quickly to the country rock; and (3) their ability to enter into reactions with the country rock while at elevated temperatures.

The physical-chemical data concerning the system MgO-CaO-CO_2-H_2O allow the following conclusions to be drawn: (1) that calcite is much less soluble than magnesium carbonate in water containing carbon dioxide; (2) that MgO forms a highly soluble carbonate when it reacts with a solution rich in carbon dioxide. As a result of these relationships, a dedolomitized dolomite, consisting of MgO (periclase) and $CaCO_3$ (calcite) will react with a solution of water rich in carbon dioxide, with the transfer of most of the magnesium but with only a minimum amount of calcium into the liquid phase. This is the mechanism proposed for the derivation of a magnesium-rich hydrothermal solution.

Acknowledgments

I wish to thank Professor Eugene Callaghan, formerly in charge of the geologic studies on magnesium minerals and rocks for the U. S. Geological Survey and now of Indiana University, for his kind interest and continuous encouragement in this work. I have derived much from him in many discussions, both in the field and in the laboratory, on the probable nature and relationships of the hydrothermal solutions which served as agents for the formation of magnesite and brucite deposits.

I am indebted to Drs. Michael Fleischer, Clarence S. Ross, and Earl Ingerson for a critical reading of the paper. Likewise, I wish to thank my colleague, H. Cecil Spicer, for a careful reading of the sections on the heat relations.

Professor W. F. Hunt, Editor, *The American Mineralogist*, and Professor Alan M. Bateman, Editor, *Economic Geology*, kindly loaned the

cuts for figures 2 and 8, and figure 3, respectively. Professor W. H. Parsons, Editor, *Journal of the American Chemical Society* granted permission to reproduce figure 5.

BIBLIOGRAPHY

Adams, L. H. (1924), A physical source of heat in springs: *Jour. Geology*, **32**, 191–194.

Ambrose, J. W. (1943), Brucitic limestones and hastingsite syenite near Wakefield, Quebec: *Royal Soc. Canada Proc. and Trans.*, 3rd Ser. **37**, 9–22.

Bain, G. W. (1924), Types of magnesite deposits and their origin: *Econ. Geol.*, **19**, 412–434.

Bär, Otto (1932), Beitrag zum Thema Dolomitenstehung: *Centralbl. Mineral.* Abt. A., 46–62.

Birch, F., and Clark, Harry (1940), The thermal conductivity of rocks and its dependence upon temperature and composition: *Am. Jour. Sci.*, **238**, 529–558 and 613–635.

Bowen, N. L. (1933), The broader story of magmatic differentiation briefly told; in Ore Deposits of the Western States (Lindgren Volume): *Am. Inst. Min. Met. Eng.*, Part 2, Chapter 3, 106–128.

Bowen, N. L. (1940), Progressive metamorphism of siliceous limestone and dolomite: *Jour. Geology*, **48**, No. 3, 225–274.

Bowen, N. L., and Tuttle, O. F. (1949), The system MgO-SiO_2-H_2O: *Bull. Geol. Soc. Am.*, **60**, 439–460.

Brown, I. C. (1943), Brucite in limestone near Wilkinson, Ontario: *Econ. Geology*, **38**, 408–419.

Buddington, A. F. (1933), Correlation of kinds of igneous rocks with kinds of mineralization: in Ore Deposits of the Western States (Lindgren Volume): *Am. Inst. Min. Met. Eng.*, 350–385.

Cameron, F. K., and Seidell, A. (1903), The solubility of magnesium carbonate in aqueous solutions of certain electrolytes: *Jour. Physical Chem.*, **7**, No. 8, 578–590.

Cameron, F. K., and Robinson, W. O. (1907), The solubility of calcium carbonate in aqueous solutions of potassium chloride and potassium sulfate at 25°: *Jour. Physical Chem.*, **11**, No. 8, 577–580.

Doerner, H. A., Holbrook, W. F., and Fortner, O. W. (1946), The bicarbonate process for the production of magnesium oxide: *U. S. Bur. Mines, Tech. Paper* **684**, 48 pp.

Dunham, K. C. (1935), The geology of the Organ Mountains: *New Mexico School of Mines, Bulletin* **11**.

Dunham, K. C. (1936), Xenoliths in the Organ batholith, New Mexico: *Am. Mineral.*, **21**, 312–320.

Engel, P., and Ville, J. (1881), Sur la solubilité du carbonate de magnésie dans l'eau chargée d'acide carbonique: *Compt. rend.*, **93**, 340–341.

Faust, G. T. (1944), The differentiation of magnesite from dolomite in concentrates and tailings: *Econ. Geology*, **39**, 142–151.

Faust, G. T. (1944–48), Thermal analysis studies: Unpublished work.

Faust, G. T., and Callaghan, Eugene (1948), The mineralogy and petrology of the Currant Creek magnesite deposits and associated rocks of Nevada: *Bull. Geol. Soc. America*, **59**, 11–74.

Frear, G. L., and Johnston, J. (1929), The solubility of calcium carbonate (calcite) in certain aqueous solutions at 25° C: *Jour. Am. Chem. Soc.*, **51**, 2082–2093.

Goudge, M. F. (1939), A preliminary report on brucite deposits in Ontario and Quebec and their commercial possibilities: *Ontario Dept. Mines, Rept. Ser. No.* **75**.

Griggs, David (1946), in Knopf, E. B., Study of experimentally deformed rocks: *Science*. *New Ser.* **103**, No. 2665, p. 103.

Haehnel, Otto (1924), Über die Löslichkeit des Magnesiumcarbonats in kohlensäurehaltigem Wasser unter höheren Kohlendioxyddrucken und über die Eigenschaften solcher Magnesiumbicarbonatlösungen: *Jour. prakt. Chemie,* **108,** 61–74.

Haehnel, Otto (1924), Über die Löslichkeit des Calciumcarbonats in kohlensäurehaltigem Wasser unter hohen Drucken und die Eigenschaften solcher Lösungen: *Jour. prakt. Chemie,* **107,** 165–176.

Halla, Franz (1936), Über die freie Energie bei der Dolomitbildung: *Min. pet. Mitt., Band* **48,** 275–278.

Harker, A. (1904), The Tertiary igneous rocks of Skye: *Great Britain Geol. Survey Mem.,* 144–151 (with definition on p. 150).

Hewett, D. F. (1928), Dolomitization and ore deposition: *Econ. Geology,* **23,** No. 8, 821–863.

Hunt, W. F., and Faust, G. T. (1937), Pencatite from the Organ Mountains, New Mexico: *Am. Mineral.,* **22,** 1151–1160.

Keith, M. L. (1946), Brucite deposits in the Rutherglen district, Ontario: *Bull. Geol. Soc. Am.,* **57,** 967–984.

Kline, W. D., (1929), The solubility of magnesium carbonate (nesquehonite) in water at 25° C. and pressures of carbon dioxide up to one atmosphere: *Jour. Am. Chem. Soc.,* **51,** 2093–2097.

Manning, P. D. V., and Kirkpatrick, J. D. (1944), Better utilization of mineral resources through new chemical technology: *Chem. Met. Eng.,* **51,** 92–96.

Mitchell, A. E. (1923), Studies on the dolomite system—part 2: *Jour. Chem. Soc. London,* **123,** 1887–1904.

Prutton, C. F., and Savage, R. L. (1945), The solubility of carbon dioxide in calcium chloride-water solutions at 75, 100, 120° and high pressures: *Jour. Am. Chem. Soc.,* **67,** 1550–1554.

Rivett, A. C. D. (1923), The phase rule and the study of heterogenous equilibria, Chapter 2, The Principle of Le Chatelier-Braun: Oxford University Press, Oxford

Rogers, A. F. (1918), An American occurrence of periclase and its bearing on the origin and history of calcite-brucite rocks: *Am. Jour. Sci.,* **46,** 581–586.

Rogers, A. F. (1929), Periclase from Crestmore near Riverside, California, with a list of minerals from this locality: *Am. Mineral.,* **14,** 462–469.

Ross, Clarence S. (1928), Physico-chemical factors controlling magmatic differentiation and vein formation: *Econ. Geology,* **23,** No. 8, 864–886.

Smyth, F. H., and Adams, L. H. (1923), The system calcium oxide-carbon dioxide: *Jour. Am. Chem. Soc.,* **45,** 1167–1184.

Terada, Kiyomatsu (1928), On the solubility of magnesium carbonate in aqueous solutions charged with CO_2: *Inst. Physical Chem. Research, Tokyo, Bull.* **7,** 452–465. (In Japanese). See also: Abstracts—*Inst. Physical Chem. Research, Tokyo, Bull.,* **1,** No. 4, 41–42, 1928 (In English).

Tillmans, J., and Heublein, O. (1912), Über die kohlensäuren kalk angreifende Kohlensäure der natürlichen Wässer: *Gesundheits-Ing. Jahrg.,* **35,** No. 34, 669–677.

Wiebe, R., and Gaddy, V. L., (1939), The solubility in water of carbon dioxide at 50°, 75° and 100° at pressures to 700 atmospheres: *Jour. Am. Chem. Soc.,* **61,** 315–318.

Wiebe, R., and Gaddy, V. L. (1940), The solubility of carbon dioxide in water at various temperatures from 12° to 40° and at pressures to 500 atmospheres. Critical Phenomena. *Jour. Am. Chem. Soc.,* **62,** 815–817.

Woodford, A. O., Crippen, R. A., and Garner, K. B. (1941), Section across commercial quarry, Crestmore, California: *Am. Mineral.,* **26,** 351–381.

Zambonini, F., and Quercigh, E. (1935), Mineralogia Vesuviano: Second Edition, Naples, p. 58.

ON THE SYMMETRY AND CRYSTAL STRUCTURE OF BORNITE

G. Tunell and C. E. Adams, *Dept. of Geology, University of California at Los Angeles, California.*

Abstract

Analysis of rotation and Weissenberg photographs of a single crystal of bornite from the Carn Brea Mine, Illogan, Cornwall, has led to the conclusion that the crystal structure of bornite is not strictly isometric, but is pseudo-isometric, and is approximated by an arrangement in a cubic cell of edge-length 5.47 Å of four sulfur atoms at 000, $\frac{1}{2}\frac{1}{2}0$, $0\frac{1}{2}\frac{1}{2}$, $\frac{1}{2}0\frac{1}{2}$, with four copper or iron atoms statistically distributed over the positions $\frac{1}{4}\frac{1}{4}\frac{1}{4}$, $\frac{3}{4}\frac{3}{4}\frac{1}{4}$, $\frac{1}{4}\frac{3}{4}\frac{3}{4}$, $\frac{3}{4}\frac{1}{4}\frac{3}{4}$, and two copper or iron atoms statistically distributed over the positions $\frac{1}{4}\frac{3}{4}\frac{1}{4}$, $\frac{3}{4}\frac{1}{4}\frac{1}{4}$, $\frac{1}{4}\frac{1}{4}\frac{3}{4}$, $\frac{3}{4}\frac{3}{4}\frac{3}{4}$, the total number of copper atoms in the cell being five and the total number of iron atoms being one on the average.

Although bornite usually occurs in nature in aggregates of anhedral grains, a few euhedral crystals have been found. These have cubic, dodecahedral, and more rarely octahedral habit.[1] In polished surfaces under the microscope most specimens of bornite appear to be isotropic, but some exhibit weak anisotropism.[2] The observation of this weak anisotropism suggested to Professor M. N. Short[3] that bornite is not truly isometric, but merely pseudo-isometric.

The crystal structure of bornite has been investigated by x-ray methods by de Jong[4] and by Lundqvist and Westgren.[5] The structure deduced by de Jong is in marked disaccord with the observed intensities, as stated by Lundqvist and Westgren.[6] The cubic unit cell of edge-length 10.91 kX[7] which de Jong determined, was, however, confirmed by Lundqvist and Westgren. de Jong made a single crystal rotation photograph in addition to a powder photograph; Lundqvist and Westgren based their conclusions solely on powder photographs.

It was noted by one of us some time ago that not all the lines of two

[1] Palache, C., Berman, H., and Frondel, C., Dana's System of Mineralogy, Seventh Edition, New York (1944), vol. 1, p. 195.

[2] Short, M. N., Microscopic Determination of the Ore Minerals: *U. S. Geol. Survey, Bull.* **825** (1931), p. 76. Schneiderhöhn, H., and Ramdohr, P., Lehrbuch der Erzmikroskopie, Berlin (1931) vol. **2**, p. 336.

[3] Oral communication.

[4] de Jong, W., Over de kristalstructuren van arsenopyriet, borniet en tetraëdriet; *Doctoral Thesis*, Delft (**1928**).

[5] Lundqvist, D., and Westgren, A., *Arkiv för kemi, mineralogie och geologi*, **12B, 1–6** (1936).

[6] The line calculated by de Jong to have the third greatest intensity (66 on the scale in which 100 represents the greatest intensity) is actually not present at all on our Weissenberg photographs.

[7] The value given by de Jong was probably in kX units although labelled in Å units.

powder photographs of bornite made with cobalt K-radiation filtered through iron foil could be indexed on the basis of the cubic unit cell of de Jong and of Lundqvist and Westgren. For this reason a rotation photograph and a set of equi-inclination Weissenberg photographs were made[8] of a single crystal of bornite from the Carn Brea Mine, Illogan, Cornwall, kindly furnished by Professor M. A. Peacock of the University of Toronto. The rotation photograph shows strong zero, sixth and twelfth layer-lines, and weak second, third, fourth, eighth, ninth and tenth layer-lines; the first, fifth, seventh and eleventh layer-lines are absent. The crystal was rotated about a "cube" edge and the identity period along this axis was calculated from the separations of the layer-lines to be 32.8 Å ± 0.1 Å,[9] that is, three times greater than the length of the cell-edge of de Jong and of Lundqvist and Westgren. Point-by-point constructions of the reciprocal lattice layers corresponding to all the equi-inclination Weissenberg photographs were carried out by the method of Schneider.[10] The reciprocal lattice layers have axes making angles of ninety degrees and with the same unit-length as that obtained by taking the reciprocal of the identity period along the rotation axis. The axes thus exhibit cubic symmetry. All the diffraction spots on the Weissenberg photographs of strong and medium intensity, as well as part of the spots of weak intensity, can be indexed in terms of the cubic cell of edge-length 32.8 Å; there are in addition, however, very many weak spots on some of the layer-lines that cannot be indexed in terms of any cell that we could find any basis for assuming. Moreover, the distribution of many of the weak spots is not in accord with isometric symmetry.

All the spots of strong and medium intensity can also be indexed in terms of a cubic cell of edge-length 5.47 Å ($=\frac{1}{6}\times 32.8$ Å). The observed intensities of the spots on the Weissenberg photographs that would result from planes in a structure with this cubic cell are listed in Table 1. With the exception of three weak spots, namely, those with indices 100, 300 and 102, all have all odd or all even indices, indicating an approximation toward a face-centered cell. If such a cell is assumed as the unit cell of a structure approximating that of bornite, its content must be taken as Cu_5FeS_4. A structure with four copper or iron atoms distributed statistically over the positions $\frac{1}{4}\frac{1}{4}\frac{1}{4}$, $\frac{3}{4}\frac{3}{4}\frac{1}{4}$, $\frac{1}{4}\frac{3}{4}\frac{3}{4}$, $\frac{3}{4}\frac{1}{4}\frac{3}{4}$, two copper or iron atoms being distributed statistically over the positions $\frac{1}{4}\frac{3}{4}\frac{1}{4}$, $\frac{3}{4}\frac{1}{4}\frac{1}{4}$, $\frac{1}{4}\frac{1}{4}\frac{3}{4}$, $\frac{3}{4}\frac{3}{4}\frac{3}{4}$, the total number of copper atoms in the cell being five and the

---

[8] This work was carried out in the Geophysical Laboratory of the Carnegie Institution of Washington while the senior author was a member of the staff.

[9] Value based on the weighted average wave-length of cobalt Kα_1 and Kα_2 1.790 Å.

[10] *Zeit. Krist.*, **69**, 41–48 (1928).

TABLE 1

Observed and calculated intensities of diffraction spots of a single crystal of bornite on Weissenberg photographs. The indices refer to a cubic cell of edge-length 5.47Å (not the true unit cell). Numerous weak spots occur on some of the Weissenberg photographs that cannot be indexed on the basis of this cell; however, all the spots of medium and strong intensity can be so indexed and are listed in this table.

hkl	$I_{\text{obs.}}$	$I_{\text{calc.}}$	*hkl*	$I_{\text{obs.}}$	$I_{\text{calc.}}$	*hkl*	$I_{\text{obs.}}$	$I_{\text{calc.}}$
100	w*	0	101	—*	0	102	w*	0
200	st	53	201	—	0	202	st	100
300	w	0	301	—	0	302	—	0
400	st	46	401	—	0	402	w	9
500	—	0	501	—	0	112	—	0
110	—	0	111	st	37	212	—	0
210	—	0	211	—	0	312	—	0
310	—	0	311	m	9	412	—	0
410	—	0	411	—	0	122	—	0
510	—	0	511	m	6	222	m	15
120	—	0	121	—	0	322	—	0
220	st	100	221	—	0	422	st	41
320	—	0	321	—	0	132	—	0
420	w	9	421	—	0	232	—	0
520	—	0	521	—	0	432	—	0
130	—	0	131	m	9	142	—	0
230	—	0	231	—	0	242	st	41
330	—	0	331	w	5			
430	—	0	431	—	0			
140	—	0	531	m	14			
240	w	9	141	—	0			
340	—	0	241	—	0			
440	st	68	341	—	0			
			441	—	0			
			151	m	6			
			251	—	0			
			351	m	14			

* Denotation of symbols: st strong, m medium, w weak, — not present.

total number of iron atoms being one on the average, and four sulfur atoms on the positions 000, $\frac{1}{2}\frac{1}{2}0$, $0\frac{1}{2}\frac{1}{2}$, $\frac{1}{2}0\frac{1}{2}$, yields calculated intensities for all the strong and medium spots in good agreement with those observed, as is shown in Table 1; such a structure gives small calculated intensities for some of the weak spots and zero calculated intensities for the remainder of the weak spots.[11]

---

[11] An equal statistical distribution of the copper and iron atoms on the eight positions $\frac{1}{4}\frac{1}{4}\frac{1}{4}$, $\frac{3}{4}\frac{3}{4}\frac{1}{4}$, $\frac{1}{4}\frac{3}{4}\frac{3}{4}$, $\frac{3}{4}\frac{1}{4}\frac{3}{4}$, $\frac{1}{4}\frac{3}{4}\frac{1}{4}$, $\frac{3}{4}\frac{1}{4}\frac{1}{4}$, $\frac{1}{4}\frac{1}{4}\frac{3}{4}$, $\frac{3}{4}\frac{3}{4}\frac{3}{4}$ gives calculated intensities in markedly less good

Lundqvist and Westgren determined the edge-length of a cubic cell for bornite to be 10.93kX.[12] Such a cell would contain 40 copper atoms, 8 iron atoms and 32 sulfur atoms. The positions of the sulfur atoms in this cubic cell are given by Lundqvist and Westgren as 32(*e*) with $x=-\frac{1}{8}$; these positions are the same as those of the sulfur atoms in the approximate structure found by us. Lundqvist and Westgren concluded that the eight iron atoms occupy the eight positions of 8(*a*), and twenty-four of the forty copper atoms occupy twenty-four of the forty-eight positions of 48(*f*) with $y=\frac{1}{4}$. These are part of the positions in which iron and copper atoms are assumed by us to be statistically distributed in the approximate structure. The calculated intensities of Lundqvist and Westgren are based on this atomic arrangement leaving out the remaining sixteen atoms of copper; they are in less good agreement with the observed intensities than are the intensities calculated from our approximate structure. Lundqvist and Westgren discussed possible locations of the omitted sixteen copper atoms and concluded that not many of them could be in the sixteenfold positions 16(*c*) and 16(*d*).[13] They stated that no matter how these sixteen copper atoms are distributed on the three positions (16(*c*), 16(*d*) and 96(*g*)), in combination with the atoms already placed, they would make the lines 422, 442, and 642[14] appear. There is no trace of any of these lines on our Weissenberg photographs, although the planes were in positions to diffract.

Since the scattering powers of copper and iron atoms differ very little, accurate values of observed intensities and careful calculations would be required to discriminate the positions of the copper and iron atoms. Our work thus far does not establish the nature of the deviations from our approximate structure. The many weak spots not accounted for indicate that bornite at ordinary temperatures is less disordered than the approximate structure that we found will account for the intensities of the strong and medium spots (as well as part of the weak spots).

---

agreement with those observed than the unequal distribution adopted as the approximate structure. In the case of the artificial phase $Cu_{1.8}S$ at 170° Rahlfs came to a similar conclusion (Rahlfs, P., *Zeit. physik. Chem.*, **31B**, 157–194, 1936). It is not surprising that the approximate structure of bornite and the structure of $Cu_{1.8}S$ at 170° are similar in view of the fact that Merwin and Lombard found that at temperatures from about 500° to about 1000° a solid solution extends from pure copper sulfide to compositions considerably richer in iron than Cu_5FeS_4 (Merwin, H. E., and Lombard, R. H., *Economic Geology*, **32**, 203–284, 1937).

[12] The value was given in Å units, but was probably in kX units.

[13] Lundqvist and Westgren suggested, however, that copper atoms might be located in these positions, which are in the centers of sulphur octahedra, and be oscillating with considerable amplitudes, in which case they would scatter with less intensities.

[14] The indices would be 211, 221, 321, referred to the cell of 5.47 Å edge-length.

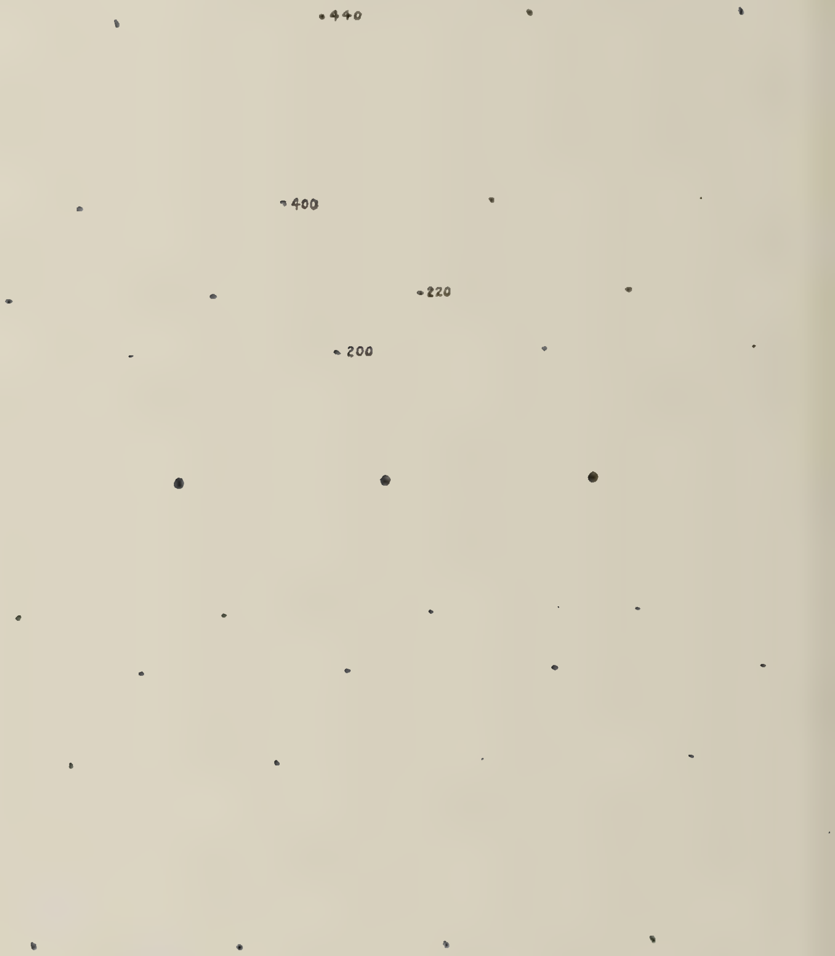

FIG. 1. Weissenberg photograph of the zero layer-line of a single crystal of bornite made with cobalt Kα-radiation. The direct beam spots along the center-line of the photograph indicate the translations of the film corresponding to 90° of rotation of the crystal. The small light areas in the centers of the direct beam spots mark the outline of the crystal. The indices of the spots refer to the cubic cell of edge-length 5.47 Å.

ACKNOWLEDGMENT

The authors wish to express their appreciation of the assistance rendered by Mrs. Ruth P. Tunell in measuring several of the films and carrying out part of the calculations.*

---

* *Note added July 21, 1949*. Shortly after the manuscript of this paper was submitted to the editor of *The American Mineralogist*, a paper entitled "Disorder in bornite, Cu_5FeS_4"

was read before the Meeting of the Crystallographic Society of America at Ann Arbor, Michigan, by A. J. Frueh, Jr. A copy of the abstract of Dr. Frueh's paper was kindly sent to us by the editor of *The American Mineralogist.* Since Dr. Frueh determined different unit cell dimensions for the ordered form of bornite existing at ordinary temperatures from those determined by us, we sent him a copy of our manuscript and a print of one of our rotation photographs. He in turn kindly wrote us and sent us prints of several of his rotation photographs. It thus became certain that bornite of two different ordered forms exists at Illogan, Cornwall, where our crystals originated, and at Bristol, Connecticut, where Dr. Frueh's crystals were formed. The results of Dr. Frueh's investigation of bornite, which constitute a part of a more general study, will appear in *The American Mineralogist.* In view of the fact that he has investigated bornite crystals from Bristol, not only in the natural ordered state, but also in the disordered state following heating and quenching, we should emphasize that we have only made *x*-ray photographs of our crystals from Illogan in the natural ordered state, and hence we cannot say what their structure would be in the disordered state after heating and quenching; it would be reasonable to assume that our "approximate structure" might be closely related to the disordered structure of the crystals from Illogan that would result from heating and quenching, and this hypothesis should be tested.

The existence of two different ordered forms of bornite in nature raises the question whether or not their compositions also differ. A polished surface of some of our crystals from Illogan showed the presence of a little chalcopyrite, chalcocite and covellite; consequently we are not able to determine the exact composition of our bornite by analysis. However, Allen has analyzed bornites from several different localities, the purity in each case having been established by mineralographic study, and he found that the composition in all cases was very close to Cu_5FeS_4; after reviewing the literature he concluded that there is no satisfactory evidence that natural bornite varies appreciably from this formula (*Am. Jour. Sci.*, (4), **41,** 409–413 (1916)). Murdoch states that "the mineralographic examination of polished surfaces of bornite from at least 30 different localities has revealed only an exceedingly slight variation in color (Microscopical Determination of Opaque Minerals, New York, 1916, page 35). The bornite crystals studied by Dr. Frueh and those investigated by us therefore probably have a composition close to Cu_5FeS_4, but the possibility of a slight difference in composition, with which the difference in structure might be connected, is not excluded.

PETROGRAPHIC DISTINCTION OF XENOTIME AND BASTNÄSITE*

WILFRID R. FOSTER, *Champion Spark Plug Company, Ceramic Division Detroit, Michigan.*

ABSTRACT

The optical properties of xenotime (YPO_4) and bastnäsite ((Ce, La, Di) FCO_3) are so nearly identical that it is impossible to distinguish between them with certainty on that basis alone. Brief ignition, however, renders them easily distinguishable under the microscope. Such treatment is recommended in order to eliminate the danger of confusing the two minerals in heavy-mineral concentrates or other types of sample.

INTRODUCTION

Several years ago a granular sample labelled "Andalusite from South Africa" was submitted to the writer for evaluation. The optical properties were found to differ decidedly from those of andalusite, and suggested rather that the material might be xenotime. The apparent detrital nature of the grains seemed consistent with such an identity, and the writer and the late Dr. Albert B. Peck concurred in calling the mineral xenotime. A qualitative chemical analysis by Mr. Arthur Rautenberg failed to confirm this identification. The mineral proved to be essentially a carbonate of cerium and lanthanum, and not the phosphate of yttrium. When apprised of these findings the suppliers of the material reported that they had inadvertently submitted a sample of bastnäsite sand from the Belgian Congo.

Hutton (5) recently dispelled the erroneous impression given by several authorities (6) (7) that it is practically impossible to distinguish xenotime from zircon by microscopic means alone. He presented reliable criteria for optically distinguishing xenotime from zircon and monazite. However, he appeared to imply that positive identification of xenotime under the microscope is not too difficult, and that only zircon and monazite need cause concern. Yet if Hutton's procedure were carefully followed the determination of xenotime would still be inconclusive because of the marked optical similarity between xenotime and bastnäsite. In the absence of a confirmatory test there is no guarantee that bastnäsite would not be wrongly identified as xenotime, as in the instance cited above.

OCCURRENCE OF XENOTIME AND BASTNÄSITE

Xenotime and bastnäsite have considerable in common as regards mode of occurrence. Xenotime occurs in granites, pegmatites, and nepheline syenites (6). Bastnäsite occurs typically in contact zones between schists and granitic or pegmatitic intrusions, but it is also found within pegmatites (3). In at least one instance the two minerals occur in the same locality, perhaps even in close association, for both have been reported with tysonite near Pike's Peak, Colorado (1). Both minerals, too, have been noted in sands or gravels (3) (5). Either mineral, therefore, might be encountered in heavy-mineral separates from sediments, and possibly also from granitic rocks. In some cases both might even occur in the same sample. Thus there is real need for caution lest the two minerals be mistaken for each other. Association with such other cerium-bearing minerals as cerite, allanite, tysonite, törnebohmite and monazite cannot be considered as too indicative of bastnäsite. Xenotime also may be accompanied by cerium minerals: tysonite, monazite, and perhaps others.

---

* Contribution from the Research Laboratories of the Ceramic Division of the Champion Spark Plug Company.

Comparison of Optical Properties

The experience of the writer in confusing xenotime and bastnäsite could easily be repeated by others. So nearly identical are these two minerals in their optical properties that even the careful measurement of refractive indices would fail to distinguish conclusively between them. Examination of the data in Table 1 reveals how they could easily be mistaken for each other. Their refractive indices and birefringence are sensibly the same, and both are uniaxial positive. Both may show weak pleochroism and may vary in color from colorless in transmitted light, to yellow, red, or brown in reflected light. Bastnäsite is said to have a perfect basal cleavage (3), whereas that of xenotime is prismatic. Herein might conceivably lie a means of distinguishing the two minerals

Table 1. Refractive Indices of Xenotime and Bastnäsite

Mineral	Source	Omega	Epsilon	Reference
Xenotime	—	1.721	1.816	Hutton (5)
Xenotine	—	1.7207	1.8155	Hutton
Xenotime	New Zealand	1.720	1.827	Hutton
Bastnäsite	Sweden	1.7220	1.8235	Glass and Smalley (3)
Bastnäsite	Colorado	1.717	1.818	Glass and Smalley
Bastnäsite	Madagascar	1.717	1.818	Glass and Smalley
Bastnäsite	New Mexico	1.718	1.819	Glass and Smalley
Bastnäsite	Belgian Congo	1.722	1.823	Glass and Smalley
Bastnäsite	Colorado	1.716	1.816	Goddard and Glass (4)
Bastnäsite	New Mexico	slightly below 1.72	very close to 1.82	Dean and Dressel (8)

in powder-mounts, since basal non-birefringent grains might be expected to be very common for bastnäsite and rare or absent for xenotime. Apparently, however, there is little tendency for such preferred orientations. Powder-mounts of bastnäsite and xenotime are very similar in appearance, and the grains of both minerals almost without exception display high birefringence.

Selection of Suitable Confirmatory Test

It is apparent that some test other than a strictly optical one is necessary to distinguish unfailingly between xenotime and bastnäsite. A simple and rapid test which dispenses with the need for spectrographic, x-ray diffraction or qualitative chemical analysis is desirable.* Ideally, the test should be applicable to isolated tiny grains as well as to large fragments and to intimate mixtures of the two minerals, either with each other or with any or all of their usual associates. In the search for such a test a number of different procedures were tried. One of these proved to be so superior to the remainder in the early trials that little time was devoted to the less promising procedures. However, it might be well to describe briefly the various techniques tested, with the reasons for rejection or acceptance.

Examination under ultraviolet light revealed no distinction between the two minerals, in the two samples of xenotime and four samples of bastnäsite at the writer's disposal. Fluorescence tests under both long (3650 A.U.) and short (2537 A.U.) radiation were in all cases negative. Hutton (5) reported that xenotime from New Zealand likewise failed to fluoresce. Such tests are useless, then, for present purposes. However, fluorescence inspection proves to be useful in distinguishing zircon from monazite and xenotime (2) and from bastnäsite.

Sandell (9) has referred to the blue fluorescence imparted to a borax bead by cerium. This should constitute a suitable procedure for distinguishing bastnäsite from xenotime. Only a few tests were made by the writer, and these were inconclusive, probably because optimum conditions were not achieved. Rejection of this method was dictated not by any doubt as to its validity, but by the realization that it would not have general applicability. Associated monazite or other cerium-bearing minerals would cause interference, and mixtures of bastnäsite and xenotime would behave in the same way as would bastnäsite alone.

Xenotime is insoluble in acids, whereas bastnäsite is very slowly attacked with accompanying evolution of carbon dioxide. For concentrated samples of appreciable size this appears to be a satisfactory method of distinction, if the possible presence of other gas-evolving minerals can be excluded. Attempts to carry out such a test in powder-mounts, using sulfuric or hydrochloric acid as the immersion medium, were not too satisfactory. Although bubbles of gas slowly accumulated beneath the cover-slip there was no visible effervescence of any of the bastnäsite grains. The test would therefore be unsuitable for samples containing both bastnäsite and xenotime, or for sparsely distributed grains in a heavy-mineral separate.

---

* The specific gravity of bastnäsite (4.99) is sufficiently different from that of xenotime (4.59) to be useful in some cases. But samples of sufficient purity and weight are not always available for such a determination.

A simple and effective test which appears to meet all the requirements consists merely of ignition at red heat in the flame of a laboratory burner for about one minute. Xenotime so treated is found, upon microscopic examination, to be unaffected, whereas bastnäsite suffers a notable reduction in birefringence and an increase in refractive indices such that both indices considerably exceed 1.80. The microscopic color is changed from colorless to yellow or yellow-brown. Every grain of bastnäsite from the smallest to the largest is similarly affected, so that even a few isolated grains of this mineral in a heavy mineral separate reveal their true identity by such treatment. Furthermore, the occurrence of both bastnäsite and xenotime in the same sample does not cause any difficulty.

DECOMPOSITION PRODUCT OF BASTNÄSITE

It might be expected that the product of the thermal decomposition of bastnäsite would be essentially a cerium oxide containing other rare earths in solid solution. To test this a sample of powdered New Mexico bastnäsite was calcined for several hours at 1450° C., and analyzed on a Norelco *x*-ray spectrometer. The diffraction pattern was strikingly similar to that of pure ceric oxide (CeO_2), although showing somewhat larger interplanar spacings. The length of the cubic unit cell is 5.57 kX, as compared to a length of 5.42 kX for the cell of ceric oxide. The enlarged cell of the decomposition product is probably to be attributed to lanthanum oxide and other rare earths present in solid solution. Microscopically the decomposed product is isotropic with index well above 1.80 and is deep yellow-brown in color. When xenotime is exposed to similar thermal treatment it yields an *x*-ray pattern identical with that given by the uncalcined mineral.

Bastnäsite heated momentarily in the burner-flame, as in the test previously outlined, is apparently not completely converted to the cubic oxide. This is suggested by its residual birefringence and by the character of its *x*-ray pattern. The latter is a poorly developed yet recognizable pattern of the ceric oxide type. Nevertheless, this rapid ignition is capable of rendering bastnäsite microscopically dissimilar to xenotime. For the purposes of our test, therefore, there is no advantage in heating to complete decomposition.

CONCLUSION

The criteria used by Hutton to distinguish xenotime from zircon and monazite do not suffice to distinguish it from bastnäsite. It is suggested that an additional confirmatory test is necessary in order to render the determination of xenotime conclusive. Such a test, which depends upon the difference in behavior of xenotime and bastnäsite upon heating is described. The decomposition product of bastnäsite is essentially a cubic ceric oxide. Hutton's recommendation of more careful immersion work in order to insure detection of certain easily overlooked minerals such as xenotime cannot be overemphasized.

ACKNOWLEDGMENTS

Grateful acknowledgment is extended to J. J. Glass, W. F. Foshag, J. M. Morris, O. C. Ralston, and George Switzer for kindly providing specimens of xenotime and bastnäsite.

REFERENCES

1. FORD, W. E., (1932), Dana's Textbook of Mineralogy, 4th Edition (John Wiley & Sons, Inc., New York, N. Y.), pp. 526, 700.
2. FOSTER, W. R., (1948), Useful aspects of the fluorescence of accessory-mineral zircon: *Am. Mineral.*, **33**, 724–735.
3. GLASS, J. J., AND SMALLEY, R. G. (1945), Bastnäsite: *Am. Mineral.*, **30**, 601–615.
4. GODDARD, E. N., AND GLASS, J. J. (1940), Deposits of radioactive cerite near Jamestown, Colorado: *Am. Mineral.*, **25**, 381–404.
5. HUTTON, C. O. (1947), Determination of xenotime: *Am. Mineral.*, **32**, 141–145.
6. JOHANNSEN, A., (1932), A Descriptive Petrography of the Igneous Rocks (The University of Chicago Press, Chicago, Illinois), Vol. II, pp. 178–179.
7. MILNER, H. B., (1940), Sedimentary Petrography, 3rd Edition (Thomas Murby & Co. London, England).
8. NOTES AND NEWS, (1944), Bastnaesite at Corona, New Mexico: *Am. Mineral.*, **29**, 157.
9. SANDELL, E. B., (1944), Colorimetric Determination of Traces of Metals (Interscience Publishers, Inc., New York, N. Y.) p. 372.

GEIKIELITE, A NEW FIND FROM CALIFORNIA*

Joseph Murdoch, *University of California at Los Angeles*,

AND

Joseph J. Fahey, *United States Geological Survey, Washington, D. C.*

Abstract

Geikielite, $MgTiO_3$, from the Jensen quarry of the Riverside Cement Company, Riverside County, California, is the second known occurrence of this mineral and the only location where it is found in place. It is closer to the theoretical end member than the Ceylon material and has a lower specific gravity. The accompanying minerals are spinel, pyrite, pyrrhotite, diopside and forsterite.

Introduction

Geikielite, $MgTiO_3$, is an exceedingly rare mineral which has previously been recorded only from Ceylon, as pebbles from gem-bearing gravels. It is thus of particular interest to report a second occurrence, in California, especially as it has been found here in place, and its mineralogical relationships can be observed.

The Ceylon occurrence was reported by Fletcher (1), and the mineral described and analyzed by Dick (2). According to him the color is bluish or brownish black, thin splinters showing a peculiar purplish red by transmitted light. Sustschinsky (3) made another analysis, and measured cleavage fragments and poor crystals on the goniometer. He observed the base poorly developed, and on one crystal a narrow face with a ρ angle of about $72\frac{1}{2}°$. The unit rhombohedron he measured on cleavage surfaces. Crook and Jones (4) analyzed a number of specimens, and observed that the color and specific gravity appeared to vary with the composition. As FeO increased, the color darkened, and the specific gravity increased. All their analyses showed considerable amounts of Fe_2O_3. Table 1 gives various analyses of geikielite, including that from California.

Occurrence

The new occurrence of geikielite is at the Jensen quarry of the Riverside Cement Company, in Riverside County, California. The quarry is in limestone which has been extensively altered by the intrusion of irregular tongues of igneous rock, with recrystallization of the calcite and development of abundant brucite. The brucite is in rounded grains and crudely octahedral crystals, and, probably as at nearby Crestmore, pseudomorphous after periclase. In addition, certain zones are particularly rich in minute grains of flesh-colored or pale-lavender spinel.

---

* Published by permission of the Director, U. S. Geological Survey.

Geikielite occurs very sparingly, as minute, ruby-red to nearly black, rounded or flattened grains in the spinel-rich layers. It is in places accompanied by minute grains of pyrite and pyrrhotite, and by colorless rounded grains of diopside and forsterite. Few of the grains are over 1 millimeter in diameter, and most are considerably less.

The geikielite appears to have been crystallized at essentially the same time as the accompanying minerals, as it is often intergrown with them, and all were developed in the crystalline limestone during the process of metamorphism. The spinel very commonly encloses microscopic grains of doubly refractive material, probably diopside or forsterite. Separation of even a few hundred milligrams of material involved dissolving a considerable volume of the rock in acid, and separation of the insoluble residue by heavy solutions. Even so, the specific gravities of spinel and geikielite are so close together that separation was poor, and final hand picking under the binocular was necessary.

TABLE 1. CHEMICAL ANALYSES OF GEIKIELITE

	I	II	III	IV	V	VI	VII
TiO_2	60.0	61.32	67.74	63.94	64.03	64.9	66.46
Al_2O_3	—	—	—	—	—	1.3	—
MgO	29.86	28.95	28.73	25.79	24.66	31.8	33.54
FeO	2.028	2.028	3.81	10.09	12.14	1.4	—
Fe_2O_3	6.90	7.75	—	.25	—	—	—
MnO	—	—	—	—	—	0.4	—
SiO_2	—	—	—	—	—	0.9	
	98.79	100.05	100.28	100.07	100.83	100.7	100.00
Sp. Gr.	3.976					3.79	

I, II Sustschinsky; III Dick; IV, V, Crook and Jones; VI Fahey; VII Mg TiO_3.

There appear to be several considerable differences in properties between the California geikielite and the Ceylon mineral. These are probably due to the variation in composition, as our material (see analysis VI) is extremely low in iron. The color is decidedly lighter, being distinctly ruby red except in the largest grains, and brownish red in transmitted light, rather than purplish as described. It is also decidedly pleochroic with ϵ pinkish, and ω brownish red. Specific gravity is lower than that of the material from Ceylon, and the calculated value in *Dana's* 7th Edition (6) from x-ray data by Posnjak and Barth (5).

CRYSTALLOGRAPHY

A number of the grains showed crystal faces, and in spite of their small size could be measured with considerable accuracy on the goniometer. Many of the thin tabular crystals showed one very good face, with traces of others, whereas some of the thicker ones yielded good measurements on a variety of forms. The base is always present and dominant, and practically always brilliantly smooth, so accurate setting of the crystals for measurement became simple. The next form in importance of occurrence and development is $r\{10\bar{1}1\}$, nearly always present as two or three faces on any crystal. It is accompanied in two instances by the negative form $\{01\bar{1}1\}$. Next in frequency, but seldom with good faces is $\zeta\{20\bar{2}5\}$. Its position is frequently fair, but the signal is usually rather poor. Another form $s\{02\bar{2}1\}$ is not common, but is of good quality and in good position. A flat rhombohedron $e\{01\bar{1}2\}$ was observed in excellent position in one crystal. In addition, three other forms have been included in the subjoined angle table; a number of doubtful forms are present which frequently were close to the calculated positions, but none of which gave really satisfactory signals.

Table 2. Partial Angle Table

	$a:c=1:1.3806$				$p_0:q_0=1.592:1$	
Forms		Quality	Measured Average		Calculated	
			ϕ	ρ	ϕ	ρ
0001	8	A	—	0°00′	—	0°00′
$10\bar{1}1$	18	A	30°05′	57 54	30°00′	57 54
$01\bar{1}1$	2	B	−30 13	57 52	−30 00	57 54
$02\bar{2}1$	5	B	−30 15	72 24	−30 00	72 35
$20\bar{2}5$	13	D	30 40	33 20	30 00	32 31
$01\bar{1}2$	1	C	−30 39	38 32	−30 00	38 33½
$2\bar{3}12$	2	C	9 59	62 34	10 53½	64 38½
$8\bar{4}\bar{4}3$	1	C	61 41	72 54	60 00	74 48
$\bar{3}034$	2	D	−30 20	50 15	−30 00	50 05½
$\bar{8}719$	1	C	23 28	52 36	23 25	53 12½

Other doubtful forms, with poor signals but fairly good position $\{21\bar{3}0\}$, $\{50\bar{5}4\}$, $\{21\bar{3}1\}$, $\{21\bar{3}6\}$, $\{61\bar{7}3\}$, $\{71\bar{8}7\}$, $\{5.2.\bar{7}.12\}$.

Measurement of an x-ray powder photograph gives the following spacings for prominent lines: 2.72, 2.22, 1.71, 1.46, 1.32.

Chemical Composition

The chemical analysis (No. VI, Table 1) was made on the whole sample, weight 137 mg., recovered from the determination of the specific gravity. After dissolving the bisulfate fusion, the SiO_2 was filtered, weighed, and volatilized with HF; a double precipitation with NH_4OH

separated the titanium, iron, and aluminum from the magnesium and the manganese. The iron was determined colorimetrically with thiocyanate and computed to FeO. Titanium was measured by passing the solution through the Jone's Reductor, the delivery tube of which was below the surface of a solution of ferric sulfate, and titrating the equivalent ferrous iron with permanganate. The alumina was determined by difference in the usual manner. Magnesia was weighed as $Mg_2P_2O_7$ and the manganese contained therein measured colorimetrically.

The specific gravity (3.79 corrected to 4° C.) was determined on 147 mg., using a fused silica Adams-Johnston pycnometer of 5 ml. capacity.

A spectrographic analysis by K. J. Murata showed aluminum present in tenths of one per cent and calcium, zinc and magnesium in hundredths.

ACKNOWLEDGMENTS

The authors are indebted to Mr. K. J. Murata of the Geological Survey for spectrographing the mineral and to Mr. Joseph M. Axelrod, also of the Geological Survey, for his *x*-ray powder photographs of the sample. Professor George Tunell, of the Department of Geology, University of California at Los Angeles, was very helpful in the calculation of spacings from the *x*-ray photograph, which Professor J. D. McCullough of the Department of Chemistry, kindly made for us.

REFERENCES

1. FLETCHER, L., Geikielite and baddeleyite, two new mineral species: *Nature*, **46**, 620–621 (1892).
2. DICK, A., On geikielite, a new mineral from Ceylon: *Mineral. Mag.*, **10**, 145–147 (1893).
3. SUSTSCHINSKY, P. V., Beitrage zur Kentniss des Geikielith, Ilmenit und Hämatit: *Zeit. Krist.*, **37**, 57–62 (1903).
4. CROOK, T., AND JONES, B. M., Geikielite and the ferro-magnesian titanates: *Mineral. Mag.*, **14**, 160–166 (1906).
5. POSNJAK, E., AND BARTH, T. F. W., Notes on some structures of the ilmenite type: *Zeit. Krist.* **88**, 271–280 (1934).
6. Dana's System of Mineralogy, 7th Ed., Vol. **1**, p. 536 (1944).

IMPROVED DIFFERENTIAL THERMAL ANALYSIS APPARATUS

J. Laurence Kulp and Paul F. Kerr,
Columbia University, New York, N. Y.

Abstract

A modification of the multiple type differential thermal analysis apparatus permits automatic pen or dot recording with a sensitivity equal to that of the galvanometer-photographic recording methods. The increased sensitivity is accomplished through the use of a stable d.c. preamplifier. With a dual furnace assembly virtually continuous operation alternating between multiple and single recording may be accomplished.

Although a wide variety of apparatus has been employed in applied differential thermal analysis, there are fundamentally four essential parts common to all experimental arrangements: (1) specimen holder, (2) furnace, (3) rate-of-heating controller, and (4) differential thermocouple recorder.

Specimen holders are ordinarily made either of pure nickel or of stainless steel. The latter material has slightly less thermal conductivity than nickel but has proved more durable. Since the rate of heat flow in stainless steel is about a hundred times that of most minerals, the slight increase in thermal conductivity obtainable by employing nickel is not sufficient to compensate for the use of less stable material. The sample holder, itself is designed with the container holes for powdered minerals spaced symmetrically relative to the axis of the furnace.

The furnaces are ordinarily of the electric resistance type, either commercial or home wound and may be mounted either horizontally or vertically. It is believed the latter is preferable since vertical mounting allows closer geometrical control, greater facility in centering the specimen holder in the furnace after placing the furnace around the holder, and also mechanical rigidity.

The rate of heating has been controlled in a number of ways. The applied voltage may be changed manually or automatically by means of a *variac* or by more precise program controllers.

The differential thermocouple voltage may be recorded by manual observation, galvanometer-photographic recording or by the use of an electronic amplifier coupled with a pen or dot recorder. About two years ago a multiple differential thermal analysis unit was developed which included an automatic program control of the heating rate combined with a 6-point electronic recorder (Kerr and Kulp, 1948). Since the description of this apparatus, a number of improvements have been made which make possible not only the original multiple feature, but high sensitivity for a single sample as well. The most significant development has been the installation of a d.c. preamplifier which gives a dot record curve comparable in sensitivity and stability with the best galvanometer-photographic recording devices. The sensitivity with the new arrangement is adequate for a wide variety of mineralogical studies.

At present the apparatus consists of the controlling and recording assembly plus two furnaces each with a sample holder. One unit uses a single sample and records through the d.c. preamplifier to the Speedomax recorder with high sensitivity. The second unit employs a multiple sample holder (six holes) and records with moderate sensitivity directly via the Speedomax. The furnaces are run alternately, one heating while the other cools. In a normal day it is feasible to obtain thermal curves for three samples with high sensitivity and eighteen samples at moderate sensitivity. Since the time required for cooling and loading about equals the time required for an analysis, the program controller and recorder may be kept essentially in constant operation. The specific improvements will be discussed below.

Specimen Holder Block

In recent developments both an improved multiple sample holder and a single sample holder have been constructed. The plan view of an improved holder of (18-8) stainless steel for multiple differential thermal analysis is shown in Fig. 1 (drawn to $\frac{1}{2}$ scale). "*A*" refers to the recess for the inert alundum while "*S*" refers to the recess for the specimen. The holes for an "*A*"-"*S*" pair are centered symmetrically parallel to a vertical axis with identical radii. The dashed lines indicate the connecting differential thermocouple. The holder is drilled from a 1$\frac{3}{4}$″ cylindrical stainless steel block and is 1″ thick. The sample and alundum recesses are $\frac{1}{8}$″ in diameter and $\frac{1}{2}$″ deep. This arrangement makes it possible for the thermocouple head to be above or below the center of the

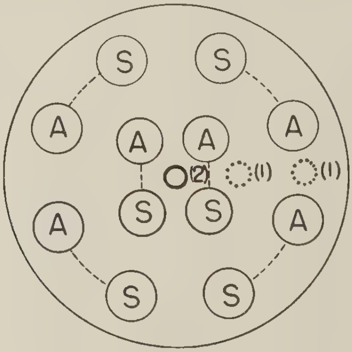

Fig. 1. Modified stainless steel holder for multiple differential thermal unit.

sample by as much as $\frac{1}{8}''$ without appreciably changing the heat flow to the head, since the heat flow is primarily determined by the closest distance from the head to the stainless steel wall. Furthermore, this simplifies centering the thermocouple head in the hoizontal plane so that it coincides with the central vertical axis of the hole. Thus, the geometrical arrangement is essentially reproducible and the baselines of the thermal curves show few irregularities due to thermal gradients and the sensitivity of a particular thermocouple head becomes quite constant over a series of runs.

The multiple specimen holder is held in place by a stainless steel collar attached to a vertical alundum tube. The latter is V-clamped to a universal vice which fits a track on the table. This assembly facilitates the centering of the specimen holder block after the furnace has been lowered to surround the block and supporting alundum tube. A $\frac{1}{4}''$ thick disk with the same diameter as the sample block supported on $\frac{1}{8}''$ long pins is placed over the sample holes as a shield against direct furnace radiation.

The small holes indicate the positions of the temperature recording thermocouples (1) and the temperature controlling thermocouple (2). The former is placed in the block at the same height and on the same radius as the thermocouple head within the sample. The temperature controlling thermocouple is brought through both the block and the lid into the open space of the furnace directly exposed to the furnace coils. This arrangement has been found to give a highly linear heating rate.

Although it has not been constructed, it is believed that a multiple specimen holder for twelve specimens is feasible, if such a number of samples of a routine nature may be required for a particular problem. In such a case the description would be essentially the same as above except that a furnace of larger diameter would be required. The recording and controlling equipment now available should be adequate for a twelve-sample apparatus.

In the case of high sensitivity, still more precise symmetrical location of the sample in the block is required. Figure 2 shows plans and elevations drawn to $\frac{1}{2}$ scale of the specimen holder used. The top section of the block I is $1\frac{3}{4}''$ diameter and the sample holder $\frac{3}{8}''$ diameter. The symbols have the same meaning as in Fig. 1. The block is also supported in the manner described above and has a comparable lid.

In order to provide long life and to allow precise spot welding, Pt-Pt10%Rh thermocouples B.S.×22 are used. The desired placement of the thermocouple head at the center of the sample and the alundum is obtained by accurately spot welding a measured length of Pt10%Rh wire to two long pieces of pure Pt wire. The centering in the vertical direction is fixed as the block is machined in such a way that the thick-

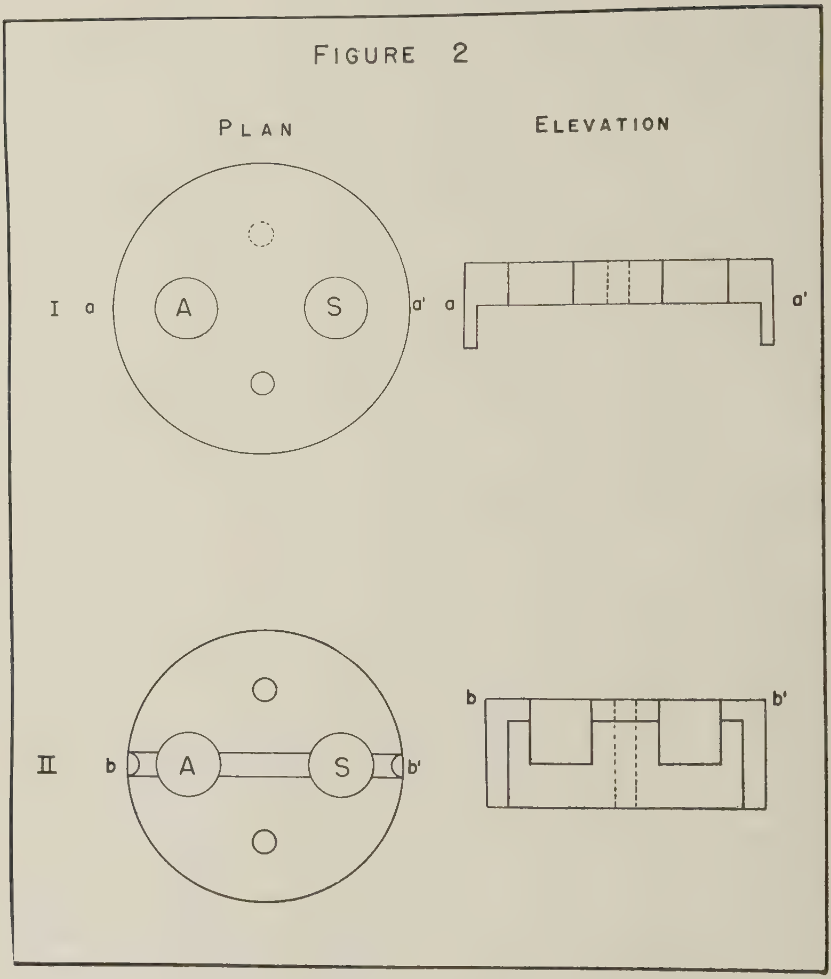

FIG. 2. Stainless steel holder for single differential unit of high sensitivity.

ness of sample above and below the trough in which the thermocouples lies is the same. The slightly larger sample hole radius compared with the multiple unit has been found desirable for this application.

FURNACE

No essential change has been made in the furnace except to remove the alundum tube which prevents direct radiation from the resistance coils to the specimen holder. This change permits more effective control of the heating rate and eliminates drag at the top of the heating range. Although the coils are relatively thick ($\frac{1}{8}''$ diameter) and although they are separated by about $\frac{1}{2}''$ this does not cause any noticeable gradient in the sample block.

PROGRAM CONTROLLER

The Leeds and Northrup Micromax Program Controller described in the earlier paper has required no major modification. Heating rate control begins at room temperature and although there is an initial lag in the sample temperature, by the time a temperature of 100° C. is reached in the sample, the heating rate becomes essentially linear at $12\frac{1}{2}$ degrees per minute. The heating rate indicator which the actual thermocouple temperature should follow has been arranged to move continuously at a uniform rate of $12\frac{1}{2}$ degrees per minute in contrast to the previous method of intermittent movement which only *averaged* $12\frac{1}{2}$ degrees per minute.

RECORDER

The six samples in the multiple unit are recorded on the six point Speedomax mentioned in the previous paper. This Speedomax is being converted at the present time to a sixteen point recorder of the same speed (2.5 seconds between points) and range (full scale 3.0 millivolts) which will have twelve of the sixteen points on the differential couples and the other four on absolute temperature. This will make it possible to run twelve samples at one time with moderate sensitivity and in addition will offer the great advantage of having the actual temperature printed on the same sheet with the differential curves. Further, if desirable, up to four different temperatures of the samples from different portions of the block may be printed simultaneously.

The high sensitivity differential thermocouple (Pt-Pt10%Rh) is connected by a screw junction to a shielded cable which leads directly into the d.c. amplifier preamplifier of the "chopper" type especially built by Leeds and Northrup on an experimental basis to be coupled to the Speedomax. Soft solder joints were found unsatisfactory causing considerable "noise" in the highest sensitivity record. Hence clean screw connections were employed. The d.c. amplifier has the following arbitrary sensitivity scales: 50, 100, 200, 500, 1,000, and 2,000. The table below gives the approximate range of the Speedomax chart for the various settings on the amplifier.

Amplifier Scale	Approximate Full Range on Speedomax	Amplification
not in circuit	1500 microvolts	× 1
2000	800	2
1000	400	4
500	200	10
200	40	20
100	20	40
50	10	80

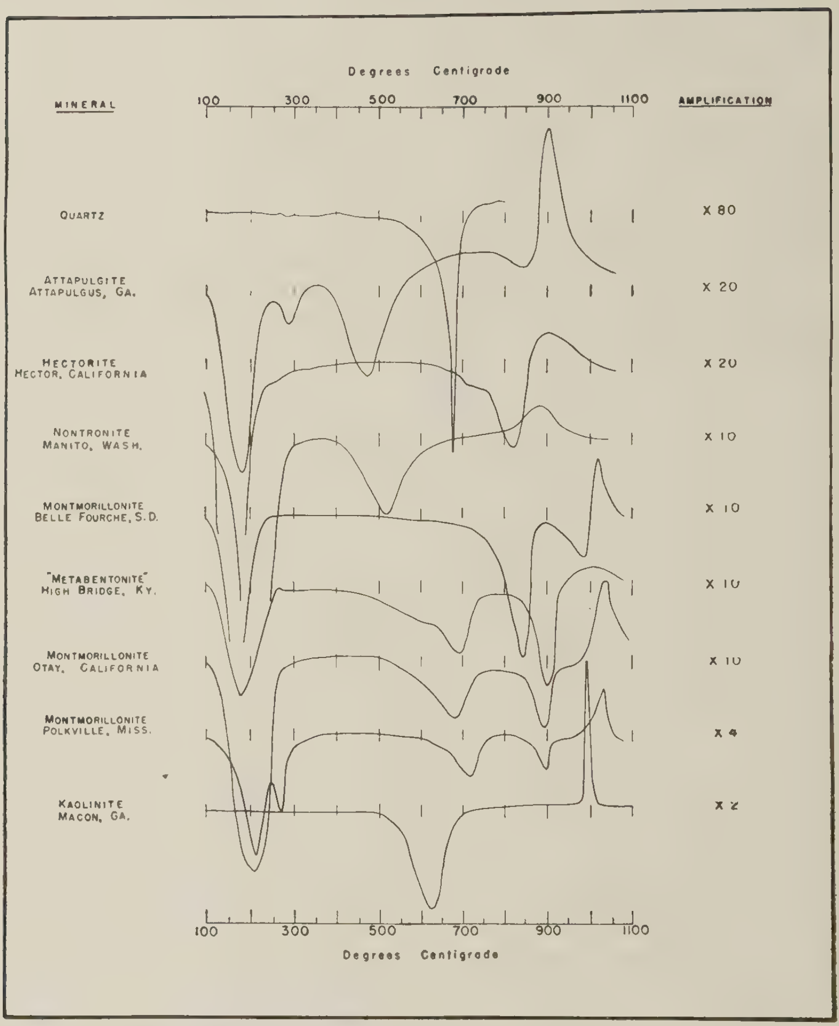

FIG. 3. Representative differential thermal curves at amplifications ×2 to ×80.

A personal communication from Dr. Ben B. Cox of Gulf Research and Development Laboratory indicates that his laboratory has developed with the cooperation of Leeds and Northrup, an automatic rotating switch that will reproducibly and rapidly switch voltages on the order of microvolts or less. This may make it possible to accomplish multiple thermal analyses with an increased sensitivity. On account of the precise geometrical requirements involved in any type of multiple sample holder, it appears that as yet, in order to achieve highest sensitivity and at the same time stability of the base line, a single sample type may be essential.

Figure 3 shows a set of representative thermal curves taken at different amplifications. Comparison of such curves with curves in the literature demonstrates the adequacy in quality and sensitivity of the differential thermal curves produced by this apparatus.

A versatile differential thermal analysis apparatus is now available which combines the features of multiple analysis, direct non-photographic recording, maximum sensitivity useful with the method, and simple operation. Such apparatus with one program controller and one recording outfit plus two furnaces, permits continuous operation of the controller and recorder.

Acknowledgments

The developments outlined in this paper have been made possible through assistance derived from Project 49, Clay Mineral Standards, of the American Petroleum Institute.

References

Kerr, P. F., and Kulp, J. L. (1948), Multiple differential thermal analysis: *Am. Mineral.*, **33**, 387–419.

LINEAR THERMAL EXPANSION OF CALCITE, VAR. ICELAND SPAR, AND YULE MARBLE

Joseph L. Rosenholtz and Dudley T. Smith,
Rensselaer Polytechnic Institute, Troy, New York.

Abstract

A new autographic dilatometer of high sensitivity for the measurement of linear thermal expansion is described. Results are given from 20° to 700° C. for calcite, var. Iceland spar, from Chihuahua, Mexico, and for Yule marble from Yule Creek, Colorado. The data for calcite is an approximate mean of previously published, low temperature values for orientations parallel and perpendicular to the *c* axis. Results for Yule marble indicate a possible correlation between linear thermal expansion and fabric analysis. The abnormal values for the marble are explained tentatively on the basis of recrystallization and residual strain.

Introduction

Since our program of mineral expansion studies was discontinued six years ago, a constant search has been made for newer equipment which would have greater sensitivity and be automatic in operation. Many devices were studied and several were built for test. As a result of the great strides in instrumentation in recent years, a combination of instruments has been adopted having all of the most desirable operational details for research in this field. This will permit the continuation of studies on mineral expansion and inversions, as well as associated studies on rocks.

Equipment

Furnace temperatures are controlled by a special Leeds & Northrup Micromax program controller. This is a versatile instrument in that the furnace may be heated and cooled at any predetermined rate, within the limits of the characteristics of the furnace. It has the further advantage of maintaining a preset temperature at the end of a heating cycle when this is desired before the cooling cycle begins. A continuous-line recorder is integral with the control unit and gives a temperature-time curve.

When changes occur which result in expansion variations, such as from inversions, a Leeds & Northrup Type K2 potentiometer is used to determine precise temperatures. In all cases, a platinum-platinum 10% rhodium thermocouple is used with a zero cold junction.

The recording dilatometer equipment was built for this research by the Baldwin Locomotive Works. It is quite unique in several respects, notably its sensitivity to length changes as small as three-millionths of an inch. Being constructed of invar, variations in room temperature produce very small changes which may be corrected for by conducting a blank determination. Line voltage variations may be disregarded completely because the operation of the measuring equipment depends upon a self-balancing transformer bridge.

The assembly of the thermal control and dilatation units is shown in Fig. 1. The furnace, fused quartz dilatometer tube and rod, and the transmitting part of the recording dilatometer are suspended on a spring-supported platform to eliminate vibrations. Tests have shown that all building vibrations are completely absorbed by this suspension.

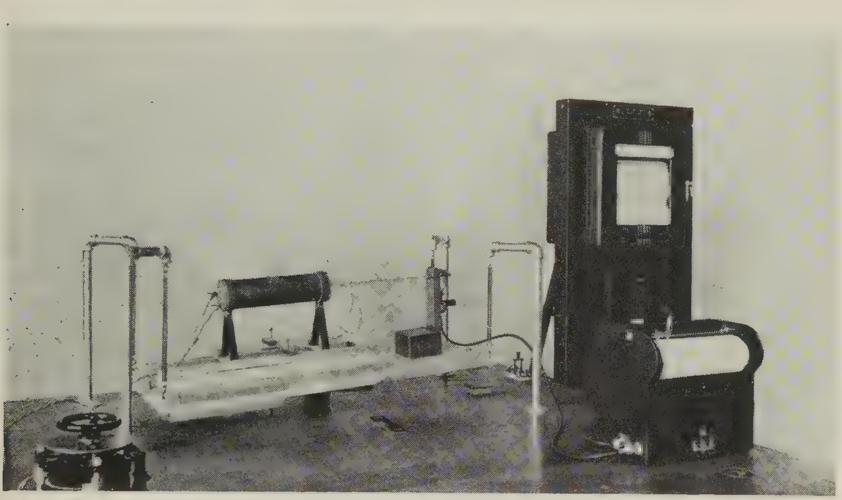

FIG. 1. Dilatometer assembly and thermal control unit.

The recording dilatometer consists of an expansion-follower assembly and an autographic recorder. In the latter, a silver wire stylus moves parallel to the axis of the recording drum at the rate of one inch per hour. The drum rotates in proportion to the length changes of the mineral or rock specimen in the dilatometer tube and will record a total length change as great as 0.02″. The recorder has three gear ratios so that magnifications of 500, 1,000 or 2,000 may be selected.

The follower assembly is shown in detail in Fig. 2. It consists of a heavy invar bar with a clamp to hold the sleeve A into which the fused quartz tube is cemented (not shown). The fused quartz rod, which is moved by length changes of the specimen in the quartz tube, makes contact with the adjustable fulcrum point *B* of the lever. The latter is supported on two knife edges at *C* and can be adjusted for contact by varying the tension on the small springs shown in the illustration. This insures that the minimum pressure will be applied which is necessary to maintain contact during expansion or contraction of the test specimen. As the lever is moved because of length changes in the test specimen, the core of the microformer (transformer) *D* changes its position and thereby unbalances the electrical circuit.

The recorder contains a second, matched microformer. The unbalanced signal from the follower is amplified and drives a servo-motor which, in turn, rotates the recorder drum. At the same time, the core of the second microformer is moved until it is brought to the position where its output balances that of the follower microformer. During this rotation the silver stylus draws a fine line on the chart paper so that an expansion-time curve is obtained. This curve is correlated with the temperature-time curve of the temperature recorder.

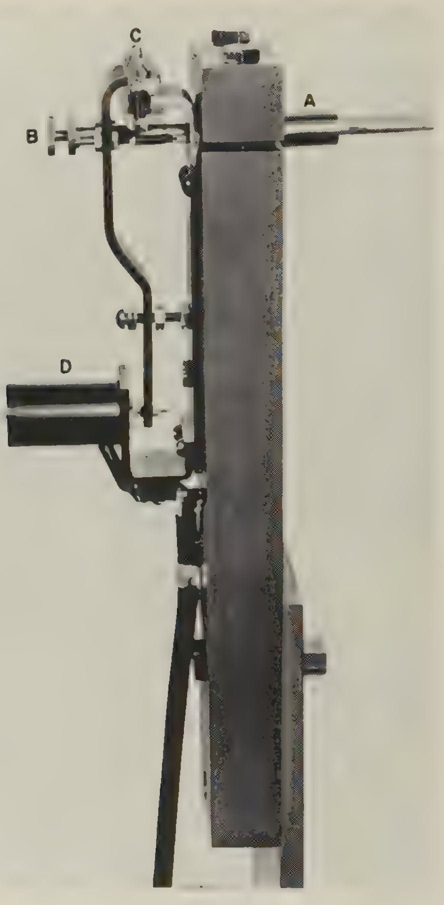

Fig. 2. Detail of the dilatation follower unit.

Two sizes of quartz tubes are used to allow for variations in specimen sizes. These depend upon the nature of the samples and they are cut at the desired orientations to either 4×4×10 mm. or 8×8×10 mm.

CALCITE, VAR. ICELAND SPAR

The specimens of calcite were cut from a large, clear cleavage from Chihuahua, Mexico. The cutting presented difficulties due to the ease of cleavage and it became necessary to develop a special saw for this purpose. Through the courtesy of the Bausch & Lomb Optical Company, information was received that a slowly reciprocating blade gave best results. To accomplish this, a device similar to a power hacksaw was built with a hard steel strip reciprocating at 48 R.P.M. The calcite was cemented to a hardwood block with glyptal and locked at the desired orientation in a universal vise. It was found that a slurry of *FF* carborundum gave best results; coarser grits resulted in cleavage.

TABLE 1. MEAN COEFFICIENTS OF THERMAL EXPANSION OF CALCITE, VAR. ICELAND SPAR

20° C. to	Linear Expansion $\parallel c \times 10^{-6}$	Linear Expansion $\perp c \times 10^{-6}$	Volume Expansion $\times 10^{-6}$ calc.
100°	23.58	−5.22	13.14
200°	26.45	−5.31	15.83
300°	27.99	−5.01	17.97
400°	29.34	−4.61	20.12
500°	30.59	−4.23	22.13
600°	31.78	−3.86	24.06
700°	32.81	−3.69	25.43

The results of the expansion studies are given in Table 1. Values are not given above 700° because a large change in the rate of expansion was noted at 706±1° which appears to be due to the initiation of dissociation of the calcite. Kôzu, Masuda and Ueda (1) found the same phenomenon but they did not indicate a specific temperature at which it occurred.

Austin, Saïni, Weigle and Pierce (2) have analyzed the data for the thermal expansion of calcite from their research and that reported by other observers. They have shown that significant differences may be attributed to variations in the samples. The results given in Table 1 are, coincidentally, an approximate mean of previously reported results to 100° (2) in which a variety of samples and instrumental methods were used. For the 20° to 700° range, there is a wide divergence between the values in Table 1 and those reported by Kôzu, Masuda and Ueda (1), especially for the orientation perpendicular to the optic axis.

YULE MARBLE

At the suggestion of Dr. Eleanora Bliss Knopf, the authors undertook expansion studies of Yule marble, from Yule Creek, Colorado. The test specimens, which were supplied by Dr. Knopf, were cut in north-south, east-west and vertical orientations, corresponding to the field orientation of the rock. These directions were chosen because they had been used in the analysis of the fabric of the marble.

The results obtained during the first heating-cooling cycle, given in Table 2, are considerably in excess of the maximum values for a single crystal of calcite. Furthermore, it was found that all specimens in all orientations acquired a permanent elongation after cooling to room temperature, this being a phenomenon which is common for marbles. It was then decided to subject all specimens to a second heating-cooling cycle and new values were obtained which are given in Table 3. Although no further length changes were observed at the end of the second cycle, measurements made several months later showed that further elongation had occurred at room temperature.

TABLE 2. COEFFICIENTS OF THERMAL EXPANSION OF YULE MARBLE. FIRST HEATING-COOLING CYCLE

20° C. to	N-S $\times 10^{-6}$	E-W $\times 10^{-6}$	Vertical $\times 10^{-6}$	Volume Coefficient $\times 10^{-6}$ calc.
100°	4.25	17.75	4.25	26.25
200°	10.56	29.33	9.67	49.56
300°	12.71	32.68	11.96	57.35
400°	13.34	33.76	13.71	60.81
500°	15.38	35.42	15.08	65.88
600°	16.29	36.72	16.26	69.27
700°	16.79	37.09	16.81	70.69
Elongation after cooling	0.50%	1.02%	0.71%	

DISCUSSION OF RESULTS

The very high coefficients obtained in the cyclic heating of the Yule marble present several intriguing problems. The first to consider is a possible correlation between the results of fabric analysis and thermal expansion. In a personal communication, Dr. Knopf has indicated that, for the east-west orientation, 50 per cent of the optic axes are concentrated in 10 per cent of the total surface of the projection hemisphere and 15 per cent are in $1\frac{1}{2}$ per cent of the surface; furthermore, 45 per cent of the entire surface is unoccupied. These percentages are the result of direct measurement but values may be computed from the coefficients of expansion.

Certain assumptions are of course necessary. In the first place, the results of the first heating-cooling cycle will not be used because, as will be discussed later, they are considered to be due in part to the relief of residual strain in the marble. Secondly, all grains are assumed to have their optic axes oriented either parallel or perpendicular to the axis of the expansion test specimen. Comparing the coefficients of expansion from 20° to 100° of calcite with second cycle Yule marble, the following results are obtained:

TABLE 3. COEFFICIENTS OF THERMAL EXPANSION OF YULE MARBLE. SECOND HEATING-COOLING CYCLE FOR ALL ORIENTATIONS

20° C. to	N-S $\times 10^{-6}$	E-W $\times 10^{-6}$	Vertical $\times 10^{-6}$	Volume Coefficient $\times 10^{-6}$ calc.
100°	−3.75	5.88	−2.62	− 0.49
200°	−2.44	8.61	−1.83	+ 4.34
300°	−1.43	11.04	−0.96	+ 8.65
400°	−0.63	11.05	−0.13	+10.29
500°	+0.85	13.02	+1.29	+15.16
600°	+2.93	16.64	+3.36	+22.93
700°	+4.71	18.44	+5.40	+28.55

East-West orientation	39% *c* concentration
North-South orientation	5% *c* concentration
Vertical orientation	9% *c* concentration

If calculations are based upon the 20° to 700° range, the E-W concentration is found to be 49% but the N-S is 13% and the vertical is 15%. There is, therefore, a good correlation between the measured and computed values in the E-W direction. The value for the N-S orientation should be zero on the basis of direct measurement. The fact that it is not zero by computation may be due either to the assumptions made in the calculations or, possibly, because of recrystallization during the first cycle with a consequent reorientation of a small number of grains; and the same reasoning applies to the other orientations.

There is one further point to consider in this connection. Fig. 3 shows the relationship between the coefficients of linear expansion from 20° to 100° for a single crystal of calcite and the angle between the *c* axis and any other direction. It is evident that appreciable changes may result from the displacement of the *c* axis. For example, for a 15° variation, the coefficient is reduced from 23.58 to 21.65×10^{-6}. In as much as

10 per cent of a hemispherical surface subtends a large angle, there is certainly added reason to expect appreciable variation between measured and calculated results. Studies now under way may make it possible to resolve the several factors mentioned and permit a revision in the method of correlation.

A second problem of considerable interest concerns the explanation for the large coefficients obtained, particularly from the first heating cycle. As shown in Tables 1 and 2, the values for Yule marble are extremely high compared with the maximum for calcite. An apparent explanation, especially in view of the permanent elongation after cooling, is that part of the expansion is due to the relief of residual strain in the marble. Such strain may have a thermal or deformational origin, or both, but part of it may have been induced by the heating during the expansion measurements.

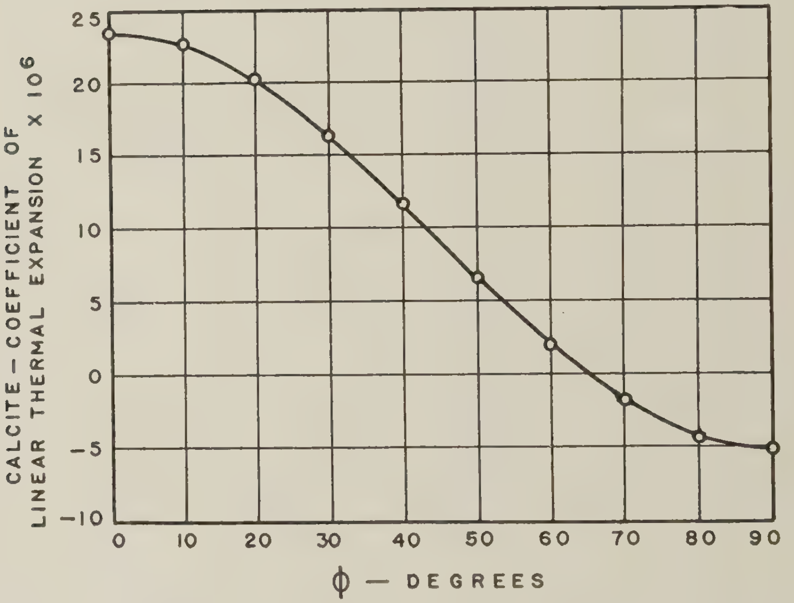

FIG. 3. ϕ is the angle between the c axis in a calcite crystal and any other direction.

Boas and Honeycomb (3, 4) found that cyclic heating and cooling produces deformation in such metals as cadmium, zinc and tin, due to the anisotropy of their thermal expansion, and that there are other significant effects such as grain boundary migration and evidence of preferential deformation in the randomly oriented grains. There is a striking parallelism between the effects reported by Boas and Honeycomb and those which may be inferred from thermal coefficients. The calculated volume coefficients of calcite and both cycles of Yule marble, plotted in Fig. 4, give the basis for the deductions which follow. It should be emphasized that, while the calculated values for calcite are correct, those for the marble are not true volume coefficients since the orientations upon which they are based are more or less random in the N-S and vertical directions and, to a lesser extent, in the E-W direction.

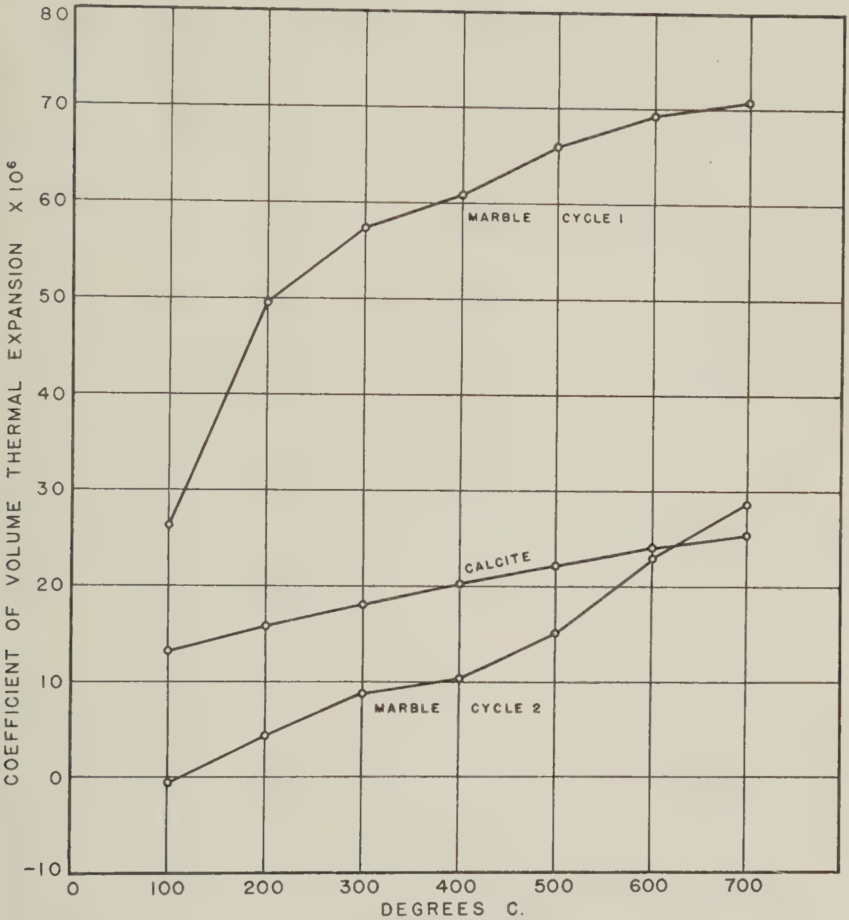

FIG. 4. Volume coefficients of expansion (calculated) for calcite and Yule marble.

SUMMARY

The Yule marble has a deformational history and, whether or not it was cyclic in character, residual strain remained which was relieved, for the most part, during the early part of the first expansion cycle. The change in curvature in the 300° to 400° range is interpreted as the zone in which recrystallization began. Continued heating introduced new strain because of the anisotropy of thermal expansion of the individual calcite grains and it is probable that much of this strain was relieved during the cooling portion of the first cycle. The low coefficients in the early part of the second cycle tend to substantiate this inference. Further heating during the second cycle again caused recrystallization in the same temperature range as before, resulting in a volume change at 700° in excess of that for calcite.

The foregoing deductions are necessarily conjectural at this time but it is expected that at least some of the questions mentioned will be clarified by further studies.

ACKNOWLEDGMENT

The authors gratefully acknowledge the grant-in-aid from the Rensselaer Polytechnic Institute Research Fund which made possible the purchase of the new dilatometric equipment.

REFERENCES

1. KÔZU, MASUDA AND UEDA, *Sci. Rep. Tohoku Imp. Univ.*, III, **3**, 247 (1929).
2. AUSTIN, SAÏNI, WEIGLE AND PIERCE, *Phys. Rev* , **57**, 931 (1940).
3. BOAS AND HONEYCOMB, *Proc. R. Soc.*, A, **186**, 57 (1946).
4. ——— *Proc. R. Soc.*, A, **188**, 427 (1947).

ABSORPTION OF INFRARED RADIATION BY POWDERED SILICA MINERALS

W. D. KELLER[1] AND E. E. PICKETT[2]

ABSTRACT

The absorption of infrared radiation over the range 2.0 to 15.0 microns by pulverized (suspended in Nujol) quartz from various localities and origins was measured in a Beckman Infrared Spectrometer. The characteristic absorption of quartz is compared to those of chalcedony, opal, alpha cristobalite, and fused silica. The effects of crystal structure apparently predominate over those of the silica molecule in the infrared absorption by pulverized silica minerals. Absorption by a single oriented plate of quartz or muscovite is dissimilar in fine detail to that of random powder.

INTRODUCTION

During a study of the absorption of infrared radiation by clay minerals (Keller, 1948) the need for information on the infrared absorption characteristics of the building units of clay minerals (silica tetrahedra, alumina and magnesia octahedra, water and OH groups) was early recognized. Although the absorption of the infrared by water and OH groups has been studied extensively by organic chemists, comparatively fewer measurements have been published on the infrared absorption by quartz, gibbsite, and brucite (see bibliography in "Infrared Spectroscopy" by Barnes, Gore, Liddel and Williams, 1944). No measurements especially on pulverized minerals were reported in the literature, but these are essential for comparisons with those of clays which must be studied in the pulverized form. Consequently before resuming work on clays, the infrared absorption by several of the silica minerals in powdered form was measured. This paper is concerned with their absorption of the infrared spectrum between 2.0 and 15.0 microns in wave length.

It will be recalled that the atoms which comprise molecules do not remain at rest but are continuously in vibration. The frequencies of their vibrations, for example those of O—H, C—O, C=O, C—H, N—H, etc., fall within the range of 10^{13} to 10^{14} cycles per second, which is the same order of magnitude as the frequencies of infrared radiation. Then if molecules of a substance whose vibrations are accompanied by a change of dipole moment are irradiated by a succession of monochromatic bands of infrared, those radiated frequencies which correspond to the intramolecular vibrational frequencies may be absorbed wholly or in part. If the per cent of radiation which is absorbed by a substance is plotted against the incident wave length (or frequency), the ensuing graph may be interpreted in terms of the intramolecular vibration. Hence certain molecules may be determined by their characteristic absorption, and may be "finger printed" by characteristic absorption graphs. A high degree of success has been achieved in the analysis of organic chemical compounds by chemists using infrared absorption as an analytical tool. To what extent the technique may be useful in mineralogy and related fields is relatively unexplored.

---

[1] Professor of Geology, University of Missouri.

[2] Assistant Professor of Agricultural Chemistry, in charge of Spectrographic Laboratory University of Missouri.

It is apparent at the outset that a knowledge of the absorption frequency of the molecules under study is essential. For simple or highly symmetrical molecules the approximate absorption frequency can be calculated by the equation:

$$\mathrm{N} = \frac{1}{2\pi c}\sqrt{\frac{k}{u}}.$$

Where N is the frequency in cm.$^{-1}$, c is the velocity of light, u is the reduced mass of the vibrating atoms, and k is the force constant which exists between the atoms. The formula has been simplified by reduction of the constants, and typical interatomic characteristics shown by Barnes et al.

A second approach to the derivation of absorption characteristics is empirical. Barnes et al. (p. 14), summarize the situation as follows:

> Although the mathematical approach has been of great value when applied to simple or highly symmetrical molecules, most of the information derived from infrared spectra is obtained by the application of the empirical method. This method consists of comparing the spectra of the largest obtainable number of different molecules having a common atomic group. By a process of elimination, it is often possible to find an absorption band whose frequency remains constant throughout the series. The presence, in an unknown, of an absorption at this frequency may reasonably form the basis for a guess that the particular atomic group is present. Confidence in this method can be obtained only by successful applications in a large number of cases.

Although mathematically derived characteristics may be tidier to the scientific purist, an empirical study may produce additional and valuable information. Even the massive lattice vibrations of crystals may absorb radiation (see second paragraph of next quotation). Hence, the empirical approach was used in evaluating the graphs shown in the subject study. A further quotation from Barnes, et al., is pertinent.

> It must not be assumed from this discussion that it is, or will be, possible to ascribe every observed absorption to a specific atomic group. Indeed, if this were true it would make more difficult the possibility of differentiating clearly between isomeric compounds. Actually only a few of the observed bands can usually be correlated in this manner. The majority of observed bands arise from normal modes of vibration which are characteristic of the molecule as a whole. These general absorption bands are very sensitive to structural changes, and so furnish us with a "fingerprint" of the molecule. They also make possible the analysis of isomeric mixtures and provide the basis for quantitative analyses of other closely related compounds.

> The normal vibrations of a molecule do not account for all of the absorption bands observed in its infrared spectrum. For example, in the far infrared there are absorptions caused by the slower rotations of the molecules or the massive lattice vibrations of crystals. Moreover, throughout the whole infrared region absorptions frequently occur at integral multiples (overtone bands) of the fundamentals, or at frequencies which are equal to the sum or difference (combination bands) of fundamentals. These bands in general absorb very much less strongly than do the fundamentals and consequently must be studied with thicker samples. Since they are so sensitive to the over-all molecular structure, they can sometimes be used more for successfully accurate fingerprinting of molecules and for the analysis of mixtures than the fundamental absorptions.

It is evident from the preceding discussion that absorption "peaks" or depressions are tell-tale characteristics of a positive nature of the irradiated compound. High transmission bands may be characteristic of certain compounds, but they constitute evidence of a negative type.

Apparatus and Technique

The apparatus used in this investigation is a Beckman Model IR-2 infrared spectrometer. Briefly, infrared radiation from a rich source is dispersed by a rock salt prism into a spectrum from which relatively narrow wave length bands are selected and transmitted along a path to a sensitive thermocouple. The intensity of the radiation transmitted is measured with the sample, and without it, in the absorption chamber, and the per cent transmission obtained thereby. High sensitivity of the instrument is achieved by suitable electronic amplification. The current infrared spectrometers embody highly advanced improvements over the apparatus which was available only a few years ago. Many of the older measurements of infrared absorption have been revised.

In this study, from 5 to 10 milligrams of the finely pulverized mineral was stirred and dispersed in 2 drops of Nujol (medicinal mineral oil) which filled the absorption chamber. The latter consists of rock salt plates which are separated by shims of variable and selected thicknesses, and held together by a metal frame. Nujol has been used as a suspending medium because it has a satisfactory viscosity, because its index of refraction lessens the scattering reflectance from the mineral particles, and because its own absorption spectrum is relatively simple. It should be recognized that the indices of refraction of both Nujol and a dispersed mineral may be radically different in the infrared range than they are in the visible spectrum. Regarding the absorption spectrum of the suspending medium, it has been suggested that a single pure substance which could be purified chemically and reproduced closely might be preferred as a suspending medium to one like Nujol which is a complex mixture. Theoretically this is correct, but practically no pure liquid is known which has a simple absorption spectrum and also possesses the other properties which are desired for the infrared work. Because Nujol is a mixture, many tiny absorption peaks of individual constituents are averaged out, and the curve is flat enough that absorptions occurring within the suspended mineral show up.

About four hours are required to make a run and plot it.

EXPERIMENTAL RESULTS

An absorption graph of Nujol alone in the specimen chamber is shown in Fig. 1. Along the base of the abscissa is plotted the wave length of the radiation in microns, 2 to 15 microns at 0.5 micron intervals, and along the top is the corresponding frequency in wave numbers or reciprocal centimeter. Transmission of radiation in per cent is plotted on the ordinate. Nujol is relatively transparent to most infrared radiation, transmitting from 80 to 90 per cent over most of the spectrum. A light absorption occurs at approximately 2.3 and 2.4 microns, and almost complete absorption (opacity) for a band at about 3.43 microns in wave length. Lesser absorption occurs from 3.6 to 3.72 microns and pronounced absorption at 6.86 and 7.28 microns. Numerous slight absorptions extend over wave lengths to about 11.0 microns and another prominent peak occurs at 13.86 microns. This "background" of absorption is unavoidably present in every measurement where a mineral was immersed in Nujol. It may be "subtracted" from the mineral graph to obtain the absorption characteristics of the mineral.

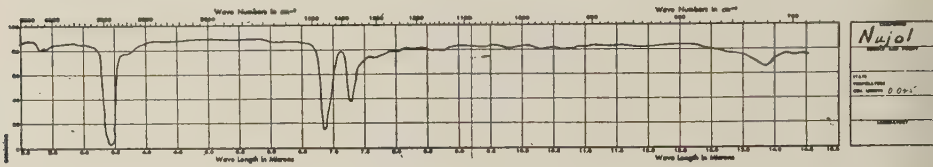

FIG. 1. Infrared spectrogram of Nujol.

QUARTZ

In Fig. 2 are shown representative absorption spectra of varieties of quartz which were finely pulverized and suspended in Nujol. Specimen No. 86 is of a clear crystal of quartz from Brazil. Omitting the absorption peaks due to Nujol, it is observed that quartz powder absorbs infrared radiation at 5.0 and 5.3 microns, and with lesser intensity at 5.93 and 6.21 microns. The second decimal figures of the latter two absorptions are taken from another measurement. A gradual increase in absorption is shown from about 4.5 microns to about 6.5 microns. Upward in wave

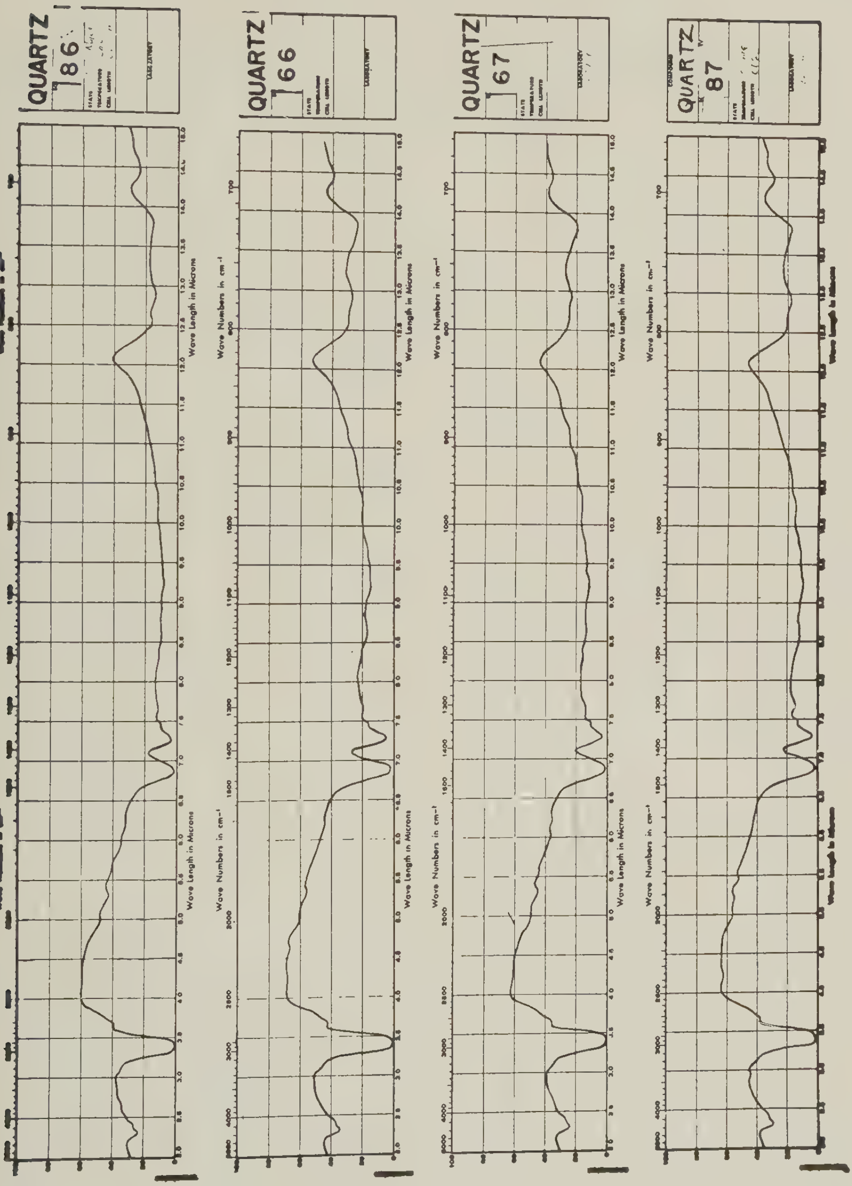

FIG. 2. Infrared spectrograms of quartz.

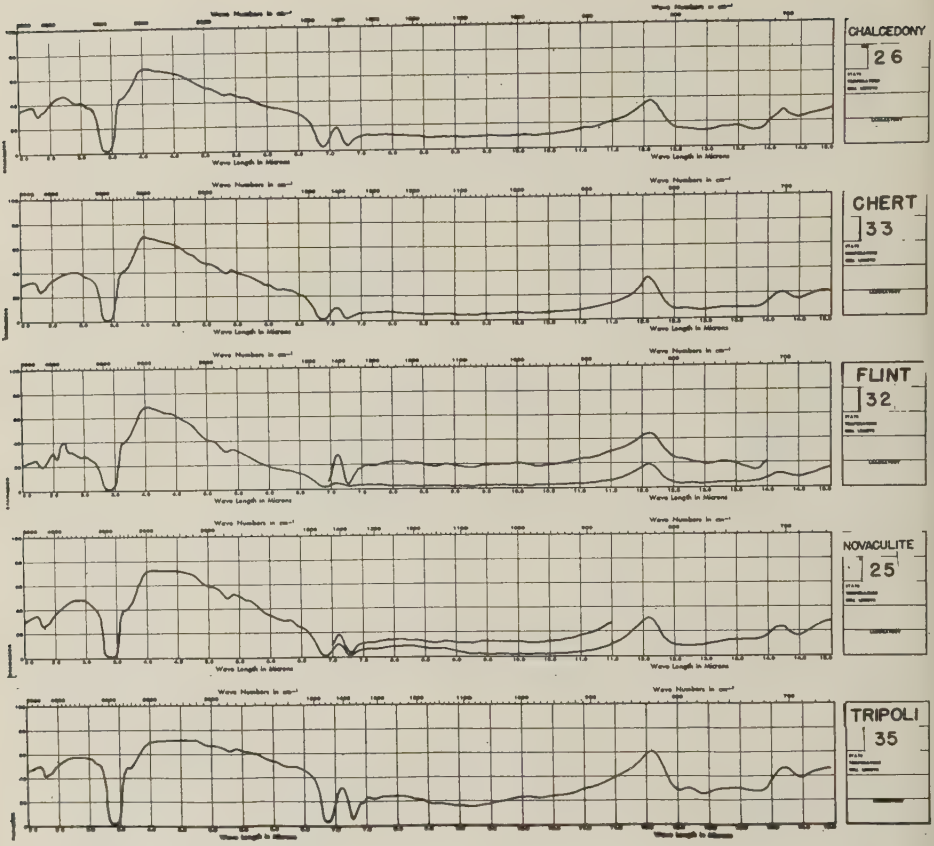

Fig. 3. Infrared spectrograms of chalcedony, chert, flint, novaculite, and tripoli.

length from the Nujol absorption at 7.9 microns the quartz powder absorbs uniformly strongly until about 9.9 microns where a gradual decrease in absorption begins and culminates at a peak of high transmission at about 12.08 microns. The transmission peak (at 12.08) is a negative measure, but it occurs so consistently with quartz powder that it has some secondary value in recognizing a quartz curve. Other absorptions occur at about 12.54 and 12.9 microns, and more strongly at 14.46 microns. The 14.46 micron absorption band appears to be highly characteristic of extended quartz-like structure. Its absence in alpha-critobalite and fused silica, which are discussed later, indicates that the absorption is a function of the quartz-type crystal structure.

Specimen No. 66, pulverized quartz from coarse-grained Missouri granite shows a graph similar to No. 86, plus an additional slight absorption at 4.64 microns. Metamorphic quartz from the Baraboo quartzite, No. 67, closely parallels the Brazil quartz. The familiar rose quartz from Custer, South Dakota, No. 87, shows absorption similar to the others previously figured.

Chalcedony, Chert and Tripoli

A specimen of chalcedony, typically fibrous and waxy when powdered, gives the absorption graph No. 26. The curve is smoother than those of quartz and the peaks are slightly subdued. An *x*-ray diffraction pattern run on this sample and compared with a pattern run on Arkansas crystal quartz, No. 54, showed peaks of slightly lower intensity and more subdued vertices than those of quartz.

Crystalline chert (pulverized), which may be composed of varying amounts of microcrystalline quartz, chalcedony and opal, is represented by absorption spectra No. 33, 32, and 25, which are respectively of chert from the Mississippian limestone near Seneca, Missouri (tripoli region), of very dark gray flint from the chalk at Dover, England, and of translucent novaculite from a hone stone quarry near Hot Springs, Arkansas. All three crystalline cherts give typical chalcedony-quartz absorption patterns. No. 32 shows extra absorption at 2.56, 2.75 and 2.95 microns. The last two are probably due to OH groups. Tripoli, No. 35, which occurs in the Seneca, Missouri, tripoli producing region has about the same absorption characteristics as the chert of that region. No. 33.

Opal

Opal collected from different sources shows somewhat different absorptions. A specimen of water-clear hyalite opal, No. 40, from Guanajuato, Mexico, exhibits relatively featureless differential absorption. Some water in OH absorption is shown by the small peaks at 2.7 microns ("unbound OH") and at 2.86 microns ("bound OH"). At longer wave lengths there is no particularly characteristic absorption. Opal No. 40 has low birefringence and shows weak undulatory extinction. The index of refraction varies a little, ranging from 1.456 to 1.458. The water lost upon calcination (actually total ignition loss) was 2.7 per cent.

Relative to the nature of "unbound and bound OH," it may be pertinent to recall here that chemists have found OH groups absorb at different wave lengths between 2.7 and 3.1 microns depending upon the degree of hydrogen bonding of these groups with each other or with other O atoms in the lattice. Where OH groups are situated independently, monomeric, within a crystal lattice the absorption is at about 2.75 microns (2.72 in the kaolin group). Where two or more OH groups are sufficiently close together, the hydrogen of the OH groups may assume a

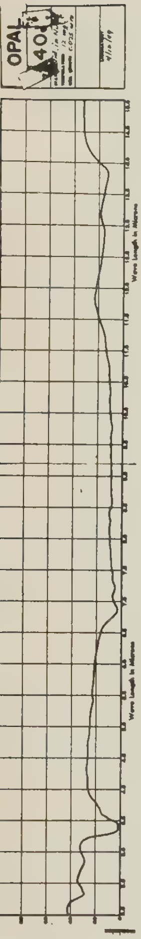
OPAL
40
Wave Numbers in cm⁻¹
Wave Length in Microns

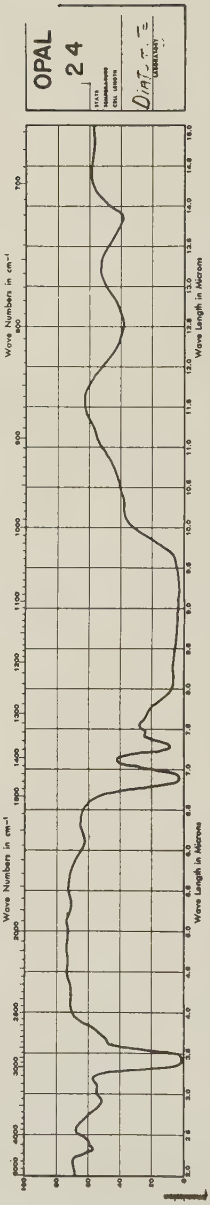
OPAL
24
STATE
TEMPERATURE
CELL LENGTH
Diat. π. =
LABORATORY
Wave Numbers in cm⁻¹
Wave Length in Microns
5000
4000
3000
2500
2000
1500
1400
1300
1200
1100
1000
900
800
700
2.0
2.5
3.0
3.5
4.0
4.5
5.0
5.5
6.0
6.5
7.0
7.5
8.0
8.5
9.0
9.5
10.0
10.5
11.0
11.5
12.0
12.5
13.0
13.5
14.0
14.5
15.0
100
80
60
40
20
0

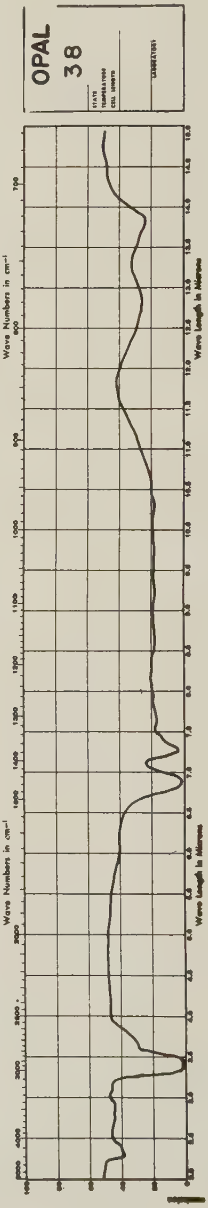
OPAL
38
STATE
TEMPERATURE
CELL LENGTH
LABORATORY
Wave Numbers in cm⁻¹
Wave Length in Microns

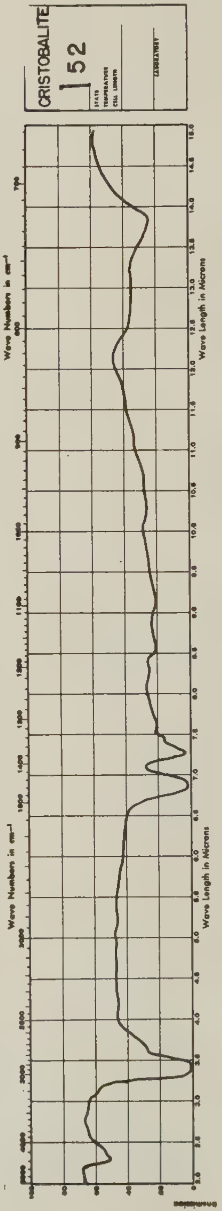
CRISTOBALITE
52
STATE
TEMPERATURE
CELL LENGTH
LABORATORY
Wave Numbers in cm⁻¹
Wave Length in Microns

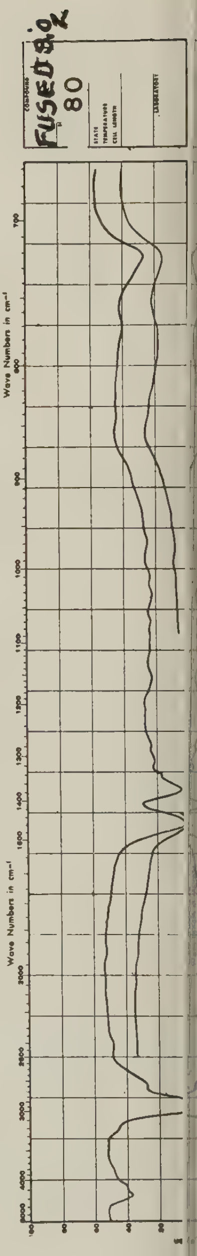
FUSED SiO2
80
COMPOUND
STATE
TEMPERATURE
CELL LENGTH
LABORATORY
Wave Numbers in cm⁻¹
Wave Length in Microns

more or less fixed position between two oxygen atoms with the formation of a resonating bond between both oxygen atoms simultaneously, the so-called hydrogen bond. The dimeric groups absorb at about 2.85 microns and polymeric groups at about 2.95 microns. Free water, H_2O, absorbs in the 6.0 to 6.1 micron band as shown in the spectrum of opal No. 24. Preliminary work on clays and other hydrated minerals indicates that the nature of their hydration merits additional research using infrared absorption.This work is in progress by the writers.

Diatomite (opal) from a Tertiary lake deposit near Quincy, Washington, gave an absorption curve shown in No. 24. The presence of bonded OH is indicated by absorption at 2.92 microns and free water at 6.1 microns. Strong absorption occurs from 8.0 to 9.6 microns, with weaker absorption from 10.2 to 10.4 microns and in a broad peak at 12.53 microns. High transmission occurs from 11.5 to 11.64 microns. Because this absorption curve differed so much from the other silica curves a check was re-run with duplicate results. The index of refraction of opal No. 24 is about 1.418. Total loss on ignition was 15.3 per cent.

A third variety of opal, opaline chert from the Monterrey formation of California,[3] absorbed infrared as shown in No. 38.

Again the absorption by OH was scanty. Strong absorption extends from 7.5 to 10.6 microns, followed by high transmission at 11.84 and a broad absorption peak centering at 12.84 microns. Obviously the several opal spectrograms are noticeably different. The absorption by the water in two opals is weaker than was expected. Taliaferro found an unexpected relationship between water in opal and densities and indices of refraction of the latter. Further research on the role of water in opal and its internal architecture is being planned. *X*-ray diffraction patterns of the diatomite and hyalite showed no well defined crystal structure.

Obviously the lattice organization of anhydrous silica in quartz and in crystalline chert[4] exerts a mass crystal effect different from the water-silica system in opal.

Cristobalite and Fused Silica

Artificially prepared cristobalite,[5] No. 52, deviated noticeable from quartz in its infrared absorption spectrum. In general, cristobalite lacks

---

[3] Furnished through the courtesy of M. N. Bramlette. Sample came from specimen shown in Plate 7B in *U.S.G.S. Prof. Paper* **212,** "Monterrey formation of California and origin of its siliceous rocks."

[4] A chert from the Franciscan formation of California (furnished by M. N. Bramlette) showed typical quartz absorption, as did the cherts previously described.

[5] Prepared through the courtesy of the A. P. Green Fire Brick Company, Mexico, Missouri. Arkansas crystal quartz was heated in a brick testing furnace and held at approxi-

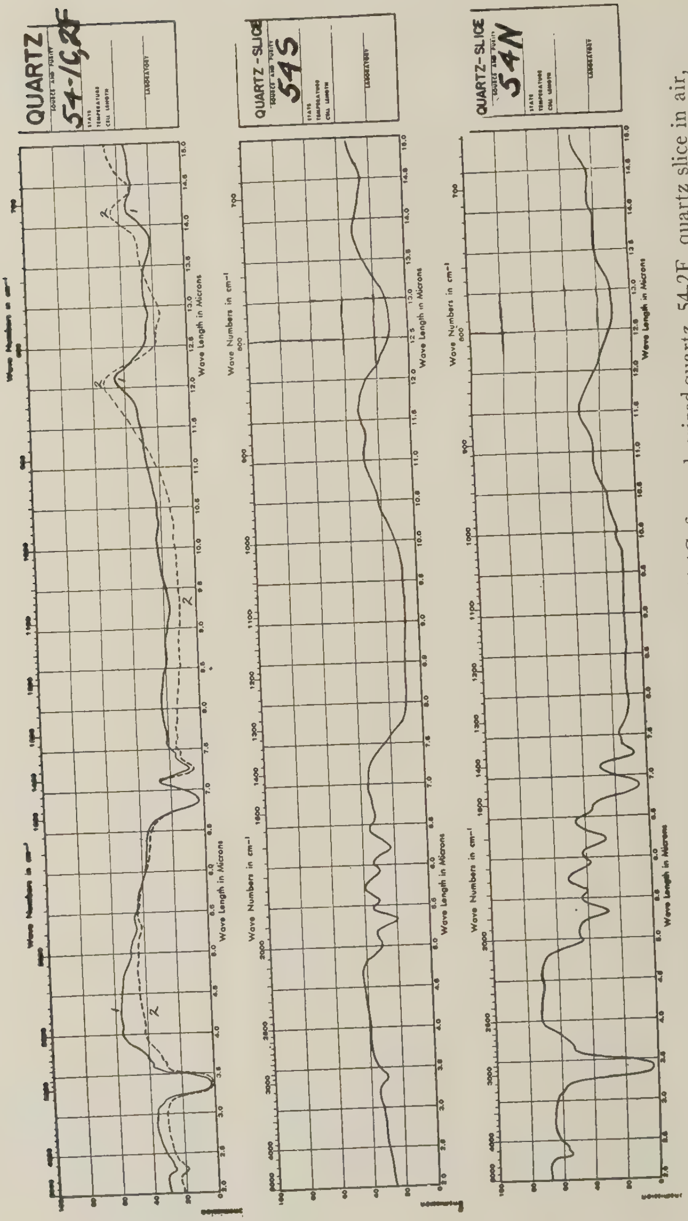

FIG. 5. Infrared spectrograms of coarse pulverized quartz, 54-1C, fine pulverized quartz, 54-2F, quartz slice in air, 54S, and the quartz slice immersed in Nujol, 54 N. Arkansas quartz.

the increasing absorption in the 4.0 to 6.5 micron range, is less absorbent of wave lengths in the range 8 to 11 microns, and specifically lacks the absorption peaks which quartz shows at 12.54, 12.9, and 14.46 microns.

The differences in absorption must be a function of crystal structure rather than characteristics of the silica molecule.

The absorption of pulverized fused silica[6] is shown in No. 80. A partial re-run of the sample for check purposes is plotted on the same graph. The absorption by fused silica resembles that of hyalite opal, but is probably more pronounced in the region 7.5 to 10.5 microns. Presumably the similar random structure of both accounts for their similar absorptions.

EFFECT OF PARTICLE SIZE

If the diameter of essentially all the particles and the wave length of the radiation were the same size the result would be strong selective scattering of this radiation. Radiation of other wave lengths would be scattered to a smaller extent. The per cent transmission would thus be lower wherever wave length and particle size are similar, giving rise to apparent absorption maxima qualitatively similar to those characteristic of the various atomic groupings present in the sample. A broad range of particle sizes in the sample would cause only a very broad general scattering, perhaps extending for many microns. This is more likely to be the case for the present samples, where a wide range of sizes exists. Nevertheless it was judged advisable to check the influence of particle size in several ways.

Sodium chloride is quite transparent to infrared radiation between 2 and 15 microns. A sample of it was powdered in a manner similar to that of the silica minerals and its absorption measured in this region. It showed no evidence of selective scattering.

A portion of No. 54, Arkansas crystal quartz, was separated by sieving and washing in alcohol into two size fractions, predominating in sizes ranging from 30 to 75 microns, 54-1C, and about 15 microns in diameter, 54-2F. Their absorption spectrograms show some differences, but these are in degree and not in kind. In the absence of any drastic differences in the spectrograms due to variation in particle size, this factor appears to have only secondary importance in affecting measurements.

---

mately 1650° C. for five hours and allowed to cool slowly (the reheat test cycle for superduty refracteries), this being repeated for a total of 6 cycles. An x-ray diffraction pattern gave the lines of alpha cristobalite. The indices of refraction of the material are: omega, 1.486; epsilon, 1.484.

[6] Donated by the A. P. Green Fire Brick Company. The index of refraction of this fused silica ranges from 1.458 to 1.461. An x-ray diffraction pattern showed no lines indicative of crystalline structure.

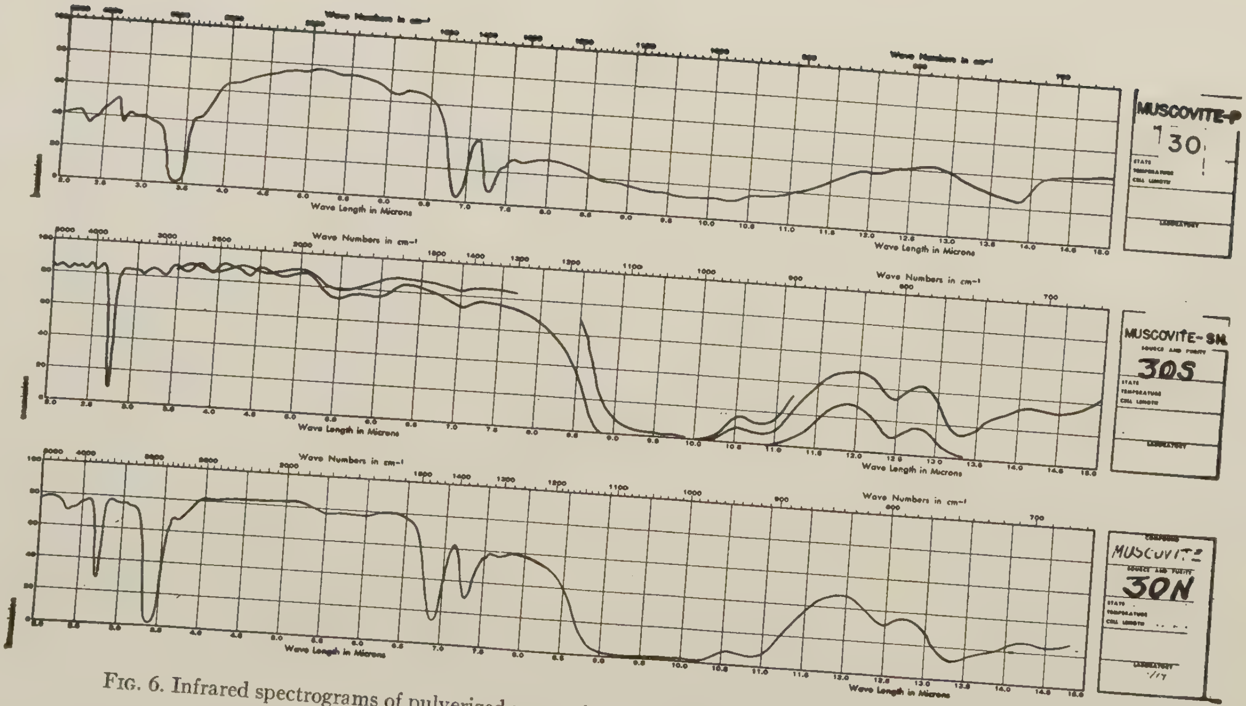

FIG. 6. Infrared spectrograms of pulverized muscovite in Nujol, No. 3, sheet muscovite in air, No. 30 S, and the same sheet immersed in Nujol, No. 30 N. Muscovite from Jackson, N. Car.

Since this paper went to press, the Carter Oil Company laboratory at Tulsa has shown notably sharper resolution in *IR* spectrograms of mineral particles whose diameter is smaller than the wave length of the incident radiation. (Personal communication, Mr. Parke Dickey, October, 1949).

POWDER AND SINGLE CRYSTAL MEASUREMENTS

Conventionally, infrared absorptions have been measured on single-piece solids, as on glass plates or on slices of large crystals. However, powders were measured in this study to provide a basis of comparison with clays which are being measured and which obviously are not available in large crystals. In order to relate the measurements between powders and plates two minerals, quartz and muscovite, were tested in both forms. As an extra control the mineral slices were re-measured while immersed in Nujol. Curves 54-1C and 54-2F which were described immediately above; 54-S, a slice of Arkansas crystal quartz cut with the *c*-axis lying in the plane of the slice; and 54-N, which is 54-S immersed in Nujol, show the variations on material all coming from the same crystal source. (Fig. 5)

Considerable deviation in details is found between powder and wafer absorption. In 54-S, the dry slice, and in 54-N, the immersed slice, details of absorption between 4.7 and 6.6 microns are shown which are much subdued in the powder. The characteristic high transmission at about 12.1 microns for the powder is not present in the slices which show a gentler transmission peak at 11.5 to 11.6 microns. Powder and slices show common absorption in the 12.7 to 12.9 micron region. The 13.8 micron absorption of the powder is not found with the slices.

A parallel series was run with muscovite, Fig. 6, using a cleavage flake of mica for the mineral slice, 30-S. Curves 30 and 30-N show the result run on the powder and on the slice immersed in Nujol, respectively. The high absorption at 2.72 to 2.74 microns is due to the unbound OH group. The strong absorption in the region 9.0 to 11.0 microns and at 12.48 and 13.3 microns with the sheet mica is subdued in the powder. We are uncertain whether the pronounced details of absorption which are shown in the single mineral plate, as contrasted to the powder, are due primarily to the physical difference in size, or to the single orientation of the slice and random orientation of the powder. Certainly the polarizing and crystallographic properties of the mineral crystal should play some part in the absorption.

On the basis of the differences in infrared absorption shown by slice and powder of quartz and muscovite, it is concluded that fine details of the infrared absorption characteristics of the two forms of minerals cannot be predicted one from the other.

SUMMARY

Pulverized quartz absorbs characteristically certain bands of radiation in the infrared range of 2.0 to 15.0 microns. Igneous, vein, sedimentary, and metamorphosed quartz absorb similarly. Specific absorptions occur at 5.0, 5.3, 5.93 and 6.21 microns. High, fairly uniform absorption occurs from about 7.9 to 9.9 microns from where it decreases with longer wave lengths until it reaches a minimum at about 12.08 microns. At still longer wave lengths it absorbs at 12.54, 12.9 microns, and more intensely at 14.46 microns.

Chalcedony absorption curves are slightly more subdued than those of quartz.

Hyalite opal from Guanajuato, Mexico, shows almost no differential absorption. Diatomite from Quincy, Washington, and opaline chert from the Monterrey formation of California show some absorption bands which suggest departures from hyalite. Fused silica absorbs much like opal. Artificially prepared alpha cristobalite shows fewer absorption bands than does quartz. It is concluded from the differences in infrared absorption by the different silica minerals that the absorption must be a function of crystal structure rather than of the silica molecule.

All of the observations summarized above were made on pulverized materials suspended in Nujol. Variation in particle size distribution from less than 15 to about 75 microns in cross section affects infrared absorption in degree, but not in kind.

Comparison measurements made on plates of quartz and muscovite mounted dry, also immersed in Nujol, and in powder form suspended in Nujol, show notably more detail on the plates than on the powder. Results cannot be predicted for one form from the other. Probably the differences should be attributed to differences in mineral orientation.

Acknowledgment. The cost of running the infrared measurements and the x-ray patterns was defrayed by University of Missouri Research Council Grants Nos. 319 (302) and 327 (302).

REFERENCES

BARNES, R., BOWLING, GORE, ROBERT C., LIDDEL, URNER, AND WILLIAMS, VAN ZANDT, Infrared spectroscopy, Industrical applications and bibliography, Reinhold Pub. Co. (**1944**).

KELLER, W. D., Absorption of infrared radiation by clay minerals (abstract): *Bull. Geol. Soc. Am.*, **59**, 1332 (1948).

TALIAFERRO, N. L., Some properties of opal: *Am. Jour. Sci.*, 5th ser., **30**, No. 179, 450–474 (1935).

SUPPRESSION OF THERMAL REACTIONS IN KAOLINITE

R. M. Gruver, E. C. Henry and H. Heystek,
The Pennsylvania State College, State College, Pennsylvania.

Abstract

Suppression of thermal reactions in kaolinite by fluxing impurities present in brick clays may cause considerable modification of thermal analysis results. Heat effects obtained by thermal analysis of complex mixtures may be misleading.

Introduction

In an investigation of brick clays from Pennsylvania by the techniques of *x*-ray diffraction and differential thermal analysis, the following observations were made:

1. After samples were tested in the differential thermal analysis furnace, many were slightly sintered and could be removed from the platinum bucket in one piece. The maximum temperature reached in the furnace on each run was 1050° C.
2. Although the *x*-ray diffraction patterns on many of the clays indicated the presence of an appreciable amount of kaolinite, it was not always possible to make the same deduction from the differential thermal curves.
3. In the case of a few clay samples that were more refractory than the others, no sintering was observed at 1050° C. The presence of a small amount of kaolinite in these was definitely indicated by the differential curves.

As a result of these observations, an attempt was made to simulate the sintering conditions occurring in the impure brick clays at low temperatures by adding small amounts of ferric oxide and sodium carbonate to Langley kaolin.

Materials and Methods

The thermal analysis apparatus used for this investigation has been described in a previous paper[1] along with the method by which the samples were run.

The samples to be tested were prepared by weighing the proper amounts of Langley kaolin and C.P. sodium carbonate, ferric oxide, or other materials to give a 2.500 gram batch. This batch was placed in an automatic mortar and pestle grinder, where the dry materials were ground for twenty minutes to obtain a uniform mixture.

From this mixture a 0.500 gram sample was taken for thermal analysis; an equal amount of calcined alumina was used for the standard reference

---

[1] Gruver, R. M., Precision method of thermal analysis: *Jour. Am. Ceram. Soc.*, **31**, 324–328 (1948).

TABLE 1

Composition of Samples, Weight Per Cent							Result of Thermal Analysis					
							Endothermic Reaction			Exothermic Reaction		
Sample No.	Kaolin	Na_2CO_3	Fe_2O_3	NaCl	$MgCl_2 \cdot 6H_2O$	Calcined Kaolin	Area Under Curve	Depth of Peak	Peak Temp. (±3°)	Area Under Curve	Height of Peak	Peak Temp. (±3°)
1	100	—	—	—	—	—	7.7	3.1	595	0.6	4.75	976
2	98	2	—	—	—	—	7.4	3.0	597	0.75	4.25	973
3	96	4	—	—	—	—	7.3	2.9	598	0.7	3.1	975
4	94	3	3	—	—	—	7.0	2.9	598	0.7	3.3	974
5	94	6	—	—	—	—	6.8	2.8	598	0.5	2.1	976
6	94	—	6	—	—	—	6.7	2.9	599	0.8	4.8	975
7	90	4	6	—	—	—	6.6	2.8	600	0.6	2.2	976
8	94	—	—	—	—	6	6.6	2.8	599	0.7	4.8	976
9	90	—	10	—	—	—	6.3	2.65	590	0.75	4.4	976
10	90	6	4	—	—	—	6.3	2.5	587	0.45	1.5	972
11	90	10	—	—	—	—	6.2	2.3	590	0.4	0.85	974
12	94	—	—	—	6	—	5.7	2.5	592	0.6	2.15	965
13	94	—	—	6	—	—	5.4	2.3	583	0.35	1.05	973

material. These materials were heated at 400° C. per hour; the sensitivity of the recorder for the differential couple was set at 5 millivolts for a full scale deflection.

RESULTS AND DISCUSSION

The mixtures tested by differential thermal analysis are listed in Table 1. For comparison, one sample diluted with calcined kaolin and two samples with materials which have melting points near that of sodium carbonate were included in the tests. Several of the differential thermal

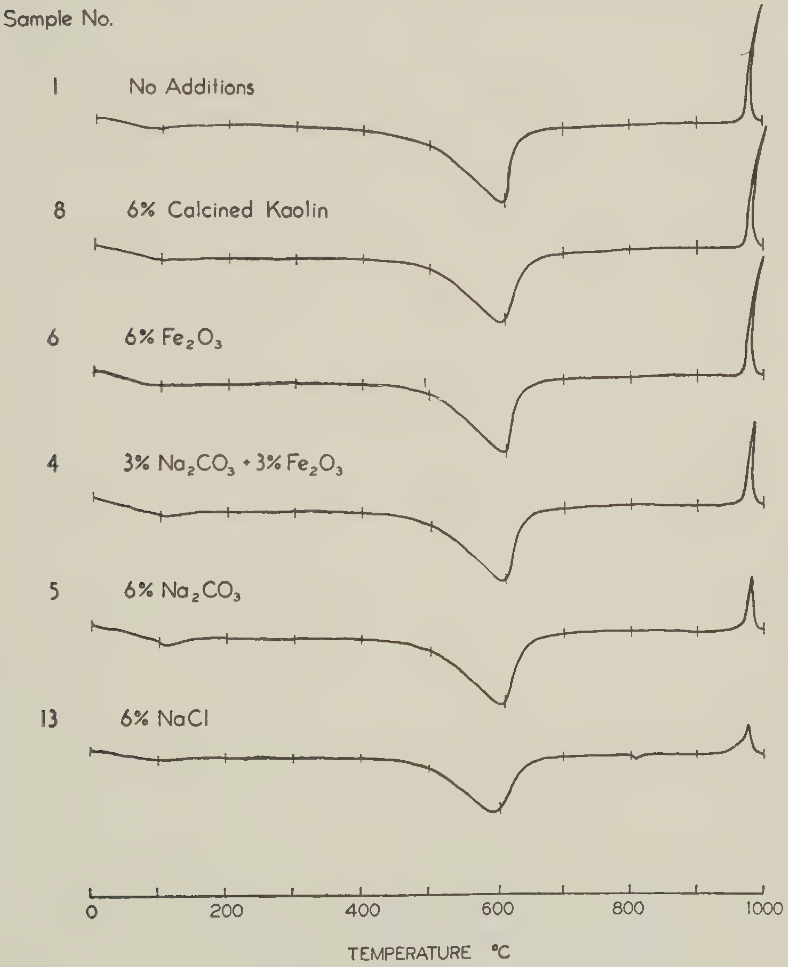

FIG. 1. Thermal analysis curves of Langley kaolin, showing the effects of various contaminants.

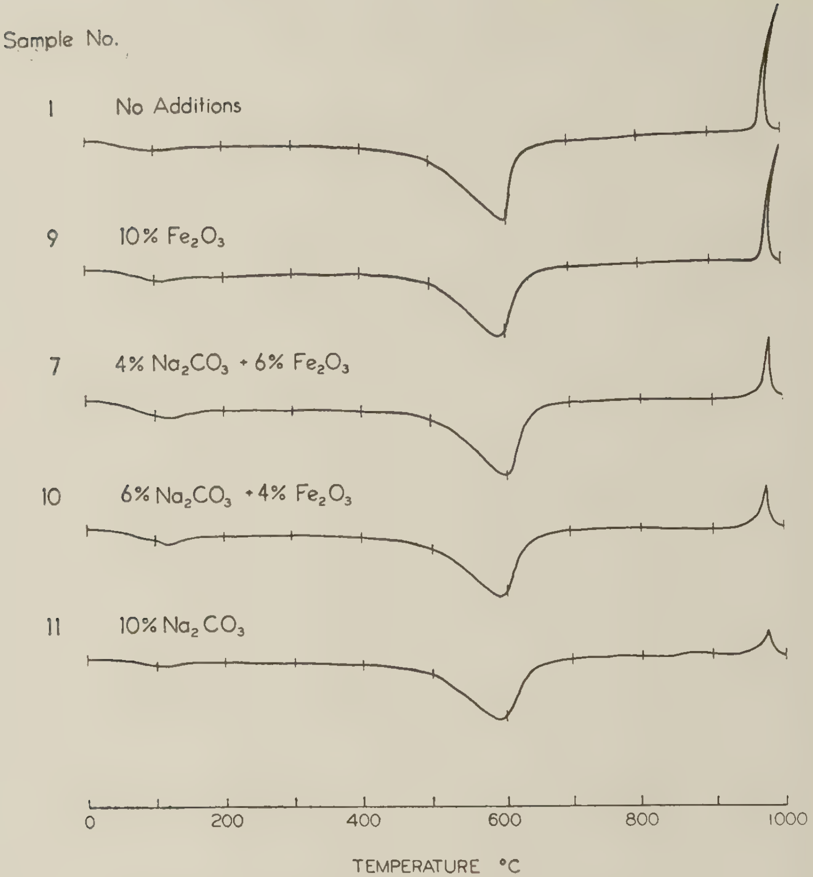

FIG. 2. Thermal analysis curves of Langley kaolin, showing effects of sodium carbonate and ferric oxide.

curves which portray the suppression of the thermal reactions are shown in Figs. 1 and 2.

As shown in Table 1, suppression of the heat effects of kaolinite is dependent on both the amount and type of contaminant present. The intensity of the exothermic reaction near 975° (transformation of amorphous alumina to gamma alumina) is affected more than that of the endothermic (dehydration) reaction at about 595°. Referring to Fig. 1, it appears that effective suppression is caused by fusible impurities in the kaolin. The peak is little affected by iron oxide or calcined kaolin alone, evidently because no fusion takes place. The curves in Fig. 2 seem to indicate that the presence of iron oxide in combination with a flux such as sodium carbonate does not suppress the formation of gamma alumina much more than does sodium carbonate alone.

The results indicate the possibility that impurities present in brick clays may react with the clay minerals and alter their normal heat effects. If a sample is sufficiently impure and reaction takes place while the material is being heated for differential thermal analysis, there is a good chance that one does not have mineralogically at elevated temperatures the same material which he had at room temperature. Thus, the heat effects due to kaolinite at 600° C. and 980° C. may reflect somewhat the amounts present at those temperatures, but should not be interpreted as indicative of the amount of kaolinite originally present.

From this picture, it seems apparent that observations of the magnitude and temperatures of heat effects obtained during the thermal analysis of complex mixtures may be misleading if one attempts thus to judge the amounts of various phases present in the mixture at room temperature.

MINERAL ISOGRADS IN SOUTHEASTERN PENNSYLVANIA

HUGH MCKINSTRY, *Harvard University, Cambridge, Massachusetts.*

"It is much to be desired that the zonal method of mapping, initiated by Barrow, should be confirmed and further elaborated by its application in other countries." Alfred Harker[1]

ABSTRACT

The formations that have been grouped as the "Glenarm Series" consist of phyllites, schists and gneisses with subordinate amounts of quartzite and marble. Within this series, a general, though by no means regular, increase in intensity of metamorphism toward the east and south has long been recognized; several authors have published small-scale maps, some based on texture and some on mineral distribution but without definite mineral isograds.

The main feature of the present paper is a map (in two sections) of the area covered by the Philadelphia and Coatesville-West Chester Folios showing reported and observed occurrences of index minerals. In the argillaceous rocks the zonal arrangement: chlorite, biotite, garnet, staurolite, cyanite, sillimanite is in accord with observations in metamorphic areas in other parts of the world. The zones are somewhat crowded and show local overlapping. In the associated carbonate rocks, tremolite appears in the middle-grade zone and sparse pyroxene in the highest grade attained. Wollastonite and garnet have not been reported in the carbonate rocks.

INTRODUCTION

The distribution of metamorphic minerals in the Wissahickon and associated formations in the Piedmont region of southeastern Pennsylvania shows a zonal arrangement indicating increasing grade of metamorphism from northwest to southeast. Despite some overlapping of zones and a few local anomalies, the general arrangement of index minerals is the same as that observed in many other tracts of aluminous schists and gneisses.[2] The sequence with increasing grade of metamorphism is: chlorite, biotite, garnet, staurolite, cyanite, sillimanite.

The main purpose of this paper is to present maps showing the distribution of index minerals. Although the metamorphic problems of the region need much more study in the field as well as in the laboratory, the data now available may help to round out the broader picture of metamorphism in the Piedmont region and at the same time point to localities where further investigation is needed.

---

[1] Harker, Alfred, Metamorphism. London, Methuen and Co. **(1932)**, p. 187.

[2] Barth, T. F. W., Structural and petrologic studies in Duchess County, New York, Pt. II: *G. S. A. Bulletin*, **47**, 775–850 (1936).

Billings, M. P., Regional metamorphism of the Littleton-Moosilauke area, New Hampshire: *G. S. A. Bulletin*, **48**, 463–566 (1937).

References to earlier studies, mainly in Scotland and Scandinavia, will be found in Turner, Francis, Mineralogical and structural evolution of the metamorphic rocks: *G. S. A. Memoir* **30**, 35, 36 (1948); also Harker, Alfred, Metamorphism, London: Methuen and Co. Ltd. (1932), p. 188.

LOCATION

The present study embraces an area of about 700 square miles in the extreme southeastern corner of Pennsylvania and includes most of the area covered by the U.S. Geological Survey's Coatesville-West Chester and Philadelphia folios (Fig. 1). It includes the southern half of Chester County, all of Delaware County and parts of Philadelphia and Montgomery Counties.

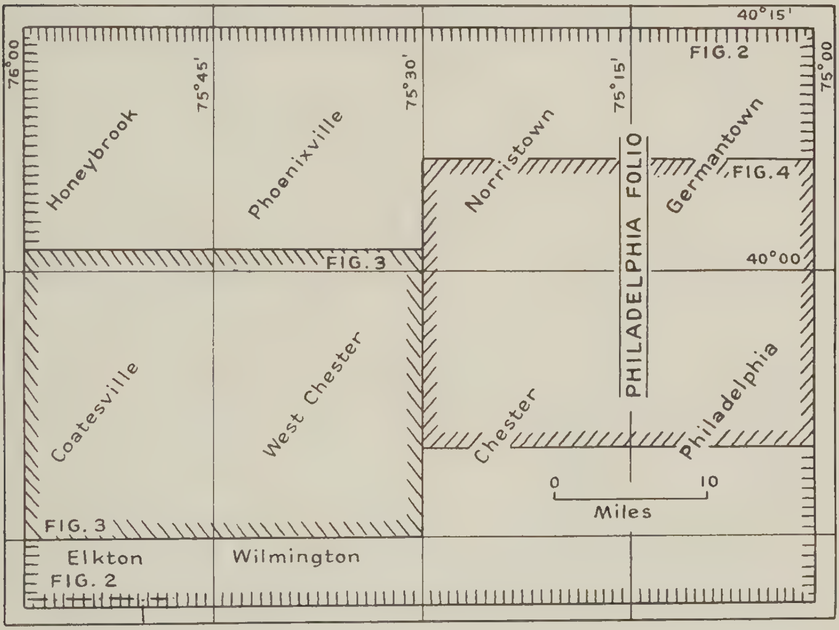

FIG. 1. Index Map to U.S.G.S. Quadrangles and to Figures 2, 3 and 4.

GENERAL GEOLOGY

Regional Setting

A glance at the geologic map of North America will show that the trend of Appalachian structure, though following a general northeasterly course from Georgia to New England, swings locally to a more easterly direction through Pennsylvania. Anyone making a traverse southerly across this trend would cross the Paleozoic rocks of the Appalachian province and enter a belt of formations of which some are unquestionably pre-Cambrian and others are of controversial age. The most southerly occurrence of undisputed Paleozoic rocks is a strip of Cambrian and Ordovician limestones[3] that finds topographic expression as a nearly straight valley forty miles long, the Chester Valley. (Fig. 2).

Age of Formations

With regard to the sequence and structure of the formations south of the valley, it is difficult to present a brief and simple statement, owing to differences of opinion. The oldest formation, the Baltimore gneiss, is unquestionably pre-Cambrian but the age of the overlying Glenarm series is controversial. Knopf and Jonas[4] regarded the Glenarm series as pre-Cambrian and in order to account for the fact that the Glenarm rocks apparently overlie the Ordovician limestones of the Chester Valley, postulated a fault-contact—the Martic overthrust. Shortly after this interpretation was proposed, the writer[5] questioned the existence of the fault and advocated a Paleozoic age for the Glenarm series. Subsequently, Miller[6] and Mackin[7] expressed similar views and still more recently the Martic Overthrust problem has been thoroughly discussed by Cloos and Hietanen[8] without reaching a definite conclusion. Finally, Stose and Stose[9] have suggested that part of the Glenarm series—the Setters and Cockeysville formations—may be Cambrian and the crystalline schists may be in part Cambrian to Ordovician, thus recalling the earliest views of Bliss and Jonas.[10] The whole problem has been reviewed in concise fashion by Swartz[11] who concludes that "there is much evidence favoring the opinion that the Glenarm series . . . is Cambro-Ordovician. . . . "

The writer is still of the opinion that the Glenarm series is Paleozoic and that the necessity for a Martic overthrust is not demonstrated. While the distribution of metamorphic minerals is quite compatible with this view, the present paper is not offered as direct evidence either for or against the Martic overthrust hypothesis.

---

[3] Limestone is used in this paper in its broader sense to include dolomite and marble.

[4] Knopf, Eleanora Bliss, and Jonas, Anna I., Geology of the McCalls Ferry-Quarryville District, Penna.: *U.S.G.S.*, *Bulletin* **799**, 71–84 (1929).

[5] McKinstry, H. E., Review, *Jour. Geol.*, **38**, 472–474 (1930).

[6] Miller, B. L., Age of the schists of the South Valley Hills, Penna.: *Bulletin G.S.A.*, **46**, 715–756 (1935).

[7] Mackin, J. Hoover, Problem of the Martic Overthrust and the age of the Glenarm series in southeast Penna.: *Jour. Geol.*, **43**, 356–380 (1935).

[8] Cloos, Ernst, and Hietanen, Anna, Geology of the "Martic Overthrust" and the Glenarm Series in Penna. and Md.: *G.S.A.*, *Special Paper* No. **35** (1941).

[9] Stose, Anna J., and George W., Geology of Carrol and Frederick Counties, Md., Physical features of Carrol and Frederick Counties: *Md. Geol. Survey*, p. 83 (1946).

[10] Bliss, Eleanora F., and Jonas, Anna I., Relation of the Wissahickon mica gneiss to the Shenandoah limestone and Octoraro schist of the Doe Run and Avondale region, Chester County, Pa.: *U.S.G.S.*, *Prof. Paper* **98-B** (1916).

[11] Swartz, Frank M., Trenton and sub-Trenton of outcrop areas in New York, Pennsylvania and Maryland: *Bull. A.A.P.G.*, **32**, 1506–1512 (1948); reprinted as *Penna. Topog. and Geol. Survey*, *Bull. G-***22**.

The alternative interpretations are compared in the accompanying stratigraphic columns:

In and North of Chester Valley	*South of Chester Valley*			
	Martic overthrust Interpretation		*Alternative Interpretation*	
Ordovician			*Glenarm Series*	
Martinsburg shale		- - - - - - - - - - - -		Peters Creek fm.
				Wissahickon fm.
Conestoga ls.		- - - - - - - - - - - -		Cockeysville marble
Cambrian				
Limestones and Dolomites				
Antietam quartzite				
Harpers schist		- - - - - - - - - - - -		Setters fm.
Chickies qte.				
Pre-Cambrian	*Glenarm Series*			
- - - - - - - - - - - - - -		Peters Creek fm.		- - - - - - - - - - - - - -
- - - - - - - - - - - - - -		Wissahickon fm.		- - - - - - - - - - - - - -
- - - - - - - - - - - - - -		Cockeysville marble		- - - - - - - - - - - - - -
- - - - - - - - - - - - - -		Setters qte.		- - - - - - - - - - - - - -
Pickering Gneiss	Baltimore Gneiss		Baltimore Gneiss	

Igneous Rocks

The pre-Glenarm rocks (Baltimore and Pickering gneisses) contain igneous intrusions ranging from ultrabasic (peridotite) through basic (gabbro) and calcic (anorthosite) to granite. Much of this igneous material is restricted to the pre-Glenarm complex but certain igneous rocks occur within the Glenarm series. There they are confined almost exclusively to the middle grade and high- rather than the low-grade zones of metamorphism.[12]

Within the Wissahickon formation are lenticular areas of serpentine up to 6 miles in length. Also partly or wholly surrounded by Wissahickon are bodies of basic rock that have been mapped as gabbro and resemble

---

[12] Two long dikes of Triassic diabase which cross the whole area are not considered in this discussion.

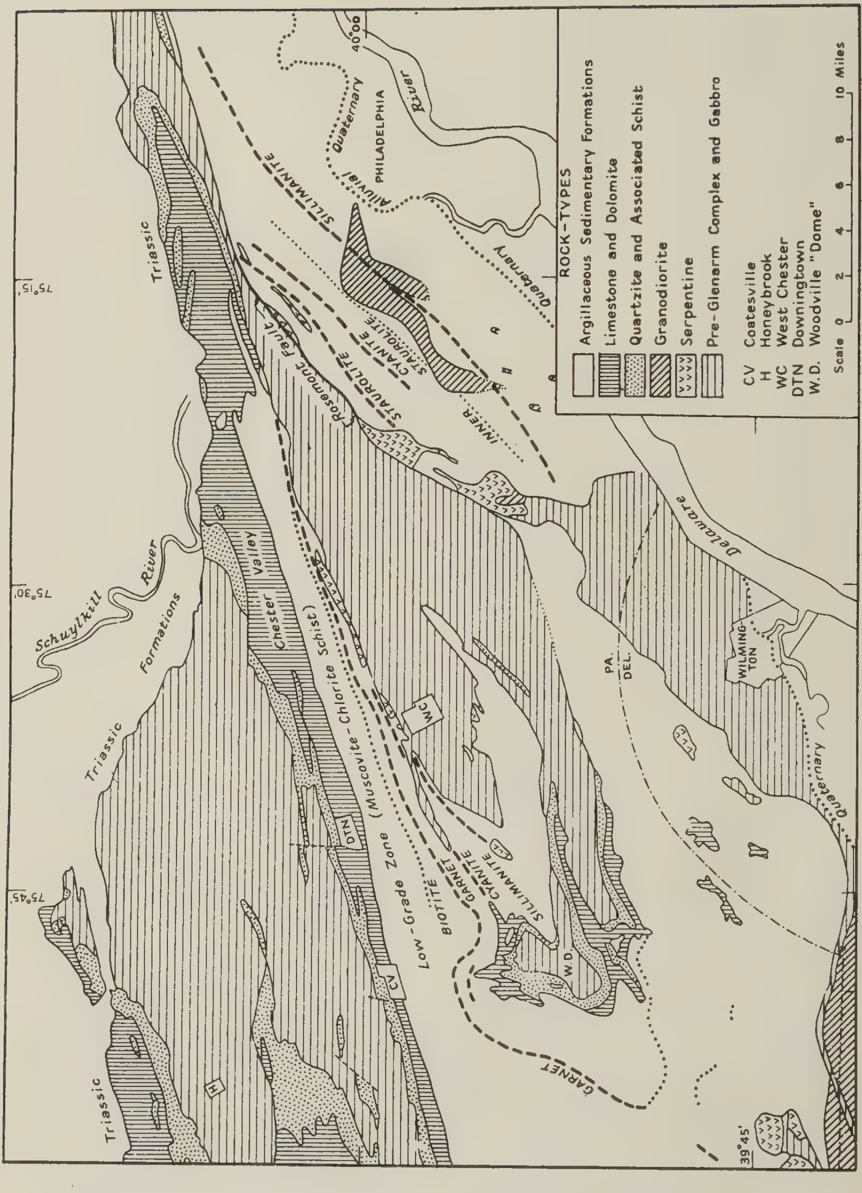

FIG. 2. Isograds in the Coatesville-West Chester and Philadelphia Districts.

some of the mafic material in the Baltimore gneiss. It is conceivable that some, though by no means all, of this material is metamorphosed basic lava, as no other equivalent of either the Catoctin greenstone or the basic volcanics of Maryland[13] have been recognized east of the Susquehanna watershed.

Insofar as metamorphism is concerned, the most significant of the igneous rocks is a granitic intrusive mapped by Bascom as granite gneiss and by Postel[14] as granodiorite. The largest body, six miles long, lies between the Rosemont Fault and the Delaware River extending approximately parallel to the fault. Here, Postel recognizes a porphyritic phase which he considers a hydrothermal replacement of the Wissahickon formation. He separates it from two "truly igneous" phases, the Springfield aplitic granodiorite and the Ridley Park granodiorite. Another large area of granodiorite, which Bascom correlates with the Springfield body as well as with the Port Deposit granite, occurs along the Maryland state line in the extreme southern edge of the area covered by Fig. 2.

Pegmatite, widespread throughout the area, has two modes of occurrence: (1) broad dike-like bodies, some of them many yards wide and up to three miles long, (2) thin sheets and lenses conforming to the contorted foliation of the mica gneisses.

Rock-Units Shown in Figures 2 to 4

The maps, figs. 2, 3, and 4 are intended to show distribution of types of rock as a basis for depiction of the metamorphic zoning. Such formation boundaries as are shown are taken mainly from the maps of the U.S. Geological Survey.[15] A few minor modifications in the West Chester

---

[13] Cloos, Ernst, Geology and structure of the Union Bridge-New Windsor areas, Carrol and Frederick Counties, Md., in Geology of the "Martic Overthrust" and the Glenarm Series in Penna. and Md.: *G.S.A., Special Paper* **35,** 85–93 (1941).

Marshall, John, Structure and age of the volcanic complex of Cecil County, Md.: *Md. Geol. Survey*, **13,** 191–213 (1937).

Jonas, Anna I., and Stose, G. W., Geol. Map of Frederick Co.: *Md. Geol. Survey* (**1938**).

Jonas, Anna I., Geol. Map of Cecil Co.: *Md. Geol. Survey* (**1928**).

[14] Postel, A. Williams, Hydrothermal emplacement of granodiorite near Philadelphia: *Proc. Acad. Nat. Sci., Phila.*, **92,** 123–152 (1940).

Watson, E. H., Emplacement of granite at Springfield, near Philadelphia: (Abstract) *G.S.A. Proc. for 1935*, p. 117 (1936).

[15] Bascom, F., and Stose, G. W., Geology and mineral resources of the Honeybrook and Phoenixville Quadrangles, Penna.: *U.S.G.S., Bulletin* **891** (1938).

Bascom, F., and Stose, G. W., Coatesville-West Chester Folio: *U.S.G.S., Folio No.* **223** (1932).

Bascom, F., *et al.*, Philadelphia Folio: *U.S.G.S., Folio No.* **162** (1909).

Bascom, F., and Miller, B. L., Elkton-Wilmington Folio: *U.S.G.S., Folio No.* **211** (1920).

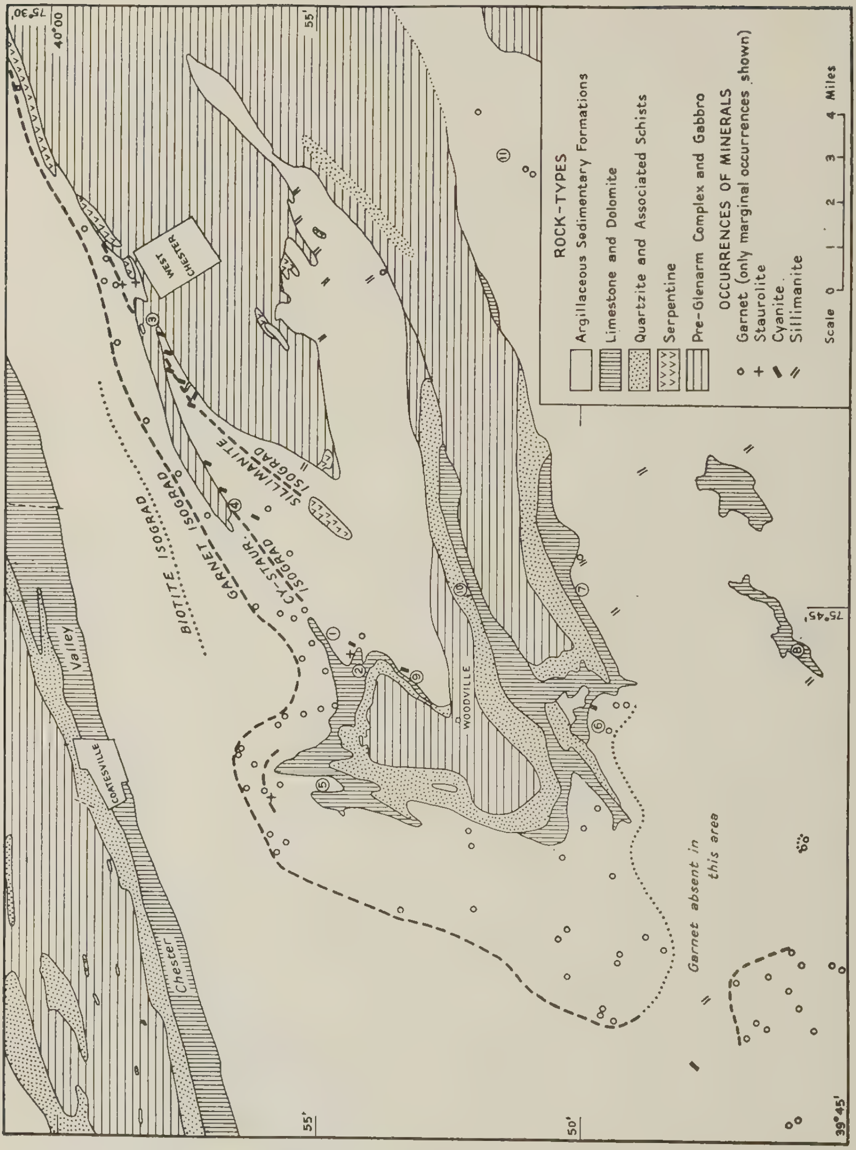

FIG. 3. Isograds and Occurrences of Minerals in the Coatesville-West Chester District. (Numbers refer to localities in Table 1.)

quadrangle are based on the writer's detailed field mapping; modifications in the Norristown and Chester Quadrangles are based on mapping by Armstrong,[16] Hietanen,[17] and Postel.[18] But as the present purpose is to show types of rock rather than stratigraphic units, certain formations which the U.S.G.S. maps show separately have been combined under a single pattern. Some explanation of this grouping seems desirable.

PRE-GLENARM COMPLEX includes the Pickering and Baltimore gneisses, which are both pre-Cambrian and presumably contemporaneous. The same pattern is used for gabbro; actually separation of pre-Glenarm from post-Glenarm gabbros and amphibolites would have been highly desirable, but the writer doubts that such a separation can be made consistently in the present state of knowledge.

QUARTZITE AND ASSOCIATED SCHISTS. A single pattern is used for the Cambrian Chickies and Antietam quartzites together with the intervening Harpers schist. The same pattern is used south of the Chester Valley for Setters formation. The quartzites of the Setters are indistinguishable lithologically from the quartzites mapped as Cambrian north of the Chester Valley; both are hard quartzites showing micaceous flakes and tourmaline needles on bedding planes.

LIMESTONES. In the Philadelphia district the limestones of the Chester Valley have been mapped by Bascom as Shenandoah limestone, but in the quadrangles farther west Stose and Jonas[19] have subdivided the Cambro-Ordovician group into seven formations. The carbonate rocks of this belt are in general gray or bluish to white and finely granular. The limestones south of the Chester Valley are marmorized and have been mapped as Cockeysville marble.

ARGILLACEOUS SEDIMENTARY ROCKS. The argillaceous sediment of the Wissahickon formation grades upward into material containing an increasing amount of quartz. Although the transition is gradational, the contrast is sufficient to warrant recognition of the more highly quartzose beds as a separate formation, the Peters Creek schist. Such a distinction is not difficult within the low-grade zone, but there is reason to doubt that Peters Creek can be distinguished from Wissahickon in the middle grade

---

[16] Armstrong, Elizabeth, Mylonitization of hybrid rocks near Philadelphia: *Bulletin G.S.A.*, **52**, Plate 1 (1941).

[17] Cloos, Ernst, and Hietanen, Anna, Geology of the "Martic Overthrust" and the Glenarm Series in Penna. and Md.: *G.S.A., Special Paper No.* **35**, Plate 20 (1941).

[18] Postel, A. Williams, Hydrothermal emplacement of granodiorite near Philadelphia: *Acad. Nat. Sci. Phila.*, **92** (1940).

[19] Stose, G. W., and Jonas, A. I., Lower Paleozoic section of southeastern Pennsylvania: *Wash. Acad. Sci. Jour.*, **12**, 358–366 (1922).

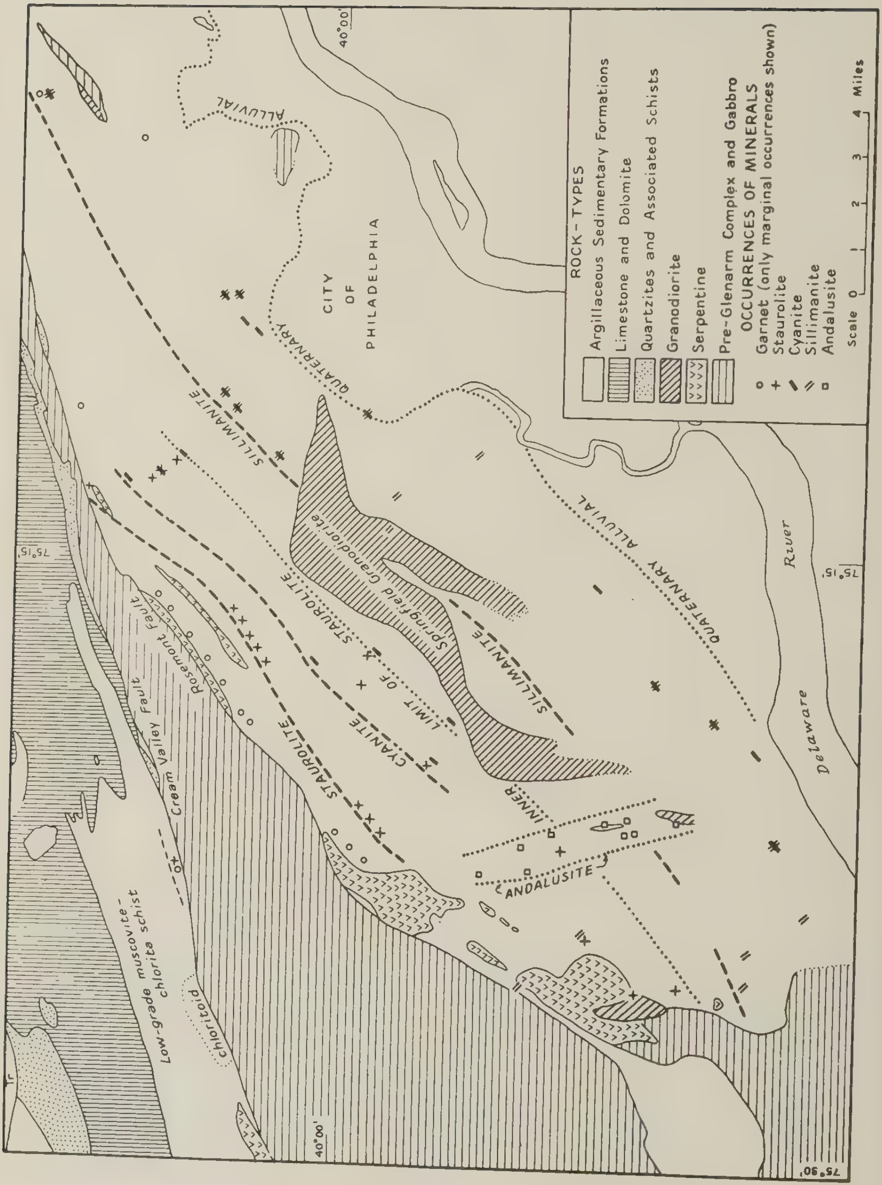

FIG. 4. Isograds and Occurrences of Minerals in the Philadelphia District.

and high-grade zones if it occurs there. The two formations have been shown by a single pattern in Figs. 2, 3 and 4 in order to avoid confusion of lines. The Peters Creek schist occurs in a syncline between the Chester Valley and the pre-Glenarm gneiss of Buck Ridge and the Woodville "Dome" line of structures.

Structure

Contacts of formations have a general northeasterly strike (N40 to 60E) except, of course, on the noses of major folds. Most of the folds are overturned to the north and some are recumbent. South of the Chester Valley, the broader structure is outlined by anticlines cored with Baltimore gneiss and bordered successively by Setters and Cockeysville formations, though either or both of these formations are locally missing so that in places the Wissahickon formation lies directly on the Baltimore gneiss.

The most northerly emergence of Baltimore gneiss south of the Chester Valley is in a fold which Bascom has termed the Buck Ridge Anticline. On its western prolongation stands the borough of West Chester. Still farther west, in line with this fold is the so-called Woodville dome, bootshaped in plan. (W.D. Fig. 2). The suggestion of Bailey and Mackin[20] that this is a recumbent fold has been confirmed by the writer's detailed observations of fold axes and plunge lines. Accordingly, the embayment of schist between the Woodville dome and the end of Buck Ridge is interpreted as a nappe-like recumbent syncline.

The next anticline to the south, termed by Bascom the Avondale anticline merges eastward with the Buck Ridge anticline, the cores of the two uniting to form a broad area of Baltimore gneiss. Still farther east the gneiss is all but cut off along a lineament which Armstrong has named the Rosemont Fault.[21] This fault, striking more northerly than the general trend of formations, curves on approaching the Chester Valley to a more easterly direction and merges with the Huntington Valley fault which, in the eastern part of the area, separates the Baltimore on the north from the Wissahickon on the south.

DISTRIBUTION OF METAMORPHIC MINERALS

Previous Observations

A general southeastward increase in intensity of metamorphism in this region has long been recognized. Thus Bascom[22] noted that "crystallinity increases eastward in all formations. . . ." More recent publications depict variation in degree of metamorphism but, except as noted below, the existing maps are generalized and do not show mineral isograds.

---

[20] Bailey, E. B., and Mackin, J. Hoover, Recumbent folding in the Pennsylvania Piedmont: *Am. Jour. Sci.*, ser. 5, **33**, 187–189 (1937).

[21] Armstrong, Elizabeth, Mylonization of hybrid rocks near Philadelphia, Pa.: *Bulletin G.S.A.*, **52**, 684 (1941).

Knopf and Jonas[23] published a small-scale map (about 30 miles to the inch) showing diagrammatically the distribution of metamorphic intensity in the crystalline schists of the Piedmont Province in Pennsylvania and Maryland. "Metamorphic intensity" was based on both texture and mineralogical composition, but the occurrence of index minerals was not shown specifically. Within the area described in the present paper, their map shows strong metamorphism in the southeast corner of the Coatesville-West Chester district and, except for a belt of "weak metamorphism" one to two miles south of the Chester Valley, "moderate metamorphism" in the northwestern half.

Zoning of metamorphic minerals in the area was observed by the writer about 1936 and described in a paper read before the Philadelphia Mineralogical Society in 1937, but pending an opportunity for further field work, no observations were published. Since then, Cloos and Hietanen[24] have published a map of a much larger area (scale not stated but approximately 15.5 miles to the inch) showing "distribution of metamorphic facies." In the same volume (p. 177) Hietanen shows the distribution of chlorite schist, chloritoid schist, garnet schist and staurolite schist in an area three by ten miles just west of the Schuylkill River, and on page 128 the distribution of similar rock types between Mine Ridge and the Susquehanna River (west of the present area.)

Sources of Data

Most of the occurrences of metamorphic minerals within the West Chester and Coatesville quadrangles (Fig. 3) are based on the writer's field observations made at intervals during the past fifteen years. In contrast, the occurrences in the Philadelphia district are chiefly from records in the literature, many of them from Gordon's[25] compilation. Such observations, although made by mineral collectors rather than by geologists primarily interested in metamorphism, yield a wealth of information, some of which is no longer available from the field now that so many quarries and exposures in the city and suburbs have been filled in or built upon. Despite the existence of the records, it was not until the occurrences had been plotted that any systematic distribution became evident. However, a more detailed and accurate portrayal of mineral isograds in this part of the area will doubtless emerge from a study of the Wissahickon formation in the Philadelphia district in preparation by Dr. Judith Weiss[25a] of the U.S. Geological Survey. Meanwhile, the map (Fig. 4) is presented here in order to show broader relationships than are available in the Coatesville-West Chester district alone.

---

[22] Bascom, F., Description of geology, Piedmont Plateau Area, Pre-Triassic metamorphic rocks: *U.S.G.S., Philadelphia Folio No.* **162** (1909).

[23] Knopf, Eleanora Bliss, and Jonas, Anna I., Geology of the McCalls Ferry-Quarryville District, Penna.: *U.S.G.S., Bulletin* **799,** 122 (1929).

[24] Cloos, Ernst, and Hietanen, Anna, Geology of the "Martic Overthrust" and the Glenarm Series in Pa. and Md.: *Geol. Soc. Am., Special Paper No.* **35** (1941).

[25] Gordon, Samuel G., Mineralogy of Pennsylvania: *Acad. Nat. Sci. Phila., Special Publication No.* **1** (1922). In addition, data for a ten-mile belt west of the Schuylkill River were taken from Hietanen's map. Cloos and Hietanen, *Op. cit.*, p. 137.

In the Pre-Glenarm Complex

The Baltimore gneiss is a complex of hornblendic and biotitic gneisses with basic and granitic intrusives. It suffered intense metamorphism prior to the deposition of the Glenarm Series and must also have experienced the metamorphic influences that affected the Glenarm, but no attempt is made here to disentangle the two processes nor, for that matter, to discuss the metamorphism of the pre-Glenarm rocks. Where the Baltimore and its basic intrusives adjoin the high-grade zone of the Wissahickon formation and especially along zones of shearing, the gabbroic and hornblendic rocks are converted into coarse biotite gneiss and in such places there is room for difference of opinion as to the correct position of the contact. Metamorphism of gabbro associated with the Baltimore gneiss has been investigated by Watson.[26]

In Argillaceous Rocks

Except for narrow belts of Harpers and Setters schist, the principal argillaceous formations of the area are the Wissahickon and Peters Creek.

LOW-GRADE ZONE. Within the low-grade zone, the Wissahickon formation is a fine-grained phyllitic schist consisting chiefly of muscovite, quartz and albite. Chlorite is present but in most places subordinate. A chloritoid-bearing belt about a mile wide and two miles long within this zone has been recognized by Hietanen eight miles west of the Schuylkill River (Fig. 4).

[25a] Weiss, Judith, Wissahickon schist at Philadelphia, Pa.: *Bulletin G.S.A.*, **60**, 1689–1726 (1949). Appeared after the present paper was in type. The only conspicuous discrepancy between Dr. Weiss' isograds and mine is in the extrapolation of "sillimanite isograd" north of "City of Philadelphia" in my figures 2 and 4. As figure 4 clearly shows, this extrapolation is postulated on incomplete data. Dr. Weiss' map shows both the cyanite and staurolite isograds extending in a more northerly direction north of Philadelphia.—H.E.McK.

[26] Watson, E. H., Alteration of gabbro near Philadelphia: (Abstract) *Am. Mineral.*, **21**, pp. 200, 201 (1936).

The schist of the low-grade zone has an even slaty cleavage interrupted by local warping and by zones of buckling. Flakes of mica and chlorite are 0.1 mm., or less in diameter usually too fine to be distinguished macroscopically so that cleavage surfaces have a silvery rather than a sparkling luster. A thorough description of the microscopic and petrofabric characteristics of the Wissahickon formation in the Norristown quadrangle has been published by Hietanen.[27] It is noteworthy that she found no evidence of retrogressive metamorphism (diaphtoresis) in the Octoraro schist[28] but states that the "sequence of recrystallization indicates progressive metamorphism contemporaneously with the deformation" (p. 135).

In the present study, however, a series of specimens taken along the West Branch of Brandywine Creek (from two to six miles southeast of Coatesville) showed consistent evidence of biotite altering to chlorite, an effect that might correctly be designated retrogressive metamorphism. Nevertheless, there is no evidence of any profound retrogressive reconstitution of the rock. On the contrary, barring this late chloritization of biotite, the transition from the low-grade to the middle-grade zone is characteristic of progressive metamorphism—deformation of smooth cleavage planes of the phyllite accompanied by recrystallization and coarsening of the mineral constituents of the rock. With this gradual increase in grain size the cleavage surfaces become less silvery and more sparkling and with incipient deformation they become warty or wavy with wave length on the order of two to four inches and amplitude one-half inch. Shortly biotite is recognizable. Within another mile, as measured in the West Brandywine section, the rock becomes a mica gneiss rather than a mica schist and garnet begins to appear.

The most definite reference line for descriptive purposes is the garnet isograd as mapped from observations of megascopically visible garnet. On the map (Fig. 3) each circle represents an occurrence of garnet observed in the field. The mapping of megascopic occurrences has the advantage of yielding a much better sampling than would be possible without a prohibitive number of thin sections. The limited number of thin sections examined would indicate that consistent occurrences of microscopic garnet are not to be expected more than a few thousand feet to the low-grade side of the isograd as mapped, although it is true that rare and sporadic microscopic crystals have been noted as much as three miles away from it.

---

[27] Cloos and Hietanen, *Op. cit.*, pp. 139–185.

[28] The low-grade facies of the Wissahickon formation in the Philadelphia District was mapped by Bascom as "Octoraro Schist."

The biotite isograd is less easy to locate than the garnet isograd, partly because of the chloritization of biotite already mentioned. Because of the difficulty of defining it sharply in the field, the biotite isograd has been mapped in only part of the area. In the West Brandywine section there is an interval of 3½ miles between the first sparse appearance of biotite and the last occurrence of chlorite, and chlorite persists to half a mile inside (i.e., on the high-grade side of) the garnet isograd. The first abundant biotite makes its appearance a little more than a mile north of the garnet isograd. For purposes of description the garnet isograd is taken as the approximate boundary between the low and the middle-grade zones, recognizing, of course, that the more conventional boundary, the biotite isograd, is probably one to two miles outside it.

As already noted, the Glenarm series is separated into two tracts by the mass of Baltimore gneiss that lies west of the Rosemont fault. Although zoning of metamorphic minerals is noted in each of the tracts, the trends of isograds on opposite sides of the Baltimore gneiss are not in line with each other. Therefore, it will be convenient to discuss the two districts separately.

ISOGRADS IN THE COATESVILLE-WEST CHESTER DISTRICT. The northern boundary of the middle-grade zone, as marked by the garnet isograd, lies north of the Buck Ridge anticline. From the Schuylkill River it strikes S. 70° W. for twenty miles, roughly paralleling the Chester Valley and the regional strike. Farther west it swings southward around the Woodville "Dome," where it is separated from the Cockeysville marble by a horizontal distance of one to four miles.

Staurolite appears a mile or less south of the garnet isograd. Although staurolite is not common in the West Chester-Coatesville district, the six localities in which it has been noted all lie within a belt ½ to 1½ miles wide, parallel to the garnet isograd.

Cyanite occurrences form a well-defined belt about a mile south of the garnet isograd, extending for ten miles from near West Chester to the margin of the Woodville dome. This belt is marked by abundant pegmatite in the gneiss—more than is found either north or south of it. An occurrence of both staurolite and cyanite from a single locality[29] has been reported but not confirmed by the writer. Elsewhere, cyanite begins about $\frac{1}{4}$ mile south of the trend-line of the staurolite belt. Cyanite has not been found on the west flank of the Woodville "dome," probably because exposures in that area are few and poor. Sillimanite is found together with cyanite at one locality, but its more abundant development begins two miles or more south of the cyanite isograd.

---

[29] "Near Logan's quarry" in the East Marlborough Township, Chester County. Listed by Gordon from Dana, J. D., System of Mineralogy, 3d edition (1850), p. 615. After the present paper had gone to the printer the writer succeeded in confirming this occurrence in the field.

An anomalous feature of the metamorphism is that south of the Woodville dome and the Avondale anticline there is a belt one to four miles wide in which garnet is very scarce or absent. This can hardly be due to local lowering of the grade of metamorphism because here the gneiss is coarse grained and in at least two localities contains sillimanite. Pegmatite is abundant in the belt and in a few places garnet occurs in the pegmatite but not in the gneiss itself. The possibility that the gneiss of this belt differs in chemical composition from typical Wissahickon calls for investigation. Alternatively, the possibility that deformation in this zone was accomplished under conditions of lowered differential stress deserves consideration, for under such conditions sillimanite, but not cyanite or almandite, would be stable.

QUARTZ VEINS, PEGMATITE AND FELDSPARS. In the low-grade zone quartz is abundant in veins cutting the cleavage at various angles. The veins commonly contain cubes of pyrite and grains of an iron-bearing carbonate. Similar veinlets carry grains of albite, but pegmatitic material, except for a very few dikes, which are cleancut and well defined, does not occur in the low-grade zone. In the Peters Creek schist thin lenses and laminae of quartz, probably representing sedimentary beds, are characteristic. But at about the beginning of the middle-grade zone, similar thin lenses consist of quartz microcline and plagioclase, with or without biotite and muscovite. With increasing degree of metamorphism these lenses of pegmatitic material become thicker, coarser and more numerous. Locally they contain garnet, cyanite or tourmaline. In addition, definite veins of quartz are common. This rough correspondence between amount and texture of pegmatitic material and degree of metamorphism, as well as the similarity in mineralogy between the pegmatitic lenses and the enclosing rock, suggest that development of pegmatite is a concomitant result rather than a primary cause of the metamorphic process.

Hietanen's[30] mapping of the anorthite content of plagioclase shows that the feldspars become more calcic as one proceeds toward the southeast. At about the biotite isograd the plagioclase is An_{16}. Near the cyanite isograd it is An_{19}, and within the sillimanite isograd An_{25} to An_{30}.

ISOGRADS IN THE PHILADELPHIA DISTRICT. In the area southeast of the Rosemont fault, isograds can be drawn approximately parallel to the fault and to the axis of the Springfield granodiorite. The low-grade zone is missing, the area where it might be expected to appear being occupied by Baltimore gneiss. The staurolite and cyanite zones overlap somewhat, cyanite appearing about a mile before the disappearance of staurolite. The cyanite zone also overlaps the sillimanite zone; the two minerals occur together in several localities. The distance between the cyanite and the sillimanite isograds is about three miles.

---

[30] Cloos and Hietanen, *op. cit.*, plate 19 and p. 130.

ANTI-STRESS MINERALS. From evidence in many districts of simple thermal metamorphism it is known that cordierite and andalusite are the characteristic anti-stress minerals of argillaceous rocks.[31] In the region under discussion, cordierite has not been reported and andalusite occurs in a single restricted belt. It has been observed in eight localities, all within a belt five miles long and a mile wide in or near the valley of Crum Creek, which flows just west of Swarthmore; nowhere else in Pennsylvania is an occurrence of andalusite listed by Gordon. This belt, striking a little west of north, crosses the regional trend of isograds. However, it is parallel to the trend of local foliation and to a dikelike body of hornblende gneiss which lies on the northward prolongation of a narrow body of Springfield granodiorite. Postel[32] has observed cyanite forming borders around andalusite and similarly around bundles of sillimanite and accordingly suggests that "the region was first subjected to high-grade metamorphism and then later was acted on by high differential pressure."

In Carbonate Rocks

The Cambrian and Ordovician limestones and dolomites of the Chester Valley, being in contact (a fault contact according to Knopf, Stose and Stose) with argillaceous rocks of the low-grade zone, nowhere show tremolite or other middle-grade minerals. Cubes of pyrite are common, fluorite has been found sparingly and rutile is sparse but widespread. It would be instructive to know whether the carbonate rocks of the Cockeysville formation where surrounded by low-grade phyllites would show a similar lack of middle-grade minerals, but unfortunately their first appearance south of the valley is well within the garnet isograd in contact with argillaceous rocks that contain minerals ranging from staurolite through cyanite to sillimanite. These limestones are marmorized and have a fine to coarse sugary texture. Tremolite is present in all localities except one, namely Edward's quarry (no. 1 on Fig. 3) which is very close to the staurolite isograd.

---

[31] Harker, Alfred, Metamorphism. London, Methuen and Co., Ltd., pp. 147–151 **(1932)**.

[32] Postel, A. Williams, Hydrothermal emplacement of granodiorite near Philadelphia: *Proc. Acad. Nat. Sci. Phila.*, **92**, 128, (1940).

Within the zones designated as middle-grade and high-grade on the basis of minerals in the aluminous rocks, the minerals of the limestones do not show any striking zonal arrangement. Tourmaline (usually a brown variety) occurs in both zones. Scapolite has been found in five localities within the high-grade zone and also in the quarries near Doe Run (No. 5 on Fig. 3) which are presumably in the middle-grade zone although the position of the sillimanite isograd in this vicinity has not been well defined. Microcline of the variety chesterlite[33] occurs in two localities.

TABLE 1

	Number on Map	Fluorite	Rutile	Tourmaline	Epidote or Zoisite	Vesuvianite	Tremolite	Scapolite	Diopside	Potash feldspar	Apatite
Low-Grade Zone											
Chester Valley		x	x								
Middle-Grade Zone											
Edwards' Quarry	1	x	x	x							
Logan's Quarry	2		x	x			x				
Cope's Quarry	3				?		x	?			
Poorhouse Quarry	4		x		?		x			x	
Doe Run Quarries	5		x	x		x	x	x			x
Avondale Quarries	6		x	x	x		x				x
High-Grade Zone											
Kennett Quarries	7		x	x			x	x			
Nevin's Quarries	8		x	x			x	x			x
Bailey's (Upland)	9		x		x		x	x	x		
Willowdale	10			x		x	x	x	x	x	
Elam	11		x					x	x	x	x

Of the minerals occurring in the limestones of this region, diopside is the one generally regarded as representing the highest grade of metamorphism. If it can be taken as an index mineral, its occurrence in localities 9 and 10 near the axis of the Buck Ridge structure and its absence[34]

[33] Chesterlite from the Poorhouse quarry was originally described by Dana as a new mineral species and named for Chester County. Later, Descloizeaux used chesterlite from this locality as one of his types in establishing the species microcline.

[34] Chondrodite together with diopside occurs in limestone surrounded by Baltimore gneiss at Brinton's Bridge on the Brandywine. This occurrence has been mapped as Franklin limestone of pre-Glenarm age.

in the localities farther south (Nos. 6, 7 and 8) might suggest a belt of metamorphic intensity that is locally high and diminishes southward as well as northward. No corresponding contrast is evident, however, in the adjoining schists, which are all in the sillimanite zone. No higher grade of metamorphism than that represented by diopside was attained in the limestone, as grossularite is not observed and even where diopside is found, tremolite is still present. Whether or not a still higher intensity is reached farther east cannot be determined on the basis of calcareous rocks since none are exposed in the sillimanite zone in the Philadelphia area. As would be expected in the absence of purely thermal metamorphism, wollastonite is not known in the region.

Table 1 gives the minerals reported in the principal exposures. Numbers on the table refer to numbers on the map, Fig. 3.

Cause and Significance of Metamorphism

Discussion of a number of the questions that the zonal relationship suggests would call for a presentation of detailed structural data which the writer hopes to offer in a later paper. The answers to still other questions must remain conjectural in the absence of more than the very limited number of chemical analyses and quantitative microscopic studies now available. Nevertheless, certain observations seem warranted at the present time.

The marked increase in grade of metamorphism southward and eastward toward the areas of granitic rocks near Philadelphia and along the Maryland state line strongly suggests the influence of subjacent igneous bodies in accordance with ideas long ago proposed by Barrell.[35] The isograds are not strictly parallel to the observed boundaries of the granitic bodies. If they are spatially related to an underlying magma they reflect general proximity to a mass of igneous material rather than to relatively small exposed sills or stocks.

The metamorphism is not limited to rocks of pre-Cambrian or undetermined age, for, although within the area mapped all of the unquestionned Paleozoic rocks are in the low-grade zone, Hietanen has noted that in the McCalls Ferry Quadrangle (west of the present area), Cambrian schists show garnet-staurolite grade of metamorphism. Therefore, if a single period of igneous activity is responsible for the metamorphism its age cannot have been pre-Cambrian.

In any case, the general, though locally interrupted, increase in grade from northwest to southeast suggests that the relatively high grade of metamorphism in parts of the Glenarm series as compared with the Paleozoic rocks of the Chester Valley, as well as with tracts of Glenarm rocks adjoining it, is due to geographical position with respect to the isograds, and not to difference in age of the rocks. For this reason the observed zonal relations are entirely compatible with Paleozoic age for the Glenarm series including the Wissahickon formation.

---

[35] Barrell, Joseph, Relation of subjacent igneous invasion to regional metamorphism: *Am. Jour. Sci.*, 5th Ser., **1**, pp. 1 ff. (1921).

Acknowledgments

The writer is indebted to Mr. Alexander G. Jones of Harvard University for microscopic identification of a number of minerals; to the Harvard Department of Geology for funds to meet the cost of thin sections and other expenses; and to Professor Marland P. Billings for a critical reading of the manuscript.

NOTES AND NEWS

REFRACTIVE INDICES OF HIGH INDEX LIQUIDS BY THE PRISM METHOD ON THE TWO-CIRCLE GONIOMETER

C. W. Wolfe and Virginia Franklin, *Boston University.*

The determination of the refractive indices of liquids, utilizing a hollow prism mounted on a one-circle goniometer, is a well known procedure (Larsen and Berman, 1934). The purpose of this paper is to discuss the extension of the same method to two-circle goniometers of the Goldschmidt type. Such goniometers (Wolfe, 1948) are comprised of three structural units: the signal collimator which is fixed in position; the telescope which is movable parallel to the horizontal circle but is not attached to it; and the vertical circle unit, which is movable and which is attached to the horizontal circle. This paper stems from the lack of connection between the telescope and the horizontal circle.

The Prism. The prism used by the authors, Fig. 1, was machined by Laboratory Associates of Belmont, Mass., who provide the prism as an accessory to the *Wolfe* goniometer. A standard crystal mounting rod is firmly fixed in the rear of the prism in order that the prism may be mounted on a standard goniometer head. A prism angle of fifty degrees is most serviceable for index measurements in the usual range.

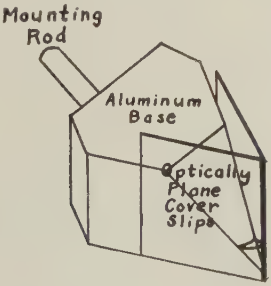

Fig. 1. Prism.

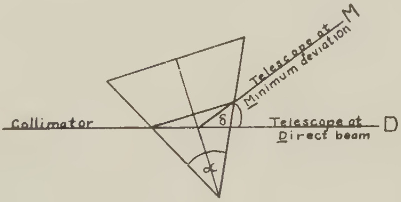

Fig. 2. Determination of δ (Delta).

Optically plane cover slips are cemented on the sides of the prism with water glass or Bakelite varnish, depending on the chemical affinities of the immersion media. Ordinary square cover slips can be used if they are optically plane. They may be tested by mounting on soft wax on the goniometer and observing whether a single, distinct signal from each side of the cover slip is obtained. If both sides are plane and parallel, the second signal will be centered after an exact rotation of 180 degrees of the vertical circle. Unfortunately, many cover slips must be tested before a satisfactory one is discovered; so the authors have resorted to the use of haemacytometer cover slips which, though optically true, are more expensive.

After the cover slips are mounted, they should be rendered opaque with black india ink to sharpen the signals and to reduce the effects of internal reflection and diffraction, leaving a small unpainted aperture in the vicinity of the liquid for passage of the light beam. Monochromatic sodium light, adequately shielded from the worker's eyes, is probably the most satisfactory light source. If greater precision is desired, a special temperature-controlled hollow prism such as that described by Butler (1933) could be machined.

Procedure. The prism is mounted on the goniometer head and adjusted. (as in crystal goniometry) until the reflections from both sides of the prism fall upon the cross hairs with rotation of both the horizontal and vertical circles in turn. The vertical circle is locked in position.

The prism angle α (alpha) is measured by obtaining the horizontal circle angular readings for the two prism faces, A and B, where A is less than B.

$$B - A = 180° - \alpha$$

or

$$\alpha = 180° + A - B$$

The prism angle is twice the angle of refraction, r, at minimum deviation (derivation in any standard description of the method of minimum deviation).

$$r = \frac{\alpha}{2} = \frac{180° + A - B}{2}.$$

Minimum deviation. Since the vertical circle, not the telescope, is attached to the horizontal circle, the procedure for determining the deviation angle between the position of the telescope when receiving the direct beam and when receiving the refracted beam at miniumum deviation Fig. 2, differs slightly from that for the one-circle goniometer where the angle can be read directly. The telescope is moved beyond the direct beam to the position of minimum deviation, which is determined by simultaneous movements of the telescope and of the vertical circle unit. If the prism be not correctly oriented, the signal will inscribe a parabola, not follow a straight line, as it is brought up to and away from the centered position.

The telescope is next locked in the minimum deviation position, and the vertical circle unit is moved until it abuts against some part of the telescope; and a reading M (*M*inimum deviation) is taken on the horizontal circle in this position. The telescope is then rotated back until the direct signal from the collimator is on the cross hairs; and the vertical circle is brought in contact with the telescope again for a second reading, *D* (*D*irect beam). *M* minus *D* gives the usual delta (δ) angle obtained in minimum deviation procedure. Calculation of n, following the formula:

$$n = \frac{\sin\left(\frac{\delta}{2} + \frac{\alpha}{2}\right)}{\sin\frac{\alpha}{2}}$$

is a simple matter; and graphs or tables showing variation of index with delta for one or more prism angles are readily prepared.

The mechanics of operation in this procedure are easier than for the one-circle goniometer, and the same accuracy is obtained. The maximum error in index determination by this method is two in the third place, and with proper controls an accuracy of three in the fourth place is easily possible.

Acknowledgment. The authors gratefully acknowledge the time and effort contributed by Laboratory Associates of Belmont, Mass., in the development of a satisfactory prism base.

Since the writing of the above note, Laboratory Associates have developed, under the direction of the senior author, a light filter which can be placed in the collimator, using the usual illumination source. The wave length of light obtained is exactly equal to that of the commercial sodium lamp. In addition to facilitating readings on the goniometer, the use of the filter has another decided advantage:—cost; for the filter can be supplied for $5.00 which is a small fraction of the cost of a sodium lamp.

References

Butler, R. D. (1933), *Am. Mineral.*, **18,** 394.
Larsen and Berman (1934), *U. S. Geol. Surv., Bull.*, **848,** 18.
Wolfe, C. W. (1948), *Am. Mineral.*, **33,** 739.

NOTE ON THE FLUORESCENCE TEST OF BENTONITE

YI HSEUNG AND C. C. YEH,

University of Missouri, Columbia, Missouri.

Brown (1) recently reported that swelling bentonites fluoresce under ultra violet light when moistened with a water solution of zinc uranyl acetate, but that non-swelling bentonites fluoresce only slightly, or not at all. He explained the cause of fluorescence as due probably to the dehydrating powers of clay involving free energy levels of the order chemisorption. He also stated that the sodium ion might play a considerable, but undetermined part in the effect. The writers have found that the sodium ion (exchangeable base) is the dominant cause.

Duplicate determinations of the fluorescence reaction were carried out by the writers on Wyoming sodium bentonite, Arizona bentonite, Mississippi bentonite, Illinois illite, and kaolinite. Fluorescence occurs only with sodium bentonite and gives negative results with calcium bentonite, calcium illite and kaolinite. However, all of the clay minerals including the kaolinite and illite groups show fluorescence when a small amount of sodium chloride is added. This fluorescence reaction appears to be due to the precipitate of the triple salt, sodium uranyl zinc acetate, having the composition $Na(UO_2)_3Zn\ (CH_3COO)_9 \cdot 6H_2O$. Feigl (2) reported that sodium zinc uranyl acetate gives a bright green-yellow fluorescence in ultra violet light, whereas zinc uranyl acetate gives no fluorescence.

To confirm the importance of sodium in causing fluorescence, a fluorescing Wyoming bentonite was leached with a calcium chloride solution to remove the exchangeable sodium and replace it with calcium. The resulting Ca-bentonite did not fluoresce with the acetate reagent. Furthermore, after the Arizona calcium bentonite (non-fluorescing) was leached with sodium chloride and washed free of NaCl, it then fluoresced. Sodium illite and sodium kaolinite which were prepared by leaching with NaCl solution fluoresced, weakly and not at all, respectively.

The quantitative effect on fluorescence of the degree of saturation by sodium of the exchangeable bases of montmorillonite and kaolinite was determined by adding known quantities of sodium (NaOH) to the respective hydrogen clays and testing the treated clays. The results are shown in table 1.

Obviously fluorescence of clay varies with the content of sodium. There is no fluorescence in montmorillonite when the saturation is less than 0.2 per cent sodium. Feigl (2) reported 2.5 gamma as the limit of identification of sodium by the fluorescence test. It is very interesting to note

TABLE 1. FLUORESCENCE REACTION OF MONTMORILLONITE AND KAOLINITE

No.	Degree of Na saturation	Gms. H-clay used	m.e. NaOH used	ml. 0.001 N NaOH used	Fluorescence* reaction
Montmorillonite, Base exchange capacity 100 m.e. per 100 grams					
1	0.1	0.08	0.00008	0.08	−
2	0.2	0.08	0.00016	0.16	−
3	0.5	0.08	0.0004	0.40	+
4	1.0	0.08	0.0008	0.80	+
5	5.0	0.08	0.004	4.00	++
6	10.0	0.08	0.008	8.00	+++
Kaolinite, base exchange capacity 2.75 m.e. per 100 grams					
7	50.0	0.1	0.00138	1.38	−
8	80.0	0.1	0.00220	2.20	−
9	100.0	0.1	0.00275	2.75	−

* − negative, + weak, ++ medium, +++ strong.

that the kaolinite when completely saturated with sodium does not fluoresce.

In addition to the above clay minerals, some sodium salts were also tested for fluorescence. Most mineral sodium salts fluoresce but some organic salts do not. Phosphates and large amounts of organic acids, such as oxalic and tartaric acids, have an interfering effect (3).

The writers wish to express sincere thanks to Dr. W. D. Keller, Dept. of Geology, Univ. of Mo., for his advice and encouragement in this test and also for furnishing samples of clay minerals.

REFERENCES

(1) BROWN, B. W., A fluorescence study of Wyoming bentonite: *Am. Mineral.*, **34,** 98 (1949).
(2) FEIGL, F., Beiträge zur anorganischen Tüpfelanalyse: *Rec. Trav. Chim.*, **58,** 473 (1939).
(3) BARBER, H. H., AND KOLTHOFF, I. M., A specific reagent for the rapid gravimetric determination of sodium: *Jour. Am. Chem. Soc.*, **50,** 1625–1631 (1928).

The American Petroleum Institute has published Preliminary Reports No. 2 and No. 3 in connection with Project 49, Clay Mineral Standards. No. 2, entitled, "Reference Clay Localities—United States," has been prepared by Paul F. Kerr and J. L. Kulp. The same authors, together with P. K. Hamilton, also have completed No. 3, "Differential Thermal Analyses of Reference Clay Mineral Specimens."

In No. 2 are descriptions of 33 clay mineral localities, kaolin group—10, montmorillonite group—15, potash bentonite—4, hydromica—2, and attapulgite and pyrophyllite—1 each. All localities save one (San Juanito, Mexico, for dickite) are in the United States. Included are 38 sketch geologic and location maps.

Preliminary Report No. 3 is divided into two parts. In the first the authors describe the method of differential thermal analysis and the equipment required for the technique. Part two presents the experimental results on the reference samples described in Report No. 2.

E. WM. HEINRICH
University of Michigan

Hugh S. Spence, Fellow of the Society, retired on September 15 from the Mineral Resources Division, Canadian Bureau of Mines, after thirty-nine years service. A graduate (1908) of the Royal Saxon School of Mines (Kgl. Sächsische Bergakademie), he specialized in mineralogy and geology under professors Kolbeck and Beck.

His work in the Bureau of Mines was mainly in the industrial and rare-element minerals field, and he is the author of numerous technical reports on these subjects. He made the first official report on the pitchblende discoveries at Great Bear Lake, and also is the author of the Prospector's Guide to Uranium and Thorium Minerals published by the Bureau in 1948. This useful little handbook has found the largest circulation of any of the Bureau's publications, and is now in its third printing.

With pegmatites as his particular interest, Mr. Spence has contributed several papers on Canadian pegmatite minerals to the *American Mineralogist*. He will engage in private practice as consulting mineral technologist, with address at 222 Argyle Avenue, Ottawa, Ontario.

Dr. A. E. Alexander, authority on gem stones and pearls, has resigned the directorship of the Gem Trade Laboratory, Inc., and has become associated with Tiffany & Co., where he will serve in an executive capacity.

Professor E. L. Bruce, Miller professor of research geology and head of the department of geology at Queen's University, died at Kingston, Ontario, on Oct. 5 from a heart ailment.

Correction

Line 7, page 696, the symbol "[100]" should be "[001]."

Line 22, page 698, "reworked" should read "reworking."

INDEX TO VOLUME 34

Leading articles are in **bold face** type; notes, abstracts, and reviews are in ordinary type. Only minerals for which definite data are given are indexed.

Absorption of infrared radiation by powdered silica minerals. (Keller, Pickett) 855
Accessory elements in pegmatites, distribution of. I. Theory. (Holland, Kulp) 35, 278
Activity measurements of microradioactive inclusions. (Yagoda) 285
Adams, C. E. with Tunell, G. Symmetry and crystal structure of bornite 824
Aggie Creek meteorite from Seward Peninsula, Alaska. (Henderson) 229
Ahlfeld, F. 133
Altaite 361
Aluminium fluoride minerals, observations on. (Ferguson) 383
American Geological Institute 620
Analcime suite of igneous rocks, Brewster Co., Texas. (Lonsdale, O'Neill) 280
Analysis of rock-forming minerals by spectrochemical methods in petrological research (Strock) 284
Anatase, occurrence in sedimentary kaolin. (Nagelschmidt, Donnelly, Morcom) 132
Anderson, J. L. Pseudotachylite of the Antietam quartzite 331
Andersonite 274
Andrews, K. W. 769
Andrewsite 534
Antimonial silver ore from Cobalt, Ontario. (Wells) 456
Antimony and tellurium minerals in western Canada, further occurrences of (Warren, Thompson) 458
Arrojadite and graftonite from the Nickel Plate Mine, South Dakota. (Lindberg) 279
Atterberg plastic limits of clay minerals. (White) 508
Axelrod, J. M. and Grimaldi, F. S. Muscovite with small optic axial angle 559
——— 274

Bader, H. Definition of Euclidean geometrical symmetry 226
———. Screw axes of symmetry and their symbols 752
Bailey, D. A. Conversion of amorphous silica to quartz 601
Bailey, R. K. Talc in the salines of potash field near Carlsbad, Eddy County, New Mexico 757
Bannister, F. A. 614
Barium mineral, new, from Benallt manganese mine, Rhiw, Carnarvonshire. (Smith, Bassister, Hey) 614
Barnes, W. H. Some comments on the Buerger precession method for determination of unit cell constants and space groups 173
———. Unit cell and space group of childrenite 12
———. Unit cell and space group of lindgrenite 163
———. Unit cell and space group of probertite 19
———. Corrections to papers on proberite and lindgrenite 611
Barshad, I. Nature of lattice expansion and its relation to hydration in montmorillonite and vermiculite 675
Baryite bearing nodules from Middle Lias of the East Midlands. (Taylor) 337
Basaltic fan jointing induced by aqueous chilling. (Fuller) 276
Bastnäsite and xenotime, petrographic distinction of. (Foster) 830
Bates, T. F. 274
Bayleyite 274
Beatty, S. v. D. *X*-ray spectrometer study of mica powders 74
Bentonite, Wyoming, fluorescence study of. (Brown) 98

Bentonite, fluorescence test of. (Hseung, Yeh)............ 000
Beraunite...................... 536
Berry, L. G.................... 275
Biotite, *x*-ray data.............. 79
Bodenbenderite, a discredited species. (Milton, Myers)......... 608
Borickite...................... 701
Bornite, symmetry and crystal structure of. (Tunell, Adams). 824
Bracewell, S.................... 339
Bragg, W. L. Acceptance of the Roebling Medal of the Mineralogical Society of America. 238
Brazilianite, optical data........ 92
Brindley, G. W................. 337
Brown, B. W. Fluorescence study of Wyoming bentonite...... 98
Buerger, M. J. Fourier summations for symmetrical crystals..... 771
Buerger precession method for the determination of unit cell constants and space groups, some comments on. (Barnes)...... 173
Buttgenbach, H................. 618

Calaverite..................... 347
Calcioferrite................... 701
Calcite, natural solid solution effects in. (Andrews).......... 769
Canadian mineralogy, contributions to.................341–469
Cancrinite from Blue Mountain, Ontario. (Phoenix, Nuffield).. 452
Charting five and six variables within the bounding tetrahedra of hypertetrahedra. (Mertie).................280, 706
Chayes, F. Simple point counter for thin-section analysis.....1, 600
———...................... 275
Childrenite, unit cell and space group of. (Barnes).......... 12
Chloritoid from Megantic County, Quebec. (Milne)........... 422
Claffy, E. W. and Ginther, R. J. with Schulman, J. H. Some observations on the crystallization of silicic acid......... 68
Clay minerals, absorption of infrared radiation by. (Keller).... 278
Clay minerals, Atterberg plastic limits of. (White)........... 508
Clay mineral names, glossary of (Kerr, Hamilton)........... 618
Clays, International Committee for Study of................ 612
Clinopyroxenes, common, chemical composition and optical properties of. Part I. (Hess)...... 621
Clinozoisite from Camaderry Mt., Glendalough, Co. Wicklow. (Johnston)................ 132
Coloradoite.................... 363
Committee on Measurement of Geologic Time, report of. 1947–48 (Marble)........... 766
Copper in California, Bull. 144, State Division of Mines. Book review.................... 768
Corrego Frio pegmatite, Minas Gerais: Scorzalite and souzalite, two new phosphate minerals (Pecora, Fahey)....... 83
Cryolite, *x*-ray data............ 384
Cryolithionite, *x*-ray powder data. 384
Crystallization of basaltic magma as recorded by variation of crystal-size in dikes. (Winkler) 338
Crystallography, Conference on teaching of. (Donnay, Fisher, Gordon, Peacock, Tunell).... 288

Dake, H. C.................... 134
Dana's Minerals and How to Study Them. (Hurlbut) Book review 616
Das Bestimmen der Mineralien. (Köhler) Book review....... 767
Dedolomitization and its relation to a possible derivation of a magnesium-rich hydrothermal solution. (Faust)........... 789
De Ment, J.................... 134
Derry, D. R.................... 275
Dervillite. (Weil)............... 618
Die Entwicklung der chemischen Elemente. Part II. (Efremov) Book review............... 617
Differential thermal analysis apparatus, improved. (Kulp,

Kerr) 839
Differential thermal analysis curves of siderite, variations in. (Rowland, Jonas) 550
Dolomite, unusual, from Portsoy, Banff. (Harry, Patterson) 615
Donnay, J. D. H. 288
Donnelly, H. F. 132
Dreyer, R. M., Garrels, R. M., and Howland, A. L. Liquid inclusions in halite as a guide to geologic thermometry 26, 276
Dufrenite problem (Frondel) 513

Early, J. W. Studies of natural and artificial selenides: I–Kockmannite, CuSe 435
Eastonite, *x*-ray data 77
Edwards, A. B. Natural ex-solution intergrowths of magnetite and hematite 759
Efremov, N. Die Entwicklung der chemischen Elemente. Part II. Book review 617
Egueite 701
Empressite 357
Enargite and tennantite, hydrothermal synthesis. (Gaines) 276
Ervin, G., Jr., and Osborn, E. F. X-ray data on synthetic melilites 717
Etching iron meteorites, improved method of. (Reberholt, Henderson) 606
Euclidean geometrical symmetry, a definition of. (H. Bader) 226
Eudialyte in quartz-bearing syenites. (Nockolds) 769
Evaporites of East Yorkshire, petrology of. (Stewart) 614
Ex-solution intergrowths, natural, of magnetite and hematite. (Edwards) 759

Fahey, J. J. with Murdoch, J. Geikielite, a new find from California 281, 835
———, with Pecora, W. T. Corrego Frio pegmatite, Minas Gerais: scorzalite and souzalite, two new phosphate minerals 83
———. Scorzalite from South Dakota, a new occurrence 282, 685
Faust, G. T. Dedolomitization and its relation to a possible magnesium-rich solution 789
Ferguson, R. B. Aluminium fluoride minerals, observations on 383
Ferrous iron and silica determinations. (Hey) 769
Fisher, D. J. 289
Forman, S. A. and Peacock, M. A. Crystal structure of rickardite, $Cu_{4-x}Te_2$ 441
Foster, W. R. Petrographic distinction of xenotime and bastnäsite 830
Fourier summations for symmetrical crystals. (Buerger) 771
Fourier Transforms and Structure Factors. (Wrinch) Book review 129
Franklin, V. with Wolfe, C. W. Refractive indices of high index liquids by the prism method on the two-circle goniometer 893
Friedman, I. I. Laboratory growth of quartz 583
Frohbergite 360
Frondel, C. Crystallography of spangolite 181
———. The dufrenite problem 513
———. Wolfeite, xanthoxenite, and whitlockite from Palermo Mine, New Hampshire 692
——— and Palache, C. Retgersite, $NiSO_4 \cdot 6H_2O$, a new mineral 188, 276
Frondelite and the frondelite-rockbridgeite series. (Lindberg) 541
Fuller, R. E. 276

Gabbro-granite transition in Norfolk County, Massachusetts, remains of. (Chayes) 275
Gaines, R. V. 276
Game, P. M. 614, 615
Garnet and associated minerals of

the Barton Mine near North Creek, N. Y., paragenesis of (Shaub).................. 573
Garnet, physical analysis of polycomponent. (Levin)......... 279
Garrels, R. M. and Howland, A. L. with Dreyer, R. M. Liquid inclusions in halite as a guide to geologic thermometry......26, 276
Gault, H. R. Frequency of twin types in quartz crystals...... 142
Gearksutite, *x*-ray powder data... 385
Geikielite, a new find from California. (Murdoch, Fahey)...281, 835
Geologic thermometer, variable inversion temperature of quartz as a. (Tuttle)............... 723
Geologic thermometry, liquid inclusion in halite as a guide to. (Dreyer, Garrels, Howland).26, 276
Geothermometer, decrepitation. (Peach).................. 413
Geothermometry, liquid inclusions in. (Peach).............. 460
Geschichte des Goldes. (Quiring) Book review............... 617
Gesteine und Minerallagerstätten. Vol. I. (Niggli) Book review.. 128
Giannetite. (Guimarães)......... 770
Ginther, R. J. with Schulman, J. H. and Claffy, E. W. Some observations on the crystallization of silicic acid............... 68
Glass, J. J. and Vhay, J. S. A new locality for ludlamite....... 335
Goldsmith, J. R. Some aspects of system $NaAlSiO_4$-$CaO \cdot Al_2O_3$. 277, 471
Golledge, A., and Grenwell-Wells, H. J., with Young, R. S. Magnetite crystals from a copper converter.................. 761
Goodspeed, G. E................. 277
Goodyear, J.................... 337
Goongarrite and warthaite discredited. (Thompson)........... 459
Gordon, S. G.................... 291
Graftonite (Lindberg)........... 279
Graham, A. R. Artificial pyrrhotite 462
Grain-thin sections and other teaching aids in optical mineralogy. (von Huene)........ 121
Grenwell-Wells, H. J. and Golledge, A. with Young, R. S. Magnetite crystals from a copper converter.................. 761
Grimaldi, F. S. with Axelrod, J. M. Muscovite with small optic axial angle.............. 559
———......................... 274
Gruver, R. M., Henry, E. C., and Heystek, H. Suppression of thermal reactions in kaolinite 869
Guimarães, D................... 770

Hale, D. R. and Hurlbut, C. S., Jr., Quartz sphere grown into a faced crystal............... 596
Halloysite-metahalloysite transition, effect of temperature and pressure. (Brindley, Robinson, Goodyear)................ 337
Halloysite, transition to metahalloysite, in relation to relative humidity. (Brindley, Goodyear)..................... 337
Handbook of Uranium Minerals. (DeMent, Dake) Book review. 134
Harry, W. T.................... 615
Hedleyite...................... 364
Heinrich, E. Wm................ 278
———. Book reviews.......... ....128, 616, 617, 764, 765
Hematite-goethite relations in neutral and alkaline solutions under pressure. (Smith, Kidd) 403
Henderson, E. P. Aggie Creek meteorite from Seward Peninsula, Alaska............... 229
——— with Hess, H. H. Moore County Meteorite; a further study with comment on its primordial environment 287, 494, 763
——— with Perry, S. H. The Wathena, Doniphan Co. Kansas, meteorite.............. 102
——— with Reberholt, B. O. Improved method of etching iron meteorites................ 606

Henry, E. C. and Heystek, H. with Gruver, R. M. Suppression of thermal reactions in kaolinite . 869
Hess, H. H. Chemical composition and optical properties of common clinopyroxenes 621
——— **with Henderson, E. P. Moore County Meteorite; a further study with comment on its primordial environment** 278, 494, 763
Hessite........................ 354
Hey, M. H.................. 614, 769
Heystek, H. with Gruver, R. M. and Henry, E. C. Suppression of thermal reactions in kaolinite 869
Hildebrand, F. A............... 274
Holdenite, Mooreite, and torreyite, x-ray study of (Prewitt-Hopkins) 589
Holland, H. D. and Kulp, J. L. Distribution of accessory elements in pegmatites. I. Theory 35, 278
Holmes, R. J. and Wright, H. D. with Kulp, J. L. Thermal study of rhodochrosite 195, 285
Howland, A. L. with Dreyer, R. M. and Garrels, R. M. Liquid inclusions in halite as a guide to geologic thermometry 26, 276
Hseung, Y. and Yeh, C. C. Fluorescence test of bentonite...... 896
Hunt, W. F. Book review........ 766
Hurlbut, C. S., Jr., Dana's Minerals and How to Study Them. Book review............... 616
——— **with Hale, D. R. Quartz sphere grown into a faced crystal** 596

Igneous rocks of the Capitan Quadrangle, New Mexico (Patton).................. 281
International Committee for Study of Clays, organization of..... 612

Jaffe, H. Visual arc spectroscopic detection of halogens, rare earths and other elements by use of molecular spectra 667
Jarlite, x-ray and optical data. (Ferguson)................ 386
Johnson, L. R. with Zerfoss, S. Crystal chemical relations in inorganic piezoelectric materials 61
Johnston, R. W................ 132
Jonas, E. C. with Rowland, R. A. Variations in differential thermal analysis curves of siderite 282, 550
Joseite A..................... 365
Joseite B..................... 367
Jujuyite (Ahlfeld).............. 133

Kaiman, S. Lattice spacing for glancing angles with iron x-radiation.................... 465
Kaolin minerals, electron microscopy of. (Bates, Hildebrand, Swineford)................ 274
Keller, W. D. and Pickett, E. E. Absorption of infrared radiation by powdered silica minerals 855
———....................... 278
Kerr, P. F. with Kulp, J. L. Improved differential thermal analysis apparatus 839
——— **with Vaes, J. F. Sengierite: a preliminary description** 109
Kidd, D. J. with Smith, F. G. Hematite-goethite relations in neutral and alkaline solutions under pressure 403
Klockmannite. (Earley) 435
Köhler, A. Das Bestimmen der Mineralien. Book review..... 767
Koktaite (Sekanina)............ 618
Kraus, E. H. Book review........ 767
Krennerite.................... 349
Kulp, J. L. with Holland, H. D. Distribution of accessory elements in pegmatites, I. Theory 35, 278
——— **with Wright, H. D. and Holmes, R. J. Thermal study of rhodochrosite** 195, 285

——— and Kerr, P. R. Improved differential thermal analysis apparatus 839

Lacroix, A., memorial of. (Orcel) .. 242
Lakeside No. 70 transparent cement, notes on. (von Huene) 125
Lane, Alfred Church, memorial of. (Larsen) 249
Larsen, E. S. Jr., Memorial of Alfred Church Lane 249
Latice expansion and its relation to hydration in montmorillonite an vermiculite (Barshad) 675
Lattice spacings for glancing angles with iron x-radiation. (Kaiman 465
Law of Rationality to the law of Bravais. (Donnay) 288
Laubmannite 534
Lepidolite, x-ray data 77
Levin, S. B. 279
Lindberg, M. L. Frondelite and the frondelite-rockbridgeite series 541
——— 279
Lindgrenite, unit cell and space group of. (Barnes) 163, 611
Liquid inclusions in halite as a guide to geologic thermometry. (Dreyer, Garrels, Howland) 26, 276
Lithium-bearing pegmatites in Northern Quebec. (Derry) 275
Lonsdale, J. T., and O'Neill, K. K. 280
Ludlamite from the Palermo mine, North Groton, New Hampshire (Wolfe) 94
Ludlamite, a new locality for. (Glass, Vhay) 335

Magnetite crystals from a copper converter. (Young, Golledge, Grenwell-Wells) 761
Manchester, James Greenfield, memorial of. (Stanton) 253
Marble, J. P. Report of committee on measurement of Geologic time, 1947–48 766
Mathias, M. 132
McKinstry, H. Mineral isograds in southern Pennsylvania 874
Melilites, synthetic, x-ray data on. (Ervin, Osborn) 717
Melonite 359
Melvin, J. H. Memorial of Lewis Gardner Westgate 256
Mertie, J. B., Jr., Charting five and six variables on the bounding tetrahedra of a hypertetrahedra 280, 706
Merumite (Bracewell) 339
Meta-halloysite, Random layer structure. (Brindley, Robinson) 337
Methyl-ethyl ketone as an index liquid. (Wherry) 613
Meteorite collections, list of catalogues of. (Spencer) 132
Mica powders, x-ray spectrometer study of. (Beatty) 74
Milne, I. H. Chloritoid from Megantic County, Quebec 422
Milton, C. and Myers, A. T. Bodenbenderite, a discredited species 608
——— 274
Mineral isograds in southern Pennsylvania. (McKinstry) .. 874
Mineral, what is a? (A. N. Winchell) 220, 284
Mineralogical crystallography, objectives in teaching of. (Fisher) 289
Mineralogical Society of America. Announcement of 30th Annual Meeting 340
———. List of correspondents, fellows, members, and subscribers 293
———. Proceedings of the twenty-ninth annual meeting at New York, N. Y. 267
Mineralogical Society (London) 132, 337, 614, 769
Mineralogy, prospect of. (M. A. Peacock) 135
Mohs' scale, correlation with Vicker's hardness numbers. (Taylor) 768

Montbrayite.................. 345
Montmorillonite and vermiculite, nature of lattice expansion and its relation to hydration in. (Barshad)................ 675
Moore County meteorite: a further study with comment on the primordial environment. (Hess, Henderson)....278, 494, 763
Mooreite, *x*-ray study of. (Prewitt-Hopkins)................. 589
Morcom, A. J.................. 132
Morenosite (optical data)........ 193
Morey, G. W.................. 281
Morphological crystallography, teaching of. (Peacock)....... 291
Moyd, L. Petrology of the nepheline and corundum rocks of southeastern Ontario........ 736
Murata, K. J.................. 274
Murdoch, J. and Fahey, J. J. Geikielite, a new find from California................281, 835
Muscovite with small optic axial angle. (Axelrod, Grimaldi)... 559
Muscovite with 3-layered monoclinic structure. (Axelrod, Grimaldi)................... 565
Muscovite, *x*-ray data........... 78
Museum, role of, in teaching crystallography. (Gordon)... 291
Muthmannite................. 373
Myers, A. T. with Milton, C. Bodenbenderite, a discredited species................... 608

Nagelschmidt, G............... 132
Nagyagite.................... 363
Naray-Szabo, I................ 133
Nepheline and corundum rocks of southeastern Ontario, petrology of. (Moyd)............ 736
Neptunite in quartz-bearing syenites. (Nockolds).......... 769
Nesterova, Y. S................ 619
New mineral names...133, 339, 618, 770
Nichols, J. B. Book review....... 768
Niggli, P. Gesteine und Minerallagerstätten. Book review... 128
Niggliite..................... 373
Nockolds, S. R................. 769
Nuffield, E. W. with Phoenix, R. Cancrinite from Blue Mountain, Ontario.............. 452

Olivier, C. P. Note on Aggie Creek meteorite................. 232
Olivines from South African melilite-basalts. (Mathias)....... 132
O'Neill, K. K.................. 280
Optical constants and thickness of thin sections, determination of. (Game)................ 615
Orcel, J. Memorial of A. Lacroix.. 242
Osborn, E. F. with Ervin, G. Jr. *X*-ray data on synthetic melilites...................... 717
Owyheeite (Robinson).......... 398

Palache, C. with Frondel, C. Retgersite, $NiSO_4 \cdot 6H_2O$, a new mineral.................188, 276
Paraguanjuatite (Ramdohr)...... 619
Parajamesonite. (Zsivny, Naray-Szabo)................... 133
Patterson, E. M................ 615
Patton, L. T.................. 281
Peach, P. A. Decrepitation geothermometer............... 413
———. Geothermometry, liquid inclusions in............... 460
Peacock, M. A. Prospect of mineralogy................... 135
———....................... 291
——— and Forman, S. A. Crystal structure of rickardite, $Cu_{4-x}Te_2$...................... 441
Pecora, W. T. and Fahey, J. J. Corrego Frio pegmatite, Minas Gerais: scorzalite and souzalite, two new phosphate minerals...................... 83
———. Scorzalite from South Dakota, a new occurrence..282, 685
Pennaite (Guimarães).......... 770
Pepinsky, R. Book review....... 129
Perry, S. H. with Henderson, E. P. The Wathena, Doniphan Co. Kansas, meteorite.......... 102

Petrographic miscroscope, inexpensive. (Winchell, Walton) . . 688
Pettijohn, F. J. Sedimentary Rocks. Book review 764
Petzite 350
Phlogopite, x-ray data 80
Phoenix, R. and Nuffield, E. W. Cancrinite from Blue Mountain, Ontario 452
Phosphoscorodite. (Shadlun, Nesterova) 619
Pickett, E. E. with Keller, W. D. Absorption of infrared radiation by powdered silica minerals 855
Piezoelectric materials, inorganic, crystal chemical relations in. (Zerfoss, Johnson) 61
Plagioclases from Sultan Hamud, Kenya. (Game) 614
Point counter for thin-section analysis. (Chayes) 1, 600
Pough, F. H. Memorial of Herbert Percy Whitlock 261
Pre-Beltian Rocks near Dillon, Montana. (Heinrich) 278
Precision lattice measurements of pyrite from Leadville, Colo., observations on. (Wasserstein) 731
Prewitt-Hopkins, J. X-ray study of holdenite, mooreite, and torreyite 589
Probertite, unit cell and space group of. (Barnes) 19, 611
Prosopite, x-ray data. (Ferguson) 391
Prospect of mineralogy. (Peacock) 135
Pseudotachylite of the Antietam quartzite. (Anderson) 331
Pyrrhotite, artificial. (Graham) . . . 462

Quartz, artificial, by hydrothermal methods. (Swinnerton) 284
Quartz, conversion of amorphous silica to. (Bailey) 601
Quartz crystals, frequency of twin types in. (Gault) 142
Quartz, laboratory growth of. (Friedman) 583
Quartz sphere grown into a faced crystal. (Hale, Hurlbut) 596
Quartz, variable inversion temperature of, as a possible geologic thermometer. (Tuttle) 284, 723
Quiring, H. Geschichte des Goldes. Book review 617

Radioactive Measurement with Nuclear Emulsions. (Yagoda) Book review 765
Ralstonite, x-ray data. (Ferguson). 393
Ramdohr, P. 619
Reberbolt, B. O. and Henderson, E. P. Improved method of etching iron meteorites 606
Refractive indices of high index liquids by the prism method on the two-circle goniometer. (Wolfe, Franklin) 893
Retgersite, $NiSO \cdot 6H_2O$, a new mineral. (Frondel, Palache) 188, 276
Retrogressive alteration following granitization and rheomorphism (Goodspeed) 277
Rhodochrosite, thermal study of. (Wright, Kulp, Holmes) . . . 195, 285
Rickardite, $Cu_{4-x}Te_2$, crystal structure of. (Forman, Peacock) . 359, 441
Riley, D. P. 132
Robertson, F. 282
Robinson, K. 337
Robinson, S. C. Owyheeite 398
Rockbridgeite, optical and chemical data. (Frondel) (Lindberg) 525, 528, 543
Roebling Medal of the Mineralogical Society of America: Presentation to William Lawrence Bragg. (Tunell) 235
Roebling Medal of the Mineralogical Society of America, acceptance of. (Bragg) 238
Roedder, E. W. 292
Rosenholtz, J. L. and Smith, D. T. Linear thermal expansion of calcite, var. Iceland spar and Yule marble 846
Rowland, R. A. and Jonas, E. C.

Variations in differential thermal analysis curves of siderite 282, 550

Schairer, J. F. 283
Shulman, J. H., Claffy, E. W. and Ginther, R. J. Some observations on the crystallization of silicic acid 68
Scorzalite from South Dakota, new occurrence. (Pecora, Fahey) 282, 685
Scorzalite and souzalite, two new phosphate minerals, Corrego Frio pegmatite, Minas Gerais: (Pecora, Fahey) 83
Screw axes of symmetry and their symbols. (Bader) 752
Sedimentary Rocks. (Pettijohn) Book review 764
Sekanina, J. 618
Selenides, natural and artificial: I-Klockmannite, CuSe (Earley) 435
Sengierite: a preliminary description. (Vaes, Kerr) 109, 763
Sengit, E. R. 132
Shaub, B. M. Paragenesis of garnet and associated minerals of the Barton Mine near North Creek, N. Y. 573
Shadlun, T. N. 619
Siderite, variations in differential thermal analysis curves of. (Rowland, Jonas) 282, 550
Silica percentage as a factor in rock classification. (Wells) 615
Silicic acid, some observations on the crystallization of. (Shulman, Claffy, Ginther) 68
Silicocarnotite, basic slag mineral, optical and *x*-ray examination of. (Riley, Sengit) 132
Smith, D. T. with Rosenholtz, J. L. Linear thermal analysis of Iceland spar and Yule marble 846
Smith, F. G. and Kidd, D. J. Hematite-goethite relations in neutral and alkaline solutions under pressure 403
Smith, W. Campbell 614
Souzalite and scorzalite, two new phosphate minerals, Corrego Frio pegmatite, Minas Gerais: (Pecora, Fahey) 83
Spangolite, crystallography of. (Frondel) 181
Spectrochemical methods of rock analysis. (Strock) 284
Spencer, L. J. 132
Stanton, G. S. Memorial of James Greenfield Manchester 253
Stewart, F. H. 614
Stobbe, H. 283
Strock, L. W. 284
Stuetzite 373
Svanbergite from Nevada. (Switzer) 104
Swartzite 274
Swineford, A. 274
Swinnerton, A. C. 284
Switzer, G. Svanbergite from Nevada 104
Sylvanite 353
System H_2O-Na_2O-SiO_2, Isothermal polybaric saturation curve at 400° in. (Morey) 281
System K_2O-MgO-Al_2O_3-SiO_2, phase equilibrium relations in the quaternary. (Schairer) ... 283
System K_2O-MgO-SiO_2. (Roedder) 282
System ($NaAlSiO_4$-$CaO \cdot Al_2O_3$, some aspects of. (Goldsmith) 277, 471

Talc in the salines of the potash field near Carlsbad, New Mexico. (Bailey) 757
Taylor, E. W. 769
Taylor, J. H. 337
Tellurbismuth 367
Telluride minerals and their occurrence in Canada. (Thompson) 342
Tellurium minerals, occurrences in western Canada. (Warren, Thompson) 458
Tennantite, hydrothermal synthesis of. (Gaines) 276
Tetradymite 370

Thermal expansion, linear, of calcite, var. Iceland spar, and Yule marble. (Rosenholtz, Smith) 846
Thermal reaction in kaolinite, suppression of. (Gruver, Henry, Heystek) 869
Thompson, R. M. Goongarrite and warthaite discredited. 459
— ——. **Telluride minerals and their occurrence in Canada.** . . 342
———with Warren, H. V. Further occurrences of antimony and tellurium minerals in western Canada. 458
Tolman, C. 282
Torreyite, x-ray study of. (Prewitt-Hopkins) 589
Tunell, G. Presentation of the Roebling Medal of the Mineralogical Society of America to William Lawrence Bragg. . 235
———. 292
——— **and Adams, C. Symmetry and crystal structure of bornite.** 824
Tuttle, O. F. Variable inversion temperature of quartz as a possible geologic thermometer. 284, 723
Twin types in quartz crystals, frequency of. (Gault) 142

Uranium minerals from the Hillside Mine, Yavapai County, Arizona. (Axelrod, Grimaldi, Milton, Murata) 274

Vaes, J. F. and Kerr, P. F. Sengierite: a preliminary description . 109
Variable inversion temperature of quartz as a possible geologic thermometer. (Tuttle) 723
Variables, charting five or six, on the bounding tetrahedra of a hypertetrahedra. (Mertie) 280, 706
Varlamoffite (Buttgenbach) 618
Vauquelinite, x-ray measurement on. (Berry) 275
Vhay, John G. and Glass, Jewell, J. A new locality for ludlamite. 335
Visual arc spectroscopic detection of halogens, rare earths and other elements by use of molecular spectra. (Jaffe) 667
Volcanic rocks of northeastern New Mexico, petrology of (Stobbe.) 283
Volcanic rocks, St. Francois Mountains, Missouri, high potash. (Robertson, Tolman) 282
Von Huene, R. Grain-thin sections and other teaching aids in optical mineralogy 121
———. Notes on Lakeside No. 70 transparent cement. 125

Walker Mineralogical Club, By-laws, officers 1948. 469
Proceedings. 133, 470
Walton, M. S. with Winchell, H. An inexpensive petrographic microscope. 688
Warren, H. V. and Thompson, R. M. Further occurrences of antimony and tellurium minerals in western Canada. 458
Warthaite discredited. (Thompson) 459
Wasserstein, B. Observations on two precision lattice measurements of pyrite from Leadville, Colo. 731
Wathena, Doniphan Co. Kansas, meteorite. (Henderson, Perry) 102
Weberite, x-ray data. (Ferguson). 395
Wehrlite. 369
Weil, R. 618
Weissite. 357
Wells, A. K. 615
Wells, R. C. Antimonial silver ore from Cobalt, Ontario. 456
Westgate, Lewis Gardner, memorial of. (Melvin) 256
Wherry, E. T. Methyl-ethyl ketone as an index liquid. 613
White, W. A. Atterberg plastic limits of clay minerals. 508
Whitlock, Herbert Percy, memorial of. (Pough) 261

Whitlockite from Palermo Mine, New Hampshire. (Frondel) 692
Winchel, A. N. What is a mineral? 220, 284
Winchell, H. and Walton, M. S. An inexpensive petrographic microscope 688
Winkler, H. G. F............... 338
Wolfe, C. W. Ludlamite from the Palermo mine, North Groton, New Hampshire 94
———, and Franklin, V. Refractive indices of high index liquids by the prism method on the two-circle goniometer..... 893
Wolfeite, xanthoxenite, and whitlockite from Palermo Mine, New Hampshire. (Frondel) 692
Wright, H. D. and Holmes, R. J. with Kulp, J. L. Thermal study of rhodochrosite. 195, 285
Wrinch, D. Fourier Transforms and Structure Factors. Book review......................... 129
Xanthoxenite from Palermo Mine, New Hampshire. (Frondel) 692
Xenotime and bastnäsite, petrographic distinction of (Foster) 830
X-ray crystallography, teaching of. (Tunell).................. 292

Yagoda, H. Radioactive Measurements with Nuclear Emulsions. Book review................ 765
———......................... 285
Yeh, C. C. with Hseung, Y. Fluorescence test of bentonite..... 896
Young, R. S., Golledge, A., and Grenwell-Wells, H. J. Magnetite crystals from a copper converter.................. 761

Zerfoss, S. and Johnson, L. R. Crystal chemical relations in inorganic piezoelectric materials 61
Zinnwaldite, *x*-ray data.......... 81
Zsivny, V...................... 133

GOLD

Nineteen hundred and forty-nine, the one-hundredth anniversary of the discovery of gold in California, is an appropriate time to announce the purchase of a magnificent collection of GOLD specimens that will be of interest to mineral collectors and museums. This collection is a large one and contains superb specimens of

GOLD IN QUARTZ
CRYSTALLIZED GOLD
WIRE GOLD
CRYSTALLIZED WIRE GOLD
GOLD NUGGETS
GOLD DUST

We have prepared a special listing of a portion of this remarkable collection and we suggest that you write for a copy if you have not already received one

Special Announcement

We are now in a position to legally go ahead with our plans to hold the Exhibition and Sale of Fine Minerals that was advertised and subsequently postponed last year in this publication.

Watch for our announcement next month giving dates and details of this long waited for special Exhibition and Sale of Fine Mineral Specimens.

SCHORTMANN'S MINERALS
6 McKinley Avenue **Easthampton, Massachusetts**

* UNIMPEACHABLE SERVICE *

Scientists habitually turn to Ward's for minerals which must meet the exact requirements of the laboratory. Ward-standards of identification and evaluation have, for nearly a century, stood the test of accuracy.

CHOICE SPECIMENS OF RECENTLY ACQUIRED ZEOLITES

CHABAZITE. Isle of Skye, Scotland. Sharp white rhombohedral crystals on basalt: 3 x 3½″, $3.00; 3 x 5″, $3.50.

HARMOTOME. Strontian, Scotland. Excellent groups of large white crystals on rock: 2 x 2½″, $3.00; 2 x 4″, $4.00; 3 x 5″, $5.00; 3½ x 6″, $6.00

PHILLIPSITE. Capo di Bove, Rome, Italy. Small, clear, glassy crystals, closely grouped, often as small spherical clusters on rock: 2½ x 3½″, $2.00; 3 x 4″, $3.00

STILBITE. Flodigarry, Isle of Skye, Scotland. Sharp, tabular crystal groups on rock: 2½ x 3″, $2.50; 3 x 4″, $3.00; 4 x 5½″, $4.00.

THOMSONITE (FAROELITE). The Storr, Isle of Skye, Scotland. Radiated, white, crystalline masses in vesicular basalt: 2½ x 3″, $2.00; 2½ x 4″, $3.00; 3 x 4″, $3.50.

OTHER ITEMS OF NOTE

BARITE. Cow Green Mine, Teesdale, Durham, England. White, lamellar aggregations with small, clear crystals projecting at the surface, forming attractive, crested groupings: 3 x 4″, $3.50; 4 x 6″, $5.00.

DIAPHORITE. Hodritsch, near Schemnitz, Czechoslovakia. Xled with quartz: 2 x ½″, $6.00

GAHNITE. Davis Mine, Rowe, Massachusetts. Dark blue, octahedral crystals with pyrite, quartz, etc.: 1½ x 2″, $2.00; 2 x 2″, $2.50; 2 x 3″, $3.00

MIMETITE, *var. CAMPYLITE.* Drygill, Cumberland, England. Very good specimens of globular and barrel-shaped, yellow-brown to brownish-red crystals grouped on quartz, etc.; 1 x 2″, $1.50; 2 x 2″, $2.00, $2.50; 2 x 3″, $3.00; 3 x 4″, $3.50, $4.00.

ROCKBRIDGEITE. Near Greenbelt, Maryland. (This material, previously considered to be dufrenite, is now identified as a new member of the dufrenite-complex. Frondel, C., *Am. Min.*, Vol. 34, Nos. 7 & 8, pp. 513-540, 1949). The rockbridgeite occurs as dark greenish black, fibrous crusts, lining cavities in limonite concretions. Single sawed halves are available in the following sizes: 3 x 3″ to 4 x 4″, $.75, $1.00, $1.50, $2.00; 4 x 5″, $2.50; 4 x 6″, $3.00.

SAFFLORITE. Cobalt, Ontario, Canada. Gray-white masses with pyrargyrite: 2¼ x 3″, $3.50; a very rich specimen: 2 x 3¼″, $6.00.

SILVER. Cobalt, Ontario, Canada. An exceptional 31½ lb. specimen of dendritic native silver with smaltite, safflorite and some rock. The polished surface is 8¾ x 13 inches and the slab is 3 inches thick. $75.00

URANINITE. Near Grafton Center, New Hampshire. Superb specimens of coal-black, dendritic uraninite with associated orange gummite, yellow uranophane and occasionally crystallized cyrtolite: 1 x 2″, $1.00; 2 x 2″, $2.00; 2 x 3″, $3.50; 3 x 4″, $7.50; 4 x 5″, $11.00; 3¼ x 5″, $12.00; 5 x 5″, $25.00; 5 x 7″, $30.00 (Shipment by express only). (*Write for Price List U-5, "Uranium and Thorium Minerals"*)

PHOTOMICROGRAPHS OF THIN ROCK SECTIONS

A new set of kodachrome microphotographs of 20 igneous, 6 sedimentary and 11 metamorphic rocks. Photographs have been taken with polarized as well as ordinary light to illustrate various rock textures and mineral assemblages as seen in thin section under the petrographic microscope.

LW74—37 slides with script, postpaid, $27.75. Ind. slides $.80.

WARD'S NATURAL SCIENCE ESTABLISHMENT, INC.
3000 RIDGE ROAD EAST · ROCHESTER 9, N.Y.

GEORGE BANTA PUBLISHING COMPANY, MENASHA, WISCONSIN